

AN ABSTRACT OF THE THESIS OF

Arianna C. Goodman for the degree of Master of Science in Water Resources Science presented on September 14, 2020.

Title: Long-Term Stream Channel Response to a Large Flood in a Forested Mountain Watershed

Abstract approved: _____

Catalina Segura

There is still scholarly debate on the impacts of large floods on the geomorphic evolution of mountain rivers. Understating the geomorphic effects of large flows in mountain rivers is challenging given the hydraulic complexity of these systems and the inherent unpredictability of large floods. Prior work has demonstrated that extreme floods in mountain regions can result in changes to channel form, the magnitude and direction of which varies not only as a function of the size of the extreme event but also on depending on local channel characteristics. Despite this variability, few long-term studies have explored the impacts of large floods. Cross sections were repeatedly surveyed from 1978 to 2011 within four, 3rd–5th order stream reaches in the HJ Andrews Experimental Forest in the Cascade Range, Oregon, USA. In February of 1996, the study site experienced mass movements and flooding in response to a storm which broadly impacted the Pacific Northwest region. At the lower gaging station, the peak flow of 1996 is the flood of record which was 290% greater than the mean annual peak flow. Repeat cross-sectional surveys showed that the flood of 1996 produced disproportionately greater effects than any moderate flood that occurred during the monitoring period. After 17 years of limited very minimal channel change in the pre-flood period, the 1996 flood induced measurable changes in sediment storage, bankfull channel geometry, and channel grain size at all of the study reaches. However, the magnitude and direction of these changes varied from reach to reach. Changes to channel form also varied within reaches. A low-gradient (1.5%), partly confined reach experienced scouring and deepening near its channel bend and deposition and depth reduction downstream of the bend. A medium-gradient (3.2%), unconfined reach experienced deposition, fining, and bankfull depth reduction upstream of a large logjam. Many of these changes persisted

through the end of monitoring in 2011. Our findings suggest large, debris-laden flows may play a fundamentally different role in fluvial adjustment than smaller, lower density flows. The placement and stability of channel-spanning logjams also affects flood response. In contrast to the other long-term monitoring sites in the western US, stream channels at this site appear relatively quiescent due in part to their more resistant lithology. While the 1996 flood produced a decadal-scale impact on channel geometry in many parts of the study reaches, grain size adjustment occurred on the 1 to 5-year time scale, which suggests that mountain streams might return to their pre-flood sediment transport conditions much more quickly than they return to their pre-flood cross-sectional geometries.

©Copyright by Arianna C. Goodman
September 14, 2020
All Rights Reserved

Long-Term Stream Channel Response to a Large Flood in a Forested Mountain Watershed

by
Arianna C. Goodman

A THESIS

submitted to

Oregon State University

in partial fulfillment of
the requirements for the
degree of

Master of Science

Presented September 14, 2020
Commencement June 2021

Master of Science thesis of Arianna C. Goodman presented on September 14, 2020

APPROVED:

Major Professor, representing Water Resources Science

Director of the Water Resources Graduate Program

Dean of the Graduate School

I understand that my thesis will become part of the permanent collection of Oregon State University libraries. My signature below authorizes release of my thesis to any reader upon request.

Arianna C Goodman, Author

ACKNOWLEDGEMENTS

I would like to express gratitude to my advisor Dr. Catalina Segura for her patience and guidance over the last two years. Her dedication to her students, to her work, and to clear science communication have helped me grow as a scientist and a researcher. I would also like to thank Julia Jones for sharing her deep knowledge of the Andrews Forest and for her patience in both the classroom and the field. I would like to thank Desiree Tullos for taking time out of her schedule to teach me new ways to look at both modeling and rivers and for repeatedly asking me to put small details into broader contexts. I offer my deep thanks to Fred Swanson, who is cited many times in this text, for his stories and his insights into Pacific Northwest landscapes.

This project would not have been possible without Greg Downing and Don Henshaw who have put in countless hours to collect and maintain these data. Thank you also to Josiah Shaver, Alberto Paredes, and Nico Vergara for assistance with field work in the summer of 2019. Thank you to Ariel Muldoon for taking the time to discuss the constraints of various statistical models with me. I left each of our meetings feeling more hopeful and less afraid of the data set.

I would like to thank Mary Santelmann for her boundless dedication to the Water Resources Graduate Program and its graduate students. Her advice and insights were essential to my success as a graduate student. Thank you also to the administrative staff of FERM and WRGP, including Cat Mullins, Madison Dudley, and Chelsea Durling who answered many emails and got me on the right track over the last two years.

Thank you also to my Snell Hall officemates, who during the pandemic became Zoom and backyard officemates. Thank you to Emily Crampe, Sami Cargill, Austin Wissler, Karla Jarecke, and Ryan Cole for continuous support, proofreading, camaraderie, and distraction. Thank you the many other friends and family members near and far who supported me daily through this process with phone calls, shared meals, beach trips, and good conversation.

This work was made possible by funding from the Lee Harris Memorial Fellowship, the Alfred W. Moltke Memorial Scholarship, the Mary McDonald Fellowship, the Arnold & Vera Meier Forestry Education Scholarship, the Lee Harris Travel Grant, and the College of Forestry Experiential Learning Grant. Funding was also provided by NSF through the LTER.

TABLE OF CONTENTS

	<u>Page</u>
1. Introduction	11
2. Site Description	5
3. Methods	12
3.1. Field Data Collection	12
3.2. Cross section data adjustment and profile interpolation	13
3.3. GIS-derived landscape attributes	14
3.4. Derived scour/deposition metrics.....	14
3.5. Derived hydraulic geometry metrics	16
3.6. Statistical Analysis	17
4. Results	18
4.1. Peak flows between 1980 and 2011 and channel change and over time.....	18
4.2. Relationship between peak flow and geomorphic response.....	20
4.3. Reach-scale responses to the 1996 flood.....	23
4.4. Geomorphic patterns of response at Middle Lookout.....	39
5. Discussion.....	45
5.1. Relationships between channel adjustment and peak flows.....	45
5.2. Patterns of geomorphic adjustment in 1996 and subsequent years.....	47
5.3. Variation within an unconfined and a confined reach.....	48
5.4. Comparison to channel adjustment in other long-term study sites	51
5.5. Implications for aquatic habitat.....	54
5.6. Opportunities for Further Research.....	55
6. Conclusions	56
7. References	57
8. Appendices	69

LIST OF FIGURES

<u>Figure</u>	<u>Page</u>
Figure 1: Shaded relief map of the Lookout Creek watershed	6
Figure 2: Maps of the four study reaches.....	10
Figure 3: Wood and channel locations in Lower Lookout over time	11
Figure 4: Conceptual diagrams	16
Figure 5: Time series of annual peak flows at the Lookout Creek and Mack Creek gages.....	19
Figure 6: Median and interquartile range of year-to-year reworked cross-sectional area	20
Figure 7: Rotal reworked channel area (i.e., area eroded plus area deposited) versus peak discharge for study reaches	21
Figure 8: Median and interquartile range of cumulative scour and deposition.	25
Figure 9: Bankfull depths as a ratio relative to the 1995 values at each reach	27
Figure 10: Bankfull widths as a ratio relative to the 1995 values at each reach.....	29
Figure 11: D_{50} in mm at each of the four reaches	30
Figure 12: Sorting (σ , unitless) at each of the four reaches	31
Figure 13: Cumulative cross-sectional deposition and thalweg aggradation from every cross section in Lower Lookout	33
Figure 14: Bankfull depths and widths from every cross section in Lower Lookout.....	35
Figure 15: D_{50} and σ from every cross section in Lower Lookout	37
Figure 16: Percent change in Shields stress from every cross section in Lower Lookout.....	38
Figure 17: Cumulative cross-sectional deposition and thalweg aggradation from every cross section in Middle Lookout	40
Figure 18: Bankfull depths and width from every cross section in Middle Lookout	42
Figure 19: D_{50} and σ from every cross section in Middle Lookout	44
Figure 20: Percent change in shields stress from every cross section in Middle Lookout	45

LIST OF TABLES

<u>Table</u>	<u>Page</u>
Table 1: Characteristics of the four study reaches	9
Table 2: Summary of R2 values for the best-fit relationship between peak discharge and mean reworked cross-sectional area	21
Table 3: Summary of R2 values for the best-fit relationship between return interval and mean reworked cross-sectional area	22
Table 4: Summary of R2 values for the best-fit relationship between return interval and net deposition.....	23
Table 5: Summary of median flood response parameters at each of the four reaches between 1995 and 1997.....	24

LIST OF APPENDIX FIGURES

<u>Figure</u>	<u>Page</u>
Figure A.1: Summary of daily maximum discharge values for the Lookout Creek gage and Mack Creek gage.	72
Figure A.2: Historical aerial photos of Lower Lookout from 1959 to 2009.....	73
Figure A.3: Historical aerial photos of Middle Lookout from 1959 to 2009	74
Figure A.4: Total reworked channel area (i.e., area eroded plus area deposited) plotted against flood return interval for all reaches.....	75
Figure A.5: Median and interquartile range of cumulative thalweg incision and aggradation relative to the start of monitoring in 1978	76
Figure A.6: Scatter plots of shear stress (Pa) versus D50 (mm) for each cross section in Lower Lookout	77
Figure A.5: Scatter plots of shear stress (Pa) versus D50 (mm) for each cross section in Middle Lookout	78
Figure B.1: Total station surveying in Lower Lookout during summer 2019	79
Figure B.2: Midchannel bar visible at low flow in Lower Lookout during summer 2019.....	79
Figure B.3: Large channel-spanning wood jam in Lower Lookout during summer 2019	80
Figure B.4: Channel-spanning wood jam in Middle Lookout during summer 2019.....	80
Figure B.5: Boulders in stream near Mack Clearcut during summer 2019	81
Figure B.6: Channel spanning logjam at Mack Old Growth	82

LIST OF APPENDIX TABLES

<u>Table</u>	<u>Page</u>
Table A.1: Table of survey years with number of cross sections surveyed at each reach.....	69
Table A.2: Substrate descriptions from survey metadata and whether or not each substrate class was included in cross-sectional change calculations.	70
Table A.3: Table of cross section-year pairs that were excluded from analysis.....	70
Table A.4: R2 values and p values for linear regressions between cross section D50 and cross section shear stress.	71

1. Introduction

The impacts of large floods on the geomorphic evolution of mountain rivers are complex and not entirely understood. Both the hydraulic complexity of mountain river systems and the inherent unpredictability of extreme flood events contribute to our lack of understanding. There is still disagreement on the role large floods play in shaping mountain rivers and the surrounding riparian landscapes over time (Major et al., 2019; Pfeiffer et al., 2019). Additionally local controls such as the confinement and the abundance of large wood affect the magnitude and direction of flood-related geomorphic changes (Stoffel et al., 2016; Surian et al., 2016). Given that these local controls are dynamic over time, hydraulic variables at a given time do not necessarily explain the geomorphic changes observed in mountain rivers after a large flood (Surian et al., 2016). In fact, changes observed in a channel at a given time might represent current conditions or the physically lagged effects from a previous year, as in the downstream propagation a sediment wave (Benda & Dunne, 1997; Miller & Benda, 2000b), or relaxation from changes induced by previous flows.

Various paradigms have been proposed to explain the role that extreme events play in shaping stream morphology. Seminal investigations suggested that the majority of fluvial sediment transport occurs at moderate, bankfull flow, rather than during catastrophic large floods (Wolman & Miller, 1960). This idea of a single dominant discharge relies on the assumption that geomorphic work is a continuous function of flow magnitude (Wolman & Miller, 1960). However, that assumption might not hold true in all contexts. Other work suggested that large flood events may in some cases represent the exceedance of an *extrinsic threshold* that divides a fluvial system's geomorphic response into two discontinuous regimes (Schumm, 1979). That is, physical processes might cause a river to respond very differently to a flood of moderate size than it does to a large flood. Research on mountain streams suggest that they may be shaped by not one but two dominant discharge classes: a regularly occurring discharge that maintains channel form and an infrequently occurring discharge that affects major changes onto channel form (Lenzi et al., 2006).

Different physical conditions, such as the degree of bed armoring might influence the thresholds that separate the effects of large flow events from those of moderate flow events

(Baker, 1977). Bed armoring, is a phenomenon in gravel bed rivers in which the particle size distribution at the stream bed surface is coarser than the subsurface particle size distribution. In armored channel beds, the transport of the subsurface finer material is limited at low flow conditions (Brummer & Montgomery, 2006; Mueller & Pitlick, 2005; Parker & Klingeman, 1982). However, during large flows, the coarse surface armor layer mobilizes, allowing for approximately equal transport of all size sediment (Mao & Lenzi, 2007; Parker & Klingeman, 1982).

Fluid density acts as a control on flow competence, which is also an important geomorphic threshold in upland rivers (Church, 2002). The downstream transport of bed and bank material combined with colluvial sediment input into a river can dramatically alter the fluid density of the streamflow and along with it, the hydraulic properties of the fluid itself (Batalla et al., 1999; Costa, 1984; Wells & Harvey, 1987). Depending on the ratio of sediment to water, flows during extreme events can range from water flows to transitional flows to debris flows. Sediment laden flows such as transitional flows and debris flows are denser and more viscous than water flows and have enormous capacity to transport large clasts and dramatically reshape channel geometry (Rickenmann, 1991; Wells & Harvey, 1987). In the forested mountain watersheds of the Pacific Northwest, road construction, forest harvest, and wildfire can all increase the likelihood of debris flows during storms (G. A. Meyer et al., 2001; Nakamura et al., 2000; Wondzell & King, 2003).

Large wood and boulders act as structural features in steep mountain streams, so their thresholds of mobility may influence the thresholds of geomorphic change (Adenlof & Wohl, 1994; Bugosh & Custer, 1989; Hogan, 1987). Large wood and large boulders act as structural controls on the longitudinal energy gradient and in steep streams (Faustini & Jones, 2003; Montgomery et al., 1995; Swanson et al., 1976), but they may be moved by sufficiently large floods (Braudrick et al., 1997; Hogan, 1987; Johnson et al., 2000; Turowski et al., 2009). Unlike large rivers which can immediately transport much of the instream wood, small mountain streams only transport wood during infrequent high flow events (Montgomery et al., 1995; Nakamura & Swanson, 2003), which means that the rare large flows that capable of moving these features might induce much more structural changes in the channel. The presence of instream wood also plays a role in the pattern of channel adjustment during and after large flows,

even when the wood is not relocated. During floods, instream wood can physically obstruct sediment transport and trigger deposition of sediment and wood features (Faustini & Jones, 2003; Hogan et al., 1998). Wood can also deflect flows and trigger bank erosion (Abbe & Montgomery, 2003; Adenlof & Wohl, 1994; Daniels & Rhoads, 2003).

There are additional factors that control the magnitude and direction of flood-associated geomorphic change in mountain streams. These factors include sediment storage (East et al., 2018), sediment supply (East et al., 2018; Gomi & Sidle, 2003; Pitlick, 1993), valley confinement (East et al., 2018; Swanson et al., 1998), and locations of river bends (de Jong, 1992). For example, sediment supply was observed to control vertical adjustment following a dam-burst flood in two streams in Colorado (Pitlick, 1993) and downstream of glacial lake outburst floods in Nepal (Cenderelli & Wohl, 2003). Valley width was found to be a controlling factor in flood-associated channel change in a mountain river in Japan (Maita, 1991), and in the Colorado Front Range, it was found to be a controlling factor in longitudinal variation in channel widening and flood response (Sholtes et al., 2018). River bend resistance and complex water surface topography associated with river bends also play a role in shaping channel reworking and deposition during floods (de Jong, 1992). Each of these controls may vary across space and time (Gintz et al., 1996; Hassan et al., 2005; Swanson et al., 1987), resulting in a complex relationship between hillslope processes, valley forms, and stream response to floods.

Extreme floods in mountain regions often result in changes in bed elevations (vertical thalweg adjustment). Extreme events do appear to reliably impact bed elevations, generally triggering aggradation and deposition (Di Silvio, 1994). For example, a set of coastal streams in California and Oregon, widely aggraded following the extreme flood of 1964 followed by a 5- to 15-year recovery period (Lisle, 1981). In Redwood Creek in Northern California floods disrupted regular patterns of bed elevations, and bed elevations showed distinct patterns based on the time since the last large disturbance (Madej, 1999). In gaged streams in the Washington Cascades and Olympics, specific gage analysis suggested that bed elevation changes are most commonly observed at flows 5–10 times the mean discharge, while smaller flows are less likely to induce bed elevation changes (Pfeiffer et al., 2019).

Researchers also frequently observe channel widening in response to large floods. In the Italian Apennines, one study found channel widening at 35 out of 39 study reaches, with more

frequent widening at reaches with slopes $< 4\%$ (Surian et al., 2016). During the 2013 Colorado Front range storm season, changes in channel width (usually widening) during the flood were associated with valley confinement variables, where more confined streams were more likely to experience greater levels of width adjustment (Yochum et al., 2017). In the Magra River in northern Tuscany study reaches widened from 3% to 90% after a large flood (Nardi & Rinaldi, 2015). Aerial photographs reveal widening of creeks in the Eel River in Northern California in response to two major peak flow events in 1955 and 1964 (Sloan et al., 2001).

Large floods may also increase sediment storage within the river channel. In a long term study at Carnation Creek, British Columbia, flows produced complex patterns of change in sediment storage, but not all large changes in storage were associated with major peak flow events (Reid et al., 2019). A study of low-flow LiDAR DEMs in the Chehalis river basin in Washington revealed a response to a 500-year flood marked by an increase in bar storage in the higher elevation headwater reaches (Nelson & Dubé, 2016). In each of the above examples, a large flood measurably altered stream morphology, but responses varied over space and time.

While flood effects can impact rivers over the decadal time scale, long term studies of floods in mountain rivers are rare due to the cost and effort involved in data collection and the unpredictability of extreme events. Only a handful of studies combine long term and simultaneous monitoring of several geomorphic parameters before and after fluvial disturbance. These include studies at the HJ Andrews Experimental Forest (Faustini, 2000; Faustini & Jones, 2003; Nakamura & Swanson, 1993), Redwood Creek in Northern California's Franciscan Complex (Madej, 1999, 2009; Madej & Ozaki, 1996), the Toutle River drainage at Mt. St. Helens (Major et al., 2019; D. F. Meyer et al., 1985), and Carnation Creek on Vancouver Island (Hartman & Scrivener, 1993; Reid et al., 2019). Each of these studies has revealed different patterns of disturbance response ranging from multidecadal adjustments at the Toutle River (Zheng et al., 2014) to cyclical interannual adjustments at Carnation Creek (Reid et al., 2019).

Other studies that examine change over long time scales utilize pre-existing long term data sets that provide limited geomorphic information such as 2D aerial photographs (Krapesch et al., 2011; Nardi & Rinaldi, 2015; Surian et al., 2016; Thompson et al., 2016; Wallick et al., 2012; Yochum et al., 2017) or the shifting stage-discharge relationships at established stream gages (Anderson & Konrad, 2019; Klingeman, 1973; Pfeiffer et al., 2019; Wallick et al., 2012).

Yet examining the response of only a single variable, such as channel width obscures the complex patterns of fluvial adjustment between depth, width, grain size distribution, and sediment supply (Major et al., 2019). Long term field data that collects multiple geomorphic variables is then poised to fill in these information gaps in our understanding of infrequent events.

In this study, we investigated geomorphic adjustment based on long term data in a mountain watershed in the Oregon Cascades. The data set includes 17 years before and 16 years after the flood of record that occurred in February 1996. This site resembles many other forested steep volcanic western watersheds of the Pacific Northwest and benefits from a long period of monitoring before the major flood event. We investigate how channel adjustment was related to peak flows over 33 years. We explore how the 1996 flood and smaller events over the subsequent 16 years influenced channel form, sediment storage, and bed particle size via effects of hydraulic processes in four reaches and how that adjustment varied between reaches with contrasting settings in terms of slope, watershed area, valley confinement, wood loading, and local mass-wasting. We compare how channels in 2011 (at the end of active monitoring) were similar to or different from 1996 with respect to channel geometry, sediment storage, and bed surface texture. We also investigate how the changes vary within two reaches (Lower and Middle Lookout) with along-stream variation in confining features, wood loading, and channel curvature.

2. Site Description

The study was conducted in the HJ Andrews Experimental Forest located on the western slope of the Cascade Range, Oregon, USA. The Andrews Forest contains the entire drainage basin of Lookout Creek, a 64 km², 5th order mountain stream (Figure 1). The Andrews Forest has been managed since 1948 for ecological and forestry research and has been an NSF-funded Long-Term Ecological Research (LTER) since 1980.

Elevation in the Andrews Forest ranges from 410 m to 1,630 m (Spies, 2016). Geology consists of Miocene to Pleistocene volcanic and volcanoclastic material (Priest et al., 1988; Swanson & James, 1975). Climate is marine temperate with mean annual precipitation ranging

from 2200 to 2700 mm and with a mean annual temperature of 9 °C (Bierlmaier, 1989; Jones & Perkins, 2010). Approximately 80% of precipitation falls between October and April, and streamflow is greatest between November and June (Figure A.1). Dominant tree species within the experimental forest are Western hemlock (*Tsuga heterophylla*), Douglas fir (*Pseudotsuga menziesii*), Pacific Silver Fir (*Abies amabilis*), Western red cedar (*Thuja plicata*), and Bigleaf maple (*Acer macrophyllum*). Experimental logging was conducted in the forest (22% of total area) from 1949 to 1991, and a network of logging and access roads was developed to facilitate both logging and research activities. However, no major logging operations have occurred since 1991 (Jones & Grant, 1996). Remnant old growth (~500 years since disturbance) covers 40% of the forest (Swanson & Jones, 2002). The study was conducted in four, 212–450-meter reaches where stream cross-sections were established in 1978 and have been resurveyed at varying intervals up to 2011 (Table 1).

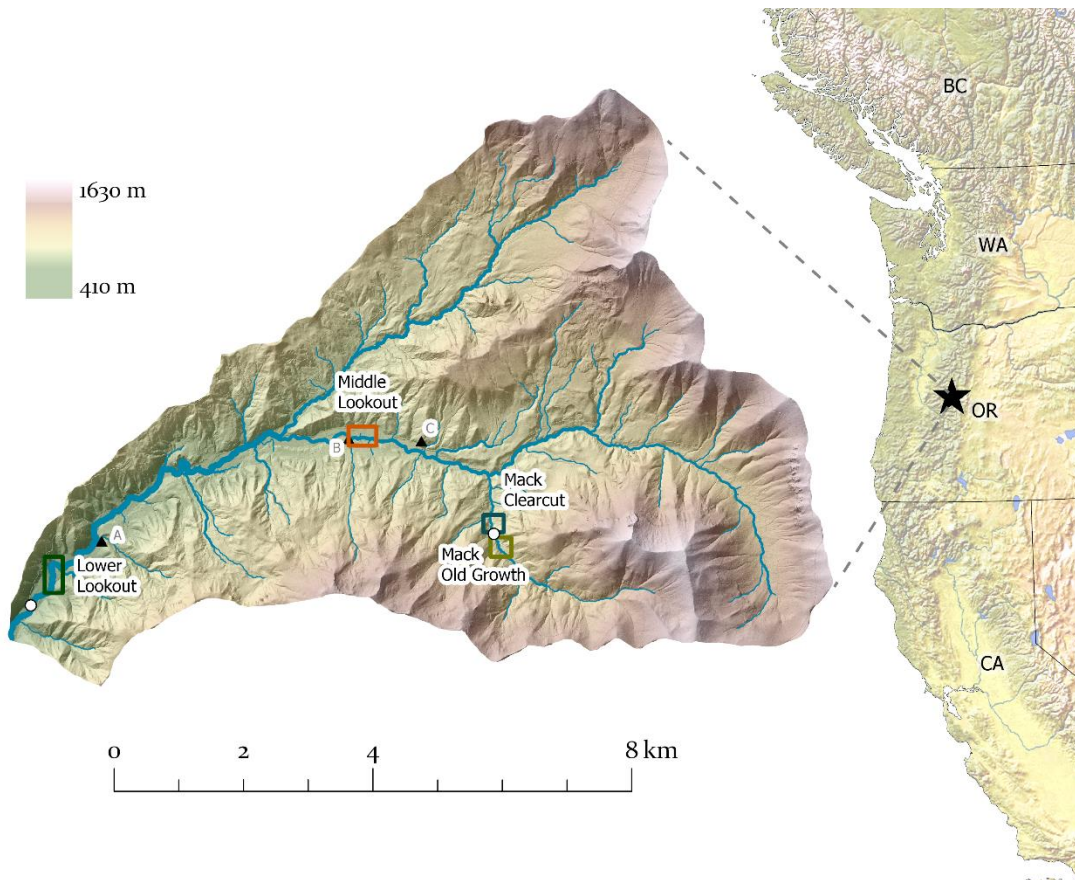


Figure 1 Shaded relief map of the Lookout Creek watershed and location within the Oregon Cascades. Study reaches are shown in boxes: dark green (Lower Lookout Creek), orange

(Middle Lookout Creek), dark blue (Mack Clearcut Reach), and olive green (Mack Old Growth Reach). White circles show selected stream gage sites: Lookout Creek (left) and Mack Creek (right). Locations of large landslide or debris flows near study reaches are shown as black triangles A, B and C. Stream network is shown as blue lines. The widths of the streams are exaggerated to show detail and do not map directly onto their true width on the landscape.

In February of 1996, a warm, wet Pacific storm induced widespread flooding in the Pacific Northwest affecting the study reaches. The storm was preceded by heavy snowfall at relatively low elevations in the Cascade Mountains. Sensible and latent heat exchange from the storm melted the snow, generating up to 3.6 meters of runoff in only a few days (Marks et al., 1998). Robison et al. (1999) documented widespread landsliding in Oregon forested lands following the 1996 flood, with substantial impacts (field-observed torrent scour and depositional features) on streams.

Snowpack conditions at the start of the storm varied across the Andrews Forest's nearly 1250-meter elevation gradient, which produced a complex, spatially heterogeneous runoff response as snow variously stored and released water. Forest practices also modulated the flood response — peak flows were greater in harvested watersheds than in old growth forest (Dyrness et al., 1996; Swanson et al., 1998). The February storm of 1996 induced the flood of record in the Lookout Creek watershed, with the Lookout Creek gage (Figure 1) recording a peak discharge of 227 m³/s, nearly four times greater than the mean annual peak discharge of 58 m³/s and 1.2 as great as the previous flood of record of 189 m³/s in 1964 (Johnson et al., 2019). Within the experimental forest, the storm initiated 36 debris slides with volumes greater than 75m³, sixteen of which generated debris flows into stream channels (Johnson et al., 1997; Swanson et al., 1998). About 60% of debris flows of any size entered 4th and 5th order channels within the Blue River Watershed which contains the HJ Andrews Forest (Nakamura et al., 2000).

Debris flows occur infrequently in the Blue River watershed. Between 1946 and 1996, 91% of all inventoried debris flows (83 out of 91 total) in the watershed occurred in just two water years, Water Year 1965 (which includes December 1964) and Water Year 1996 (Snyder, 2000). This rarity places the 1996 flood uniquely in the historical record. The 1996 storm represented the first major landsliding event in two decades (Dyrness et al., 1996) and although it produced fewer debris flows overall than the storm of 1964 (Snyder, 2000), it still produced

notable effects (Dyrness et al., 1996; Johnson et al., 2000; Nakamura et al., 2000; Swanson et al., 1998; Wemple et al., 2001). A portion of the debris flows were associated with road features on the landscape (Snyder, 2000; Wemple et al., 2001).

Channels influenced by debris flows experienced severe disturbance of the riparian forest (Johnson et al., 2000; Nakamura et al., 2000; Swanson et al., 1998). Dyrness et al. (1996) report that a large debris flows several meters thick removed riparian growth and scoured alluvium from Watershed 03, and the debris flow in Watershed 10 damaged the gaging station. In the storm's rapid, sediment-laden flows, Lookout Creek, a 5th order stream, transported boulders for at least 24 hours and relocated large wood pieces up to 30 m in length. Floodplain disturbance also occurred through the mechanism of lateral channel change (Swanson et al., 1998). The width of the flood's high energy zones varied among streams within the Andrews Forest and nearby watersheds, and the flood generally caused a decrease in the amount of instream large wood within higher order streams (Johnson et al., 2000). Johnson et al. (2000) found evidence for congested transport as well as uncongested (piecewise) transport of wood in the streams, with congested transport generally associated with debris flows. Widespread wood transport was not observed at the lower order and higher-elevation Mack Creek (Dyrness et al., 1996), where wood plays an key role in stabilizing the stream's step-pool morphology (Faustini & Jones, 2003).

This study focuses on four stream reaches within the Andrews Forest (Table 1, Figure 2). Lower Lookout (LOL, Figure 2a) is a 440-meter reach draining 62 km² with a gradient of 1.5% and valley width of 40 to 100 m (Table 1). A mid-channel bar lies near the center of the reach between cross sections LOL05 and LOL08 (check). Historic maps (Faustini, 2000; Nakamura & Swanson, 1993) show that the low-flow channel has variously occupied the right (west) side of the channel and left (east) side of the channel over time (Figure 3, Figure A.2). The placement and volume of instream wood has also varied over time (Figure 3). Debris flows from a small watershed (Watershed 03) 0.8 km upstream entered this reach during the flood of 1996 (Figure 1, point A)(Snyder, 2000; Swanson, 2014). A stream gage (USGS 14161500) located 0.5 km downstream of this reach provides a record from 1949 to the present (Johnson et al., 2019).

Middle Lookout Creek (LOM, Figure 2b) is a 295-meter reach draining 32 km² with gradient of 3.2% in a broad, 200–305 m, unconfined valley. The valley contains alluvial fill deposited in response to an earthflow-induced base level change that began at least 7,000 years

ago (Swanson & James, 1975). A persistent channel-spanning logjam has occupied the lower part of the reach potentially as early as the 1960s, and a bar-anchored logjam was emplaced in 1996. In 1996, a large debris flow entered the main channel approximately 100 m downstream of the bottom of this reach (Figure 1, point B) (Snyder 2000, Swanson 2014). A moderate-sized (336 m³ in volume) valley wall landslide occurred 0.8 km upstream of the top of the reach in 1996 (Figure 1, point C)(Snyder, 2000; Swanson, 2014).

Mack Clearcut (MCC, Figure 2c) is a 220-meter reach draining 5.9 km² with a 9.6% grade in a steep-sided 20 to 40 m-wide, steep V-shaped valley. The slopes adjacent to this reach were clearcut in the early 1960s and yarded (wood removed) in the winter of 1964-1965 (Swanson et al., 1976). Logging-related wood removal dramatically decreased instream wood density through at least 1997, and step features within this reach are associated with large boulders rather than wood pieces or wood-boulder structures (Faustini & Jones, 2003). A stream gage located between MCC and MAC provides a record from 1980 to present (Johnson et al., 2019).

Mack Old Growth (MAC, Figure 2d) is a 212-meter reach draining 5.6 km² with a gradient of 10% confined within a 15 to 50 m-wide, steep-sided V-shaped valley. The vegetation is ~500-year-old forest. No debris flows or major landslides have been inventoried near either of the two Mack Creek reaches (Swanson, 2014).

Table 1: Characteristics of the four study reaches, reproduced in part from Faustini (2000), with the addition of valley widths and presence or absence of debris flows. Slopes represent historical field measurements. Drainage areas, elevations, at lower end, and reach lengths were recalculated using a LiDAR-derived DEM (Andrews Forest, unpublished data set) Valley widths were delineated by hand in considering previous valley mapping (Grant & Swanson, 1995).

Reach Name	Lower Lookout	Middle Lookout	Mack Clearcut	Mack Old Growth
Reach Code	LOL	LOM	MCC	MAC
Number of cross sections	14	11	20	12
Drainage area (km ²)	62.0	31.8	5.9	5.7
Elevation at lower end	428	583	730	764
Mean channel gradient (m/m)	0.015	0.032	0.096	0.1
Mean channel width (m)	27.3	24.7	10.7	13
Reach length (m)	440	295	220	212

Mean valley width (m)	66	235	28	31
Mass movements > 150 m ³ observed within 1 km upstream of reach 1996	Debris flow	Slide (~336 m ²)	None	None
Mass movements > 150 m ³ observed within 1 km downstream of reach 1996	None	Debris flow	None	None

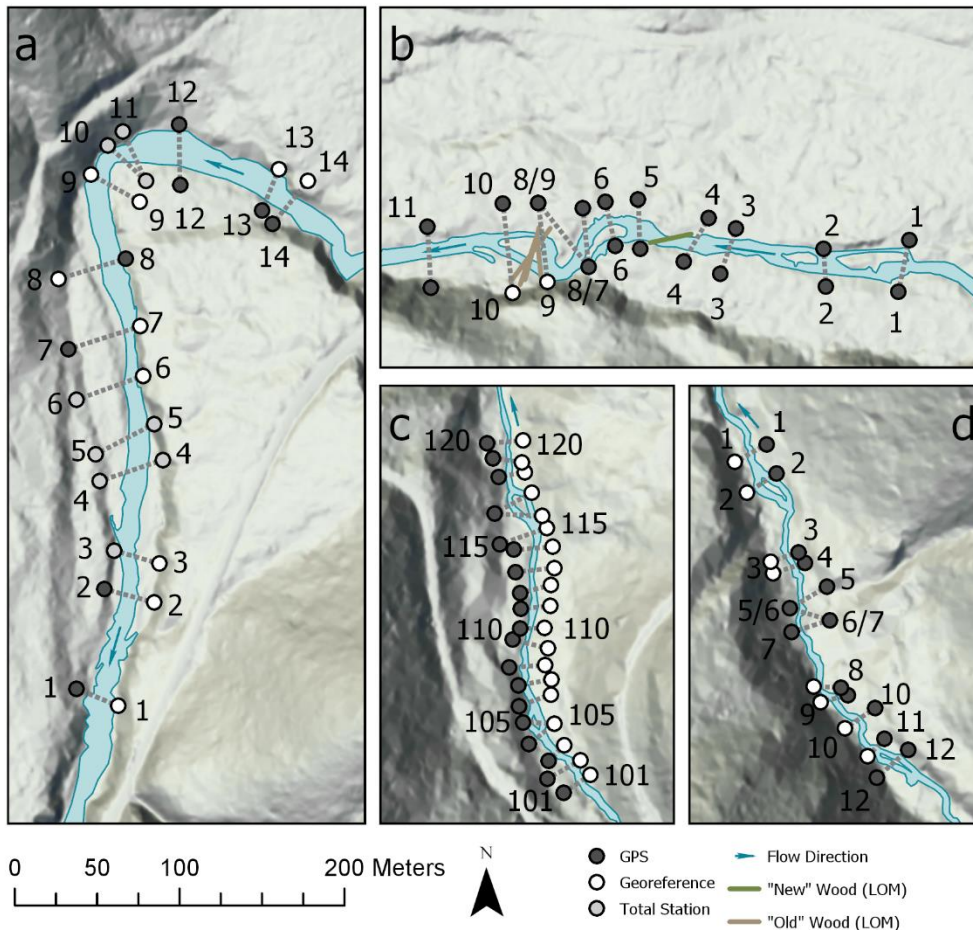


Figure 2: Maps of the four study reaches: (a) Lower Lookout, LOL, (b) Middle Lookout, LOM, (c) Mack Clearcut, MCC, and (d) Mack Old Growth, MAC. Endposts, represented by dots, are shaded according to the method used to survey their locations. Blue arrows indicate flow direction. Brown lines represent the location of a channel-spanning wood jam in Middle Lookout dated to prior to 1996 that accumulated additional wood in the 1996 flood. Green lines represent the location of an additional bar-anchored wood jam in Middle Lookout that was formed during the 1996 flood upstream of the older jam (Faustini, 2000). Wood in Lower Lookout is shown in Figure 3. Wood in Mack Old Growth and Mack Clearcut is mapped in (Faustini & Jones, 2003).

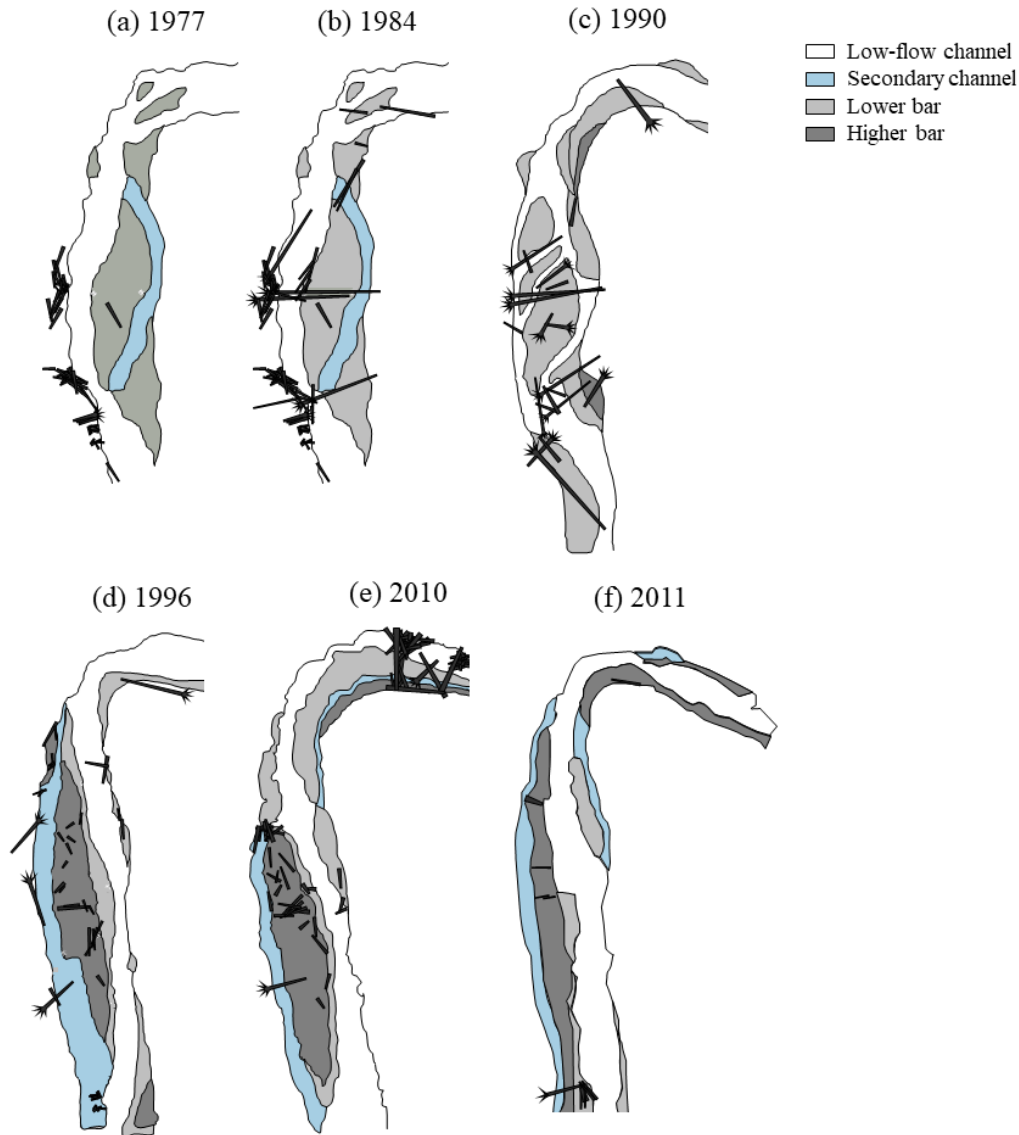


Figure 3: Wood and channel locations in Lower Lookout over time, adapted from unpublished figure produced by Jung-il Seo. Wood locations are shown as thick black lines. Low-flow channel locations are shown in white. Secondary channel locations are shown in light blue. Lower and higher bars are shown in light and dark gray, respectively. Map sources: (a) George Lienkaemper (unpublished); (b) George Lienkaemper (unpublished); (c) Futoshi Nakamura (Nakamura & Swanson, 1993); (d) John Faustini (Faustini, 2000); (e) Jung-il Seo & Kristin Kirkby (unpublished) (f) (unpublished). The flood of 1996 moved large wood pieces out of the middle of the reach and caused the relocation of the low-flow channel to the left (east) bank near the location of the displaced wood.

3. Methods

3.1. Field Data Collection

1.1.1. Cross-Sectional Surveys (1978–2011)

Eleven to twenty cross sections were established in each of four stream reaches within the HJ Andrews Experimental Forest between 1978 and 1981 (Johnson & Swanson, 2014) (Table 1, Figure 2). Cross section endpoints were marked with steel fence posts to allow for measurement of the same locations each year. End-posts that were lost to bank erosion between surveys were replaced by a secondary post placed along the same bearing as the original cross-section. During most survey years, all cross-sections in every reach were surveyed. However, a subset (18%–45%) of cross-sections were sampled within each reach at Lower Lookout from 2001–2004 and 2007–2009, at Middle Lookout in 1980, from 2001–2004, and 2007, and at Mack Clearcut in 1983 (Table A.1).

Cross sections were surveyed using a tape, stadia rod, and auto-level at 0.5 m intervals every 1 to 6 years during the summer low-flow season up until 2011. Additional survey points were collected at breaks in slope or changes in bed or bank surface material. Survey information at each point within each cross section consist of an X-coordinate, a Z-coordinate, and a “substrate class” with the X-coordinate representing horizontal distance from the right bank, the Z-coordinate representing the vertical distance above or below an arbitrary datum defined by the ground surface elevation at the right bank of each cross section, and the substrate class representing the general size and type of bed surface, bank surface, or suspended material found at that point (Table A.2). In this analysis, survey points representing features above the bed surface or banks of the stream (e.g., suspended logs) were excluded (Table A.2).

3.1.1. Wolman Pebble Counts (1995–2011)

Pebble counts (Wolman, 1954) with 100 particles were conducted at all surveyed cross sections from 1995 to 2011, except in two cases where the stream bed was not safely accessible due to streamflow conditions or logjam placement. (Table A.1). Particles were sampled within the active channel boundaries in a swath approximately one meter upstream and downstream of

the survey tape. Surveyors traversed the swath, taking one measurement for each step, until they had collected 100 diameters. In cross-sections that were too deep to wade, pebble counts were conducted by a snorkeler. Pebble counts were conducted separately from and did not include the categorical “substrate class” information taken at every survey point.

1.1.2. Real Time Kinematic (RTK) GPS Endpoint Surveys (2019)

Cross section end-posts were surveyed with a Real Time Kinematic (RTK) GPS (Leica GS14/CS15, Leica Geosystems) in the summer of 2019 and post-processed using Leica Infinity software using data from nearby base stations. Horizontal coordinates for the cross section endposts had not been recorded for all sites during prior field surveys; endpost coordinates allowed for the measurement of distances between pairs of cross sections and between cross sections and landscape features. Each end-post was surveyed for a minimum of five minutes or 300 observations. Additional surveys were conducted in Lower Lookout Creek with a total station (Nikon Nivo 5.C, Nikon-Trimble Co.). Total station data were rotated and shifted using a set of collocated GPS data to produce UTM coordinates. Surveyors did not to locate or access 36% of cross-section end-posts in 2019, but at least one end-post was surveyed for each cross section. Locations of missing end-posts were estimated by georeferencing historic maps to the GPS survey coordinates (Figure 2).

3.2. Cross section data adjustment and profile interpolation

3.2.1. Data Adjustment and Interpolation

Manual cross section data collection is sensitive to three common error types: (1) whole-number survey errors, (2) horizontal distortion, and (3) vertical datum shifts as described in Faustini (2000). We inspected and corrected cross section data for these errors prior to analysis. Individual point measurements may be exactly one or two meters above or below the true value if a surveyor was unable to see the meter-mark on the survey equipment. These errors appear as abrupt spikes in a cross-sectional profile, and they were corrected with a whole-integer correction factor. Horizontal distortion of survey data may occur due to improper tension or alignment of the survey tape. These errors appear as misalignment of cross-sectional end-posts

and bedrock features between survey years. These errors were corrected with a horizontal multiplier and/or a horizontal shift factor. Horizontal multipliers were estimated by dividing the total cross-sectional length of a correctly aligned survey in preceding and following years by the total cross-sectional length of the misaligned survey. Shift factors were estimated by subtracting the x-coordinate of the misaligned endposts from the X-coordinate of the same endposts in different years. Both correction factors were checked by eye for every survey year and manually adjusted until cross-section endposts and hard features appeared to align between survey years. Because the vertical datum (0-elevation) of each survey is determined the local ground surface elevation at the right-bank end-post, hillslope soil movement near the end-post can alter Z-coordinates from year to year. To correct for these datum shifts, measurements from different years were manually aligned based on shared features.

Data collected in 1999 or later were manually corrected by the author using the above methods, and data collected prior to 1999 were corrected by John Faustini using similar methods (Faustini, 2000). Points from each cross-sectional profile for each year were filtered to include only ground surface points (Table A.2). Cross sections that appeared poorly aligned, incompletely surveyed, or cross sections that were surveyed over a period of less than 10 years, were excluded from analysis (Table A.3).

3.3. GIS-derived landscape attributes

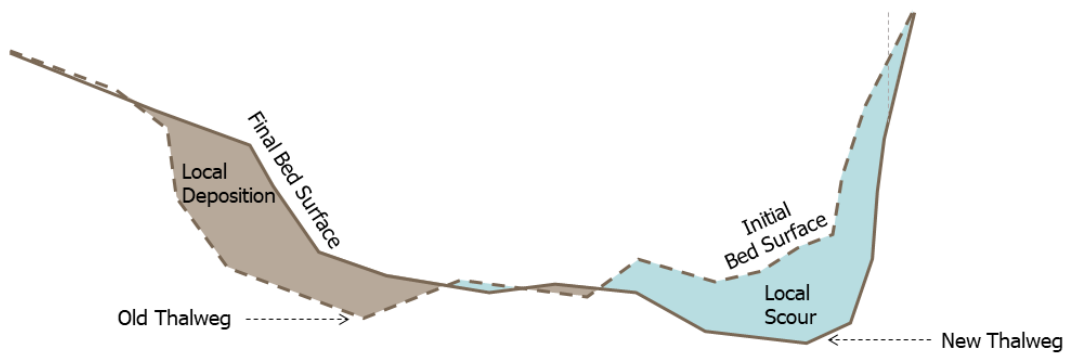
Various landscape and channel attributes were measured from a LiDAR-derived DEM (Andrews Forest, unpublished data set). Valleys were delineated by hand in ArcGIS Pro, considering previous valley delineation (Grant & Swanson, 1995). The downstream elevation of each reach was defined as the elevation of the stream bed at the most downstream cross section. Drainage areas were calculated using pour points at the downstream ends of each reach. The downstream distance value for each cross section was defined as the horizontal, along-stream distance of the cross section's midpoint to the midpoint of the most upstream cross section within each reach.

3.4. Derived scour/deposition metrics

Cross-sectional areas of scour and deposition were calculated at each cross section between every pair of survey-years (Figure 4a), (Leopold & Maddock, 1953). We calculated the

total reworked cross-sectional area as the sum of the eroded and deposited areas. We calculated net depositional area (“net deposition”) as the difference in area between the depositional areas and the scoured areas (Figure 4). We also calculated the change in the thalweg elevation at each cross section between every pair of survey-years. The thalweg was defined as the lowest point in each cross section.

a



b

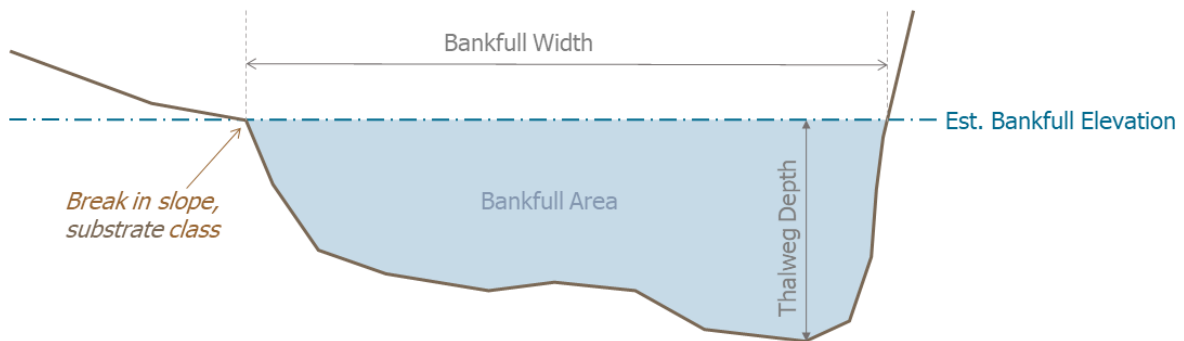


Figure 4 (a) Conceptual diagram showing areas of scour (blue areas) and deposition (brown areas) and thalweg change at one cross section between two years. (b) Conceptual diagram showing derived bankfull properties of a cross section at the second of those two years. Estimated bankfull elevation is shown as a blue dotted line. Bankfull elevation was estimated based on the location of breaks in slope and substrate size information. Thalweg depth is the vertical distance between the bankfull elevation and the lowest point of the cross section. Bankfull area is the area between the bankfull elevation and the bottom of the channel.

3.5. Derived hydraulic geometry metrics

3.5.1. Bankfull elevation

Bankfull elevations were identified as survey points that represented breaks in slope and persistent changes in substrate class (Figure 4b) (Bunte & Abt, 2001; Dunne & Leopold, 1979; Harrelson et al., 1994). For example, a persistent change in substrate class from soil on the uphill side to gravel on the downhill side of a point might be associated with the bankfull elevation. When there were multiple plausible candidates for bankfull elevation at a given cross section in a given year, we selected points that minimized year-to-year changes in bankfull elevation.

3.5.2. Bankfull channel geometry

Cross sectional area was calculated as the channel area between the bed surface and the bankfull elevation line (Figure 4b). Bankfull width was calculated as the sum of the width of the parts of the channel that were submerged between at least 5 cm below the bankfull elevation line. Channel depth was defined as bankfull area divided by bankfull width. Thalweg depth was defined as the vertical difference between bankfull water surface elevation and the lowest point in the cross-sectional profile (Figure 4). To facilitate comparison between different cross sections, we normalized cross sectional geometry each year by the values observed at the same cross section in 1995, hence channel changes were expressed as both a ratio relative to 1995 and a difference relative to 1995.

2. Derived sediment transport metrics

3.5.3. Grain size statistics

We calculated grain size statistics for each pebble count. We calculated D_n as the n^{th} percentile grain size and phi values:

$$\phi_n = -\log_2 \frac{D_n}{1 \text{ mm}} \quad (1)$$

D_{50} represents the median grain size and ϕ_{50} is the negative base-2 log of the median grain size in mm. We calculated a sorting metric (Folk & Ward, 1957):

$$\sigma_\phi = \frac{\phi_{84} - \phi_{16}}{4} + \frac{\phi_{95} - \phi_5}{6.6} \quad (2)$$

where, ϕ_{95} , ϕ_{84} , ϕ_{16} , and ϕ_5 represent phi values of the 95th, 84th, 16th, and 5th percentile grain sizes, respectively. Lower values of σ_ϕ represent a better-sorted substrate.

3.5.4. Sediment Transport

We calculated the bankfull boundary shear stress, τ , assuming uniform flow at each cross section:

$$\tau = ghS\rho \quad (3)$$

where g is acceleration due to gravity, h is bankfull channel depth, S is the reach-averaged slope as measured in the field in 1996 (Table 1), and ρ is the water density (1,000 kg/m³). We calculated the non-dimensional Shields stress, τ^* :

$$\tau^* = \frac{\tau}{(\rho_g - \rho)gD_{50}} \quad (4)$$

where ρ_g is the sediment density. We assumed the density of quartz (Buffington & Montgomery, 1997) of 2,650 kg/m³.

3.6. Statistical Analysis

We calculated return interval and area-normalized peak discharge for each year between 1978 and 2011. We used the Lookout Creek for Lower Lookout Creek and Middle Lookout Creek and the Mack Creek gage for Mack Clearcut and Mack Old Growth (Figure 1). At each site, linear regressions were fitted to predict reach-wise net deposition and total reworked cross-sectional area (dependent variables) as functions of either return interval or area-normalized discharge (independent variables). To investigate the sensitivity of each regression to the peak discharge event of 1996, regression models were fitted by Ordinary Least Squares (OLS) both with and without the 1995-1996 cross-sectional change data. Regressions included only those years in which at least 75% of cross sections were sampled in each reach (Table A.1).

4. Results

4.1. Peak flows between 1980 and 2011 and channel change and over time

At Lookout Creek, the peak flow of the 1996 flood was 290% greater than the mean annual peak flow recorded between water years 1950 and 2018. The peak flow was 20% greater than the second greatest annual peak flow on record (recorded in December 1964 [water year 1965]) and 70% greater than the second greatest annual peak flow that occurred within this study period (recorded in 2011, Figure 5). At Mack Creek the peak flow was 80% greater than the mean annual peak flow recorded between water years 1980 and 2018. The peak flow at Mack Creek was 2% greater than the second greatest annual peak flow, which was recorded in 2000. The second largest flow occurred in 2011 at Lookout Creek (120% greater than mean annual peak flow) and in 2000 at Mack Creek (70% greater than mean annual peak flow, Figure 5).

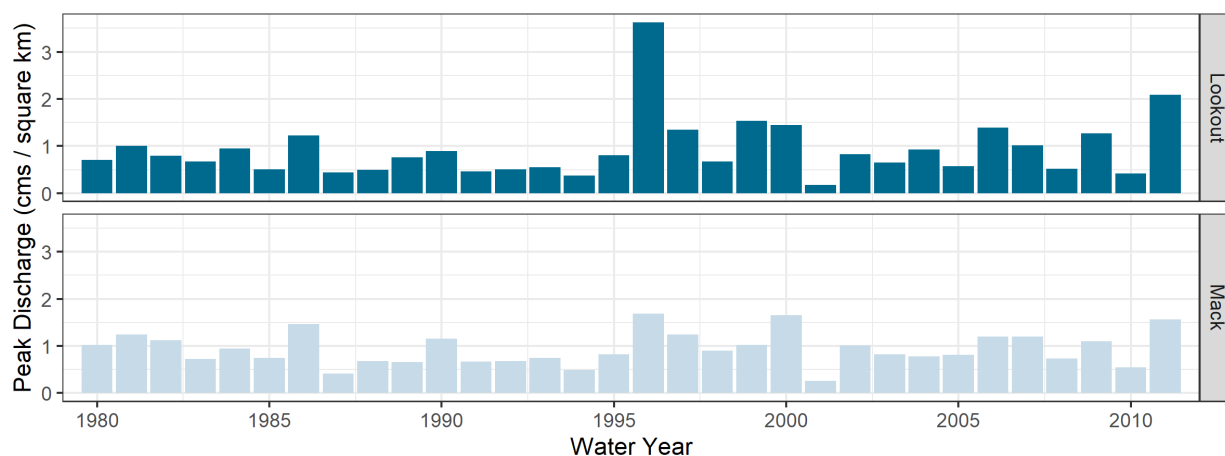


Figure 5: Time series of annual peak flows at the Lookout Creek and Mack Creek gages from Water Year 1980 to Water Year 2011. The greatest annual peak flow at both gages occurred in water year 1996. The second greatest flow within this time period occurred in 2011 at Lookout Creek and in 2000 at Mack Creek. The second greatest flow on record at Lookout Creek occurred in Water Year 1965 (December 1964).

Channel response in terms of reworked cross-sectional area paralleled peak flow magnitude at all sites. At Lower Lookout, the greatest reworked cross-sectional areas were observed between 1995 and 1996 and the second greatest were observed between 2006 and 2011. At Middle Lookout, the greatest reworked cross-sectional areas were observed between 1995 and 1996 and the second greatest were observed between 1999 and 2001. At Mack Old Growth, the greatest reworked cross-sectional areas were observed between 1995 and 1996 and the second greatest were observed between 2005 and 2011. At Mack Clearcut, the greatest reworked cross-sectional areas were observed between 1995 and 1996 and the second greatest were observed between 2005 and 2011 (Figure 6).

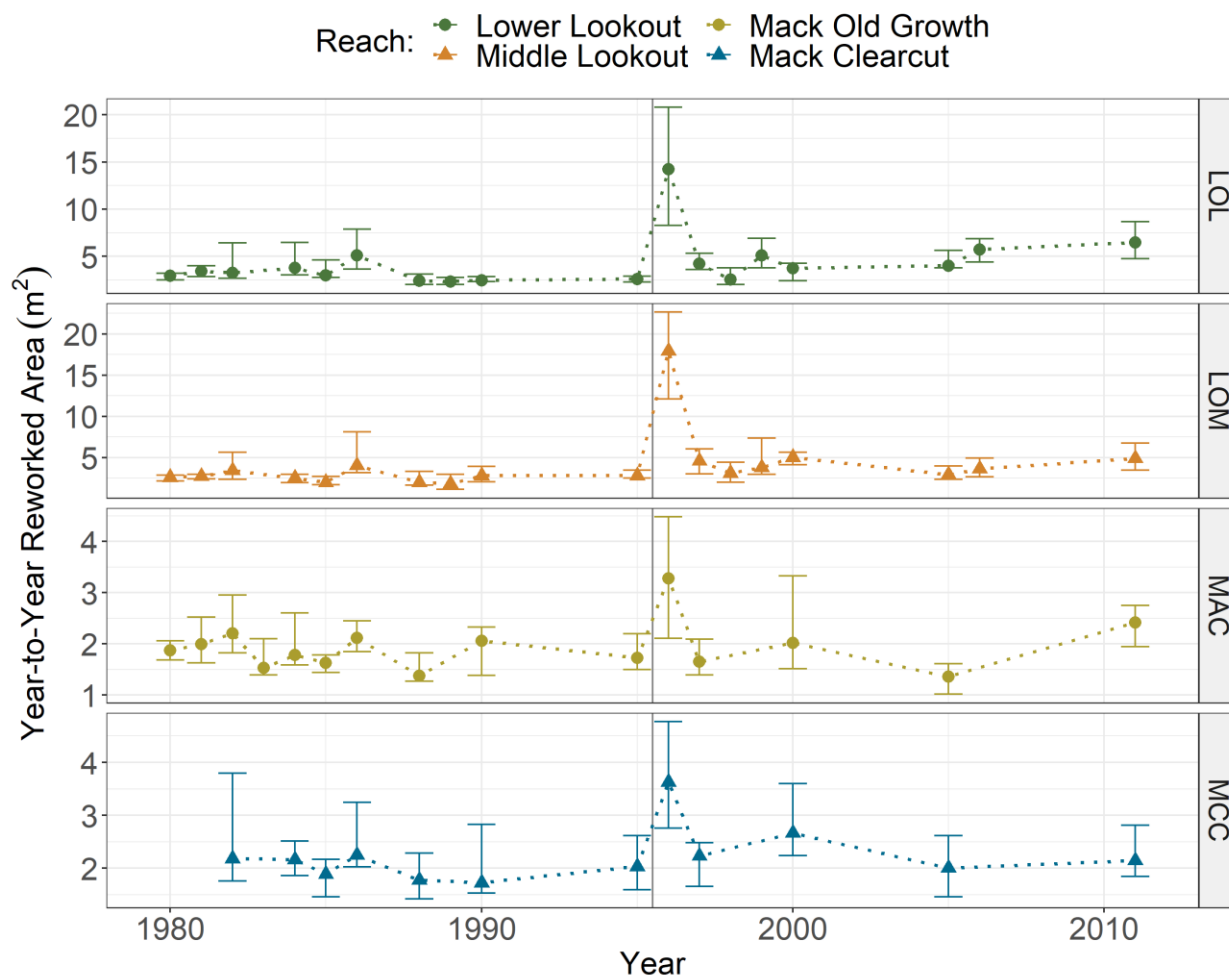


Figure 6: Median (dots) and interquartile range (bars) of year-to-year reworked cross-sectional area. Reaches experienced the most change between 1995 and 1996. The black vertical line shows the 1996 flood.

4.2. Relationship between peak flow and geomorphic response

Excluding data from 1996, reworked cross-sectional area (i.e., scoured plus deposited areas) was positively related to peak flood magnitude at three of the four reaches (Figure 7, Table 2, $R^2 = 0.38\text{--}0.57$, $p < 0.05$). Including values from 1996, linear regression yields stronger relationships (Figure 7, Table 2, $R^2 = 0.39\text{--}0.86$, $p < 0.05$). However, since the flood of 1996 was substantially larger than the next largest peak flow at Lookout creek, the 1996 data exerts substantial leverage on the overall fit of the regression (Figure 7). Residuals are not normally or evenly distributed in regressions including 1996 as they are in regressions excluding that year.

Table 2: Summary of R^2 values for the best-fit relationship between peak discharge and mean reworked cross-sectional area for each reach, including and excluding data from the 1995–1996 period. Asterisks denote $p < 0.05$.

Reach	R^2 including 1996	p -value including 1996	R^2 excluding 1996	p -value excluding 1996
Lower Lookout	0.82*	2.5×10^{-7}	0.42*	4.6×10^{-3}
Middle Lookout	0.86*	2.4×10^{-8}	0.57*	4.9×10^{-4}
Mack Old Growth	0.39*	1.2×10^{-2}	0.24	7.7×10^{-2}
Mack Clearcut	0.51*	9.2×10^{-3}	0.44*	2.7×10^{-2}

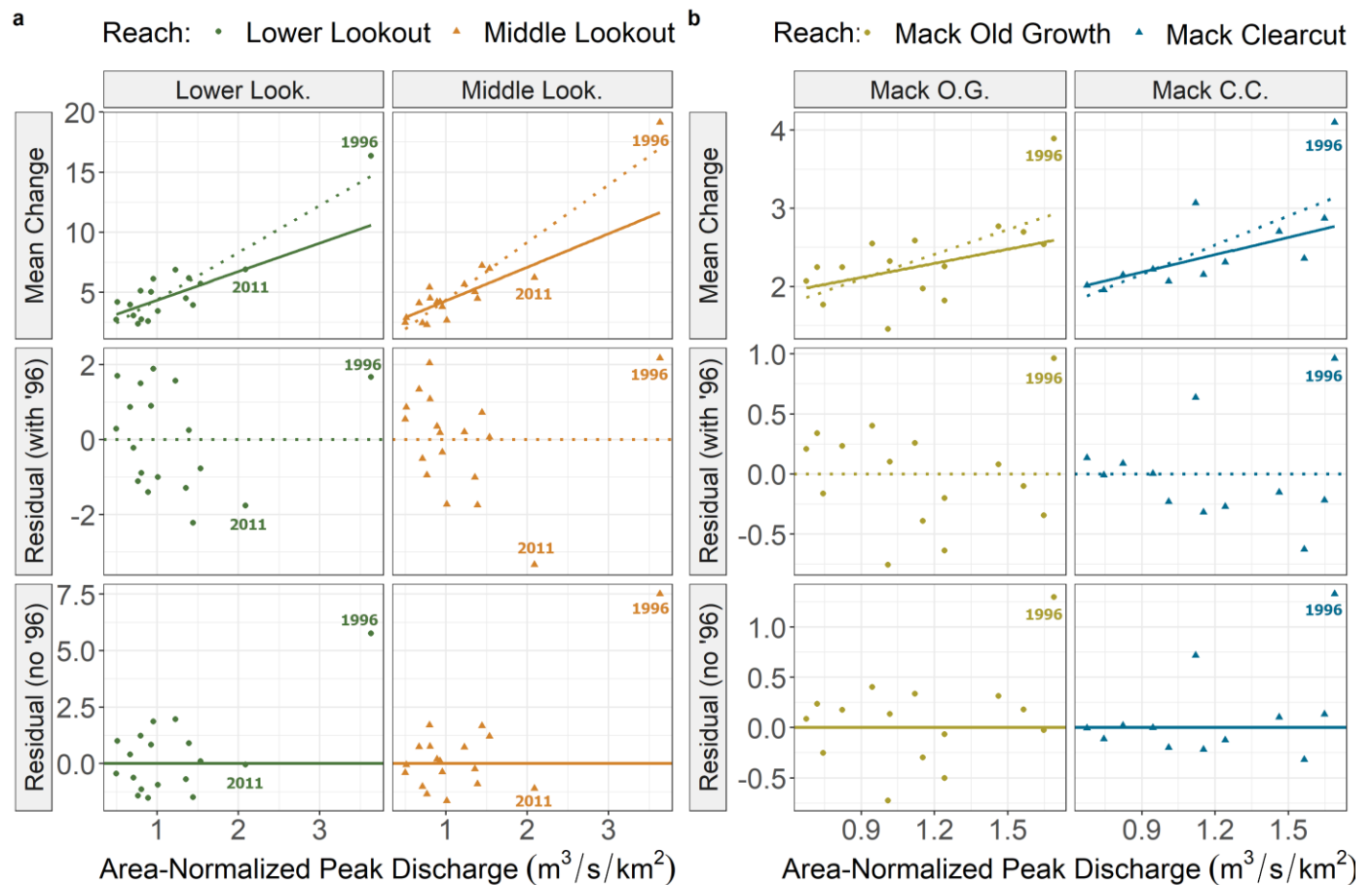


Figure 7: (a) Top row: total reworked channel area (i.e., area eroded plus area deposited) versus peak discharge for two reaches in Lookout Creek. Dashed lines represent linear regression including 1996. Solid lines represent linear regression excluding 1996. Middle and bottom rows: Residuals for each regression are shown in the second and third rows respectively. Residuals from the regression that included 1996 were not evenly distributed. Markers from 1996 and 2011 are labeled. All y-axis values are in m^2 . (b) Top row: total reworked channel

area (i.e., area eroded plus area deposited) versus peak discharge for two reaches in Mack Creek. Dashed lines represent linear regression including 1996. Solid lines represent linear regression excluding 1996. Middle and bottom rows: Residuals for each regression are shown in the second and third rows respectively. Markers from 1996 are labeled. All y-axis values are in m^2 .

The total reworked channel area in 1996 exceeded the value predicted by linear regression at all four reaches (Figure 7), regardless of whether or not the 1996 data were included in the regression. The regression that omitted 1996 resulted in a large positive residual for that year (Figure 7), at all four reaches. This suggests that the large flood of 1996 produced disproportionately greater effects than any moderate flood that occurred during the monitoring period. This residual value was greater in the two Lookout Creek reaches than the Mack Creek reaches, although the area-normalized peak flood magnitude in Lookout Creek was $3.6 \text{ m}^3 \text{ s}^{-1} \text{ km}^{-2}$ compared to $1.7 \text{ m}^3 \text{ s}^{-1} \text{ km}^{-2}$ in Mack Creek (Figure 5, Figure A.1).

Excluding data from 1996, reworked channel area was also positively related to peak flood return interval at Lower Lookout and Middle Lookout (Table 3, $R^2 = 0.35\text{--}0.46$, $p < 0.05$). Including data from 1996 yielded a positive relationship at all four reaches (Table 3, Figure A.4, $R^2 = 0.66\text{--}0.91$, $p < 0.05$). However, the 1996 data point exerts even more leverage on the overall fit in this regression for several reaches, and regressions that included this year did not have evenly or normally distributed residuals.

Table 3: Summary of R^2 values for the best-fit relationship between return interval and mean reworked cross-sectional area (i.e., area eroded plus area deposited) for each reach, including and excluding data from the 1995–1996 period. Asterisks denote $p < 0.05$.

	R^2 including 1996	p -value including 1996	R^2 excluding 1996	p -value excluding 1996
Lower Lookout	0.86*	3.4×10^{-8}	0.35*	1.2×10^{-2}
Middle Lookout	0.91*	8.3×10^{-10}	0.46*	2.8×10^{-3}
Mack Old Growth	0.66*	2.4×10^{-4}	0.23	8.0×10^{-2}
Mack Clearcut	0.77*	1.6×10^{-4}	0.35	5.3×10^{-2}

Excluding data from 1996, flood magnitude was not related to net depositional on a reach scale at any reach ($R^2 < 0.08$, $p > 0.4$, Table 4). That is, while flood magnitude might be somewhat predictive of reworked channel area, it is not predictive of whether a stream will scour

or deposit or by how much. Incorporating data from 1996 led to a positive relationship between flood magnitude net deposition only at Lower Lookout and Middle Lookout ($R^2 = 0.27\text{--}0.50$, $p < 0.05$, Table 4).

Table 4: Summary of R^2 values for the best-fit relationship between return interval and net depositional for each reach, including and excluding data from the 1995-1996 period. Asterisks denote $p < 0.05$

	R^2 including 1996	p including 1996	R^2 excluding 1996	p excluding 1996
Lower Lookout	0.27*	2.6×10^{-2}	0.03	5.3×10^{-1}
Middle Lookout	0.50*	9.6×10^{-4}	0.03	5.1×10^{-1}
Mack Old Growth	0.08	3.1×10^{-1}	0.02	6.3×10^{-1}
Mack Clearcut	0.02	6.7×10^{-1}	0.07	4.2×10^{-1}

4.3. Reach-scale responses to the 1996 flood

The 1996 flood induced measurable changes in sediment storage, bankfull channel geometry, and channel grain size at all of the study reaches. Channel characteristics changed between 1995 and 1997 in terms of net sediment deposition, channel dimensions (bankfull depth and width and thalweg elevation), and grain size (D_{50} and sediment sorting). We considered 1995–1997 because 1996 appears to have initiated directional changes in some characteristics in each reach that are well-described by comparing those two years. In the majority of cases, there are changes between the two years (Table 5), but the changes varied between reaches. Between 1995 and 1997 Lower Lookout experienced a decrease in net deposition associated with a decrease in thalweg elevation and an overall deeper bankfull channel while its width remained unchanged compared to 1995. Middle Lookout, on the other hand experienced an increase in net deposition associated with an increase in thalweg elevation, and shallower median bankfull depth while its width remained unchanged. Mack Old Growth experienced an increase in net deposition and bankfull width while its thalweg elevation and bankfull depth remained unchanged. Mack Clearcut showed an increase in thalweg elevation while net deposition, bankfull depth, and bankfull width remained the same.

Table 5: Summary of median flood response parameters at each of the four reaches between 1995 and 1997. Each parameter is marked with a +, -, or =, based on whether the median value of each parameter in 1997 moved outside of the 25th–75th percentile range of observed values for 1995.

	Net Deposition	Thalweg Elevation	Bankfull Depth	Bankfull Width	D_{50}	Sorting
Lower Lookout	- (scour)	- (lowered)	+ (deeper)	= (same)	= (same)	- (less)
Middle Lookout	+ (deposit)	+ (raised)	- (less deep)	= (same)	- (finer)	- (less)
Mack Old Growth	+ (deposit)	= (same)	= (same)	+ (wider)	= (same)	= (same)
Mack Clearcut	= (same)	+ (raised)	= (same)	= (same)	+ (coarser)	= (same)

Study reaches varied in their scour or depositional response to the 1996 flood. In the pre-flood period from 1980 to 1995, study reaches showed only minor changes in net deposition. Median values of net deposition in this pre-period ranged from -1.5 m^2 to 0.9 m^2 with an interquartile range of 1.1 m^2 to 6.9 m^2 (Figure 8). Comparison between cross-sectional profiles in 1995 and 1996 indicated that the 1996 flood resulted primarily in sediment deposition in Middle Lookout (deposition at 80% of cross sections, median depositional area 8.3 m^2) while Lower Lookout showed an erosional response (erosion at 65% of cross sections, median scour area of 1.3 m^2). After 1996, Lower Lookout continued to show an erosional response over the next 4 years between 1996 and 2000 (Figure 8). In contrast, the depositional response at Middle Lookout did not continue over the following years. The two Mack Creek reaches also showed an erosional response from 1995 to 1996 (erosion at 75% of cross sections at Mack Old Growth and 60% of cross sections at Mack Clearcut with median erosional area of 1.2 m^2 at both reaches) (Figure 8).

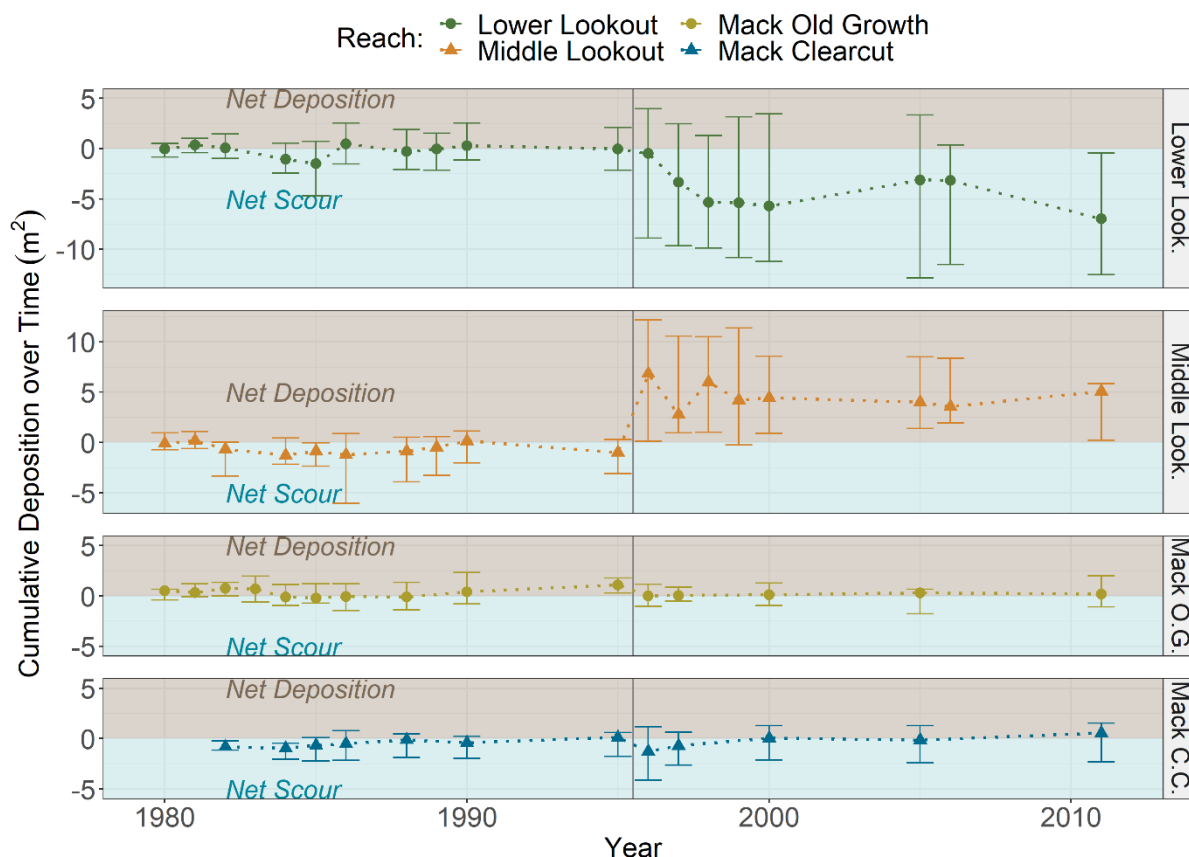


Figure 8: Median (dots) and interquartile range (bars) of cumulative scour and deposition relative to the start of monitoring in 1978 (or 1981 for Mack Clearcut). Points in the brown field (positive values) represent net deposition while points in the blue field (negative values) represent net erosion. Lower Lookout overall eroded while Middle Lookout experienced net deposition. Mack Creek reaches showed little change in median values. The black vertical line shows the 1996 flood.

Thalweg elevations were also characterized by relative stability prior to 1996 followed by rapid change after the 1996 flood. From 1980 to 1995, study reaches showed only minor changes in thalweg elevation. Median values ranged from -0.03 m to 0.06 m with and interquartile range of 0.14 m to 0.39 m². Changes in thalweg elevation paralleled sediment balance with thalweg incision at Lower Lookout and thalweg aggradation at Middle Lookout (Figure A.5). Between 1995 and 1997, median thalweg elevation incised by 18 cm (21% of the median bankfull depth in 1995) at Lower Lookout and aggraded by 37 cm (45% of the median bankfull depth in 1995) at Middle Lookout Creek. From a sediment balance perspective, neither Lower Lookout nor

Middle Lookout showed a return to pre-flood conditions by the end of monitoring in 2011 (Figure 8, Figure A.5).

In terms of bankfull dimensions, channels varied relatively little from 1978 to 1995. During this time period, the median bankfull depth variation at Lower Lookout did not exceed 12% or 9 cm relative to the 1995 values, with an interquartile range of 4%–26% or 4 cm–22 cm. Median bankfull depths at Middle Lookout varied by no more than 6% or 5 cm relative to the 1995 values, with an interquartile range of 4%–16% or 3 cm–16 cm. Median bankfull depths at Mack Old Growth varied by no more than 5% or 3 cm relative to the 1995 values, with an interquartile range of 10%–52% or 4 cm–26 cm. Median bankfull depths at Mack Clearcut varied by no more than 21% or 9 cm relative to the 1995 values, with an interquartile range of 14%–35% or 7 cm–11 cm (Figure 9).

Bankfull channel dimensions changed after the 1996 flood, and many of these changes persisted through the end of monitoring in 2011. Overall, the 1996 flood triggered a reduction of bankfull depths at Middle Lookout, deepening of bankfull depths at Lower Lookout, minor deepening in Mack Clearcut and little change in Mack Old Growth (Figure 9). Changes varied between cross sections. The variability in magnitudes and directions of change were greater in Lower Lookout and Mack Clearcut than in Middle Lookout (where most cross sections experienced a reduction in bankfull depth) or in Mack Old Growth (where most cross sections experienced minor changes, Figure 9). These changes in bankfull depths persisted over the 15 years of post-flood monitoring. At Lower Lookout, the median increase in bankfull depth from 1995 to 1996 was +46% or +29 cm. Bankfull depths then became only slightly shallower in the following 15 years at Lower Lookout. The median change in bankfull depths from 1995 to 2011 was +37% or +25 cm. At Middle Lookout, the median decrease in bankfull depth from 1995 to 1996 was -34% or -27 cm. Bankfull depths then deepened only slightly in the following 15 years. The median change in bankfull depths at Middle Lookout from 1995 to 2011 was -27% or -20 cm. At Mack Old Growth, the median increase in bankfull depth from 1995 to 1996 was only +7% or +4 cm. Bankfull depths then remained steady over the following 15 years. At Mack Clearcut, the median increase in bankfull depth from 1995 to 1996 was -20% or +8 cm. Bankfull depths then became only slightly shallower in the following 15 years. The median change in bankfull depths at Middle Lookout from 1995 to 2011 was -16% or +7 cm. (Figure 9).



Figure 9: Bankfull depths as a ratio relative to the 1995 values at each reach. Median values represented by dots and interquartile range represented by bars. Values above 1 indicate that bankfull depths deeper than those in 1995 while values below 1 indicate bankfull depths shallower than those in 1995. Median bankfull depths in Lower Lookout and Mack Clearcut increased after the flood of 1996 although both reaches displayed a wide range of post-flood variability. Median bankfull depths at Middle Lookout became shallower following the flood of 1996.

Bankfull widths also showed relatively little variation between 1978 and 1995. Prior to 1995, the median bankfull width variation at Lower Lookout did not exceed 2% or 0.6 m relative to the 1995 values, with an interquartile range of 5%–12% or 1.3 m – 3.2 m. Median bankfull

widths at Middle Lookout varied by no more than 8% or 1.6 m relative to the 1995 values, with an interquartile range of 4% – 15% or 1.1 m – 4.3 m. Median bankfull widths at Mack Old Growth varied by no more than 5% or 0.8 m, relative to the 1995 values, with an interquartile range of 5%–27% or 0.8 m – 2.7 m. Median bankfull widths at Mack Clearcut varied by no more than 10% or 1.0 m relative to the 1995 values, with an interquartile range of 9%–31% or 1.0 – 3.3 m.

Patterns in bankfull width adjustment after the 1996 flood differed from patterns in bankfull depth adjustment. At Lower Lookout, median bankfull widths did not change substantially between the start of monitoring in 1978 and the mid-2000s (Figure 10). However, the variability between cross sections increased following the 1996 flood. At both Middle Lookout and Mack Old Growth, bankfull widths increased over the course of several years following the 1996 flood. The variability in bankfull width also increase in these two reaches after 1996 (Figure 10). Middle Lookout reached an increase of 4.4 m or 17% between 1995 and 2000, and Mack Old Growth reached an increase of 1.6 m or 10% in the same time period. Neither of these reaches narrowed back to their pre-flood widths by the end of monitoring in 2011 (Figure 10). Mack Clearcut also showed some post-flood narrowing, but the scale and variability of the change at this reach was not unique to this time period matching patterns displayed at that reach in the 1980s (Figure 10).

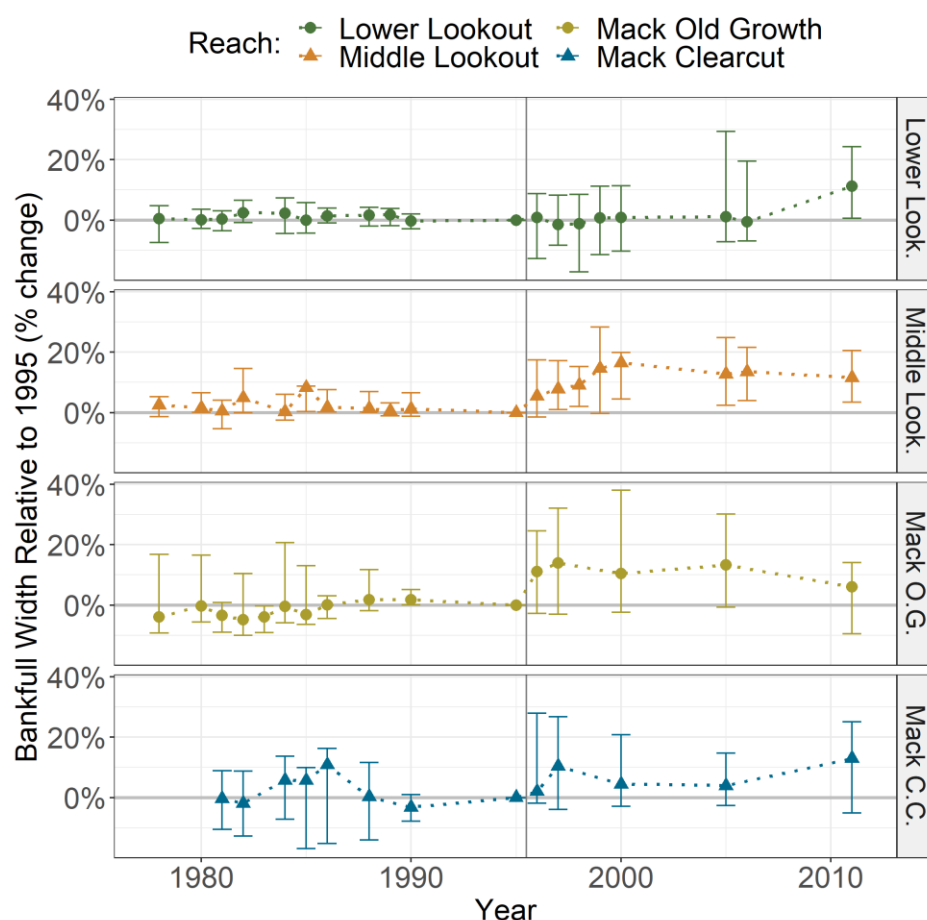


Figure 10: Bankfull widths as a ratio relative to the 1995 values at each reach. Median values represented by dots and interquartile range represented by bars. Lower Lookout shows stable median values from the start of monitoring through the mid-2000s, while Middle Lookout and Mack Old Growth show widening bankfull widths for several years following the 1996 flood. Mack Clear Cut displays fluctuating bankfull widths throughout the full time series.

Grain size changes in terms of the median size, D_{50} , (Figure 11) and the sorting (Figure 12) appeared to lag the flood event, often reaching extreme values in 1997 rather than 1996. It is possible that these extreme values were triggered by the peak flow of Water Year 1997, which was relatively high (6th largest annual peak discharge between 1979 and 2011). Between 1995 and 1997, the median D_{50} among cross sections in Lower Lookout rose from 104 mm to 118 mm while in Middle Lookout it dropped from 142 mm to 85 mm. At Mack Old Growth, median D_{50} dropped from 95 mm to 90 mm while at Mack Clearcut, it rose from 63 mm to 125 mm (Figure 11). After 1997, grain size adjustment varied by reach. At Lower Lookout, median D_{50} dropped

slightly to 93 mm in 1998 before slowly rising to 111 mm in 2000 and 120 mm in 2011. At Middle Lookout, median D_{50} remained relatively fine at 88 mm in 1998 before slowly rising to 110 mm in 2000 and 125 mm in 2011. At Mack Old Growth, median D_{50} remained relatively stable at 90 mm in 2000 before rising to 120 mm by 2011. At Mack Clearcut, median D_{50} remained relatively stable at 112 mm in 2000 before rising slightly to 130 mm in 2011 (Figure 11).

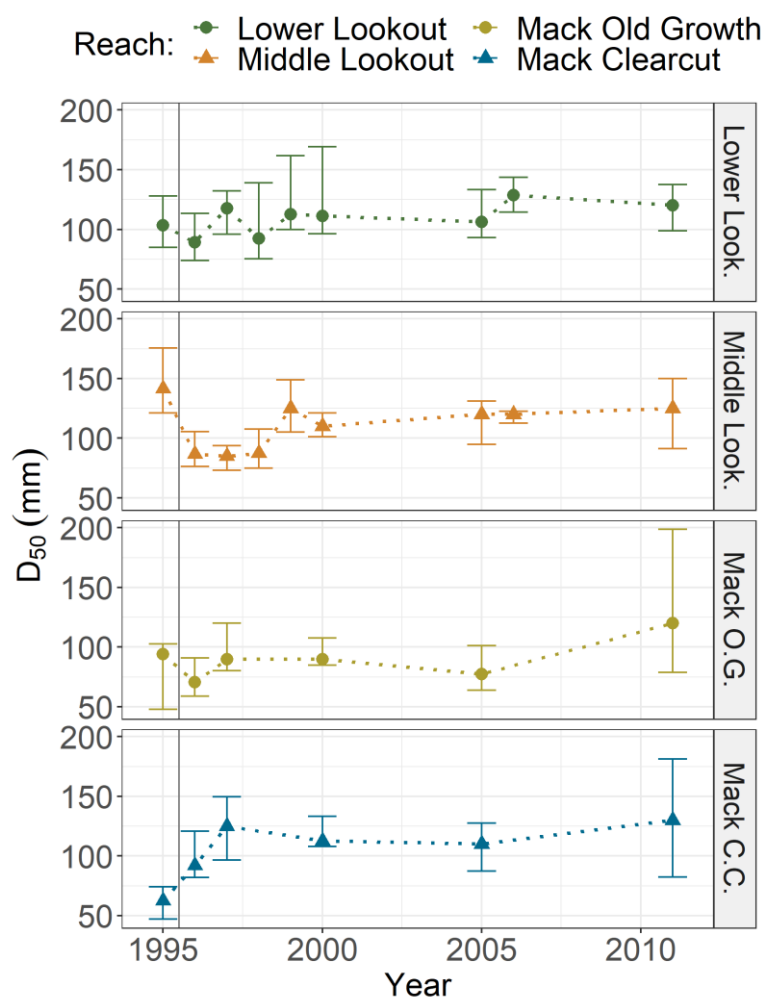


Figure 11: D_{50} in mm at each of the four reaches. Median values represented by dots and interquartile range of D_{50} values represented by bars. Lower Lookout shows fluctuating fining then coarsening of D_{50} grain sizes. Middle Lookout shows fining following the 1996 flood followed by gradual coarsening. Mack Clearcut shows coarsening following the 1996 flood with no return to pre-flood grain sizes.

The trends in sediment sorting are similar between reaches. Particle counts show that the bed surface texture became less sorted between 1995 and 1996 at all reaches but became more

sorted after that over a period of 3 years at Lower Lookout and Middle Lookout with a local minimum of σ in 1999. All reaches showed the lowest σ values in 2005 (Figure 12) indicating the narrowest distribution of particle sizes. Although we lack grain size data from before 1995, it appears that both Lower Lookout and Middle Lookout displayed conditions similar to pre-1996 grain size and grain sorting conditions by the end of monitoring in 2011. That is, the D_{50} and σ values in 2011 are closer to the 1995 values than the 1996 or 1997 values.

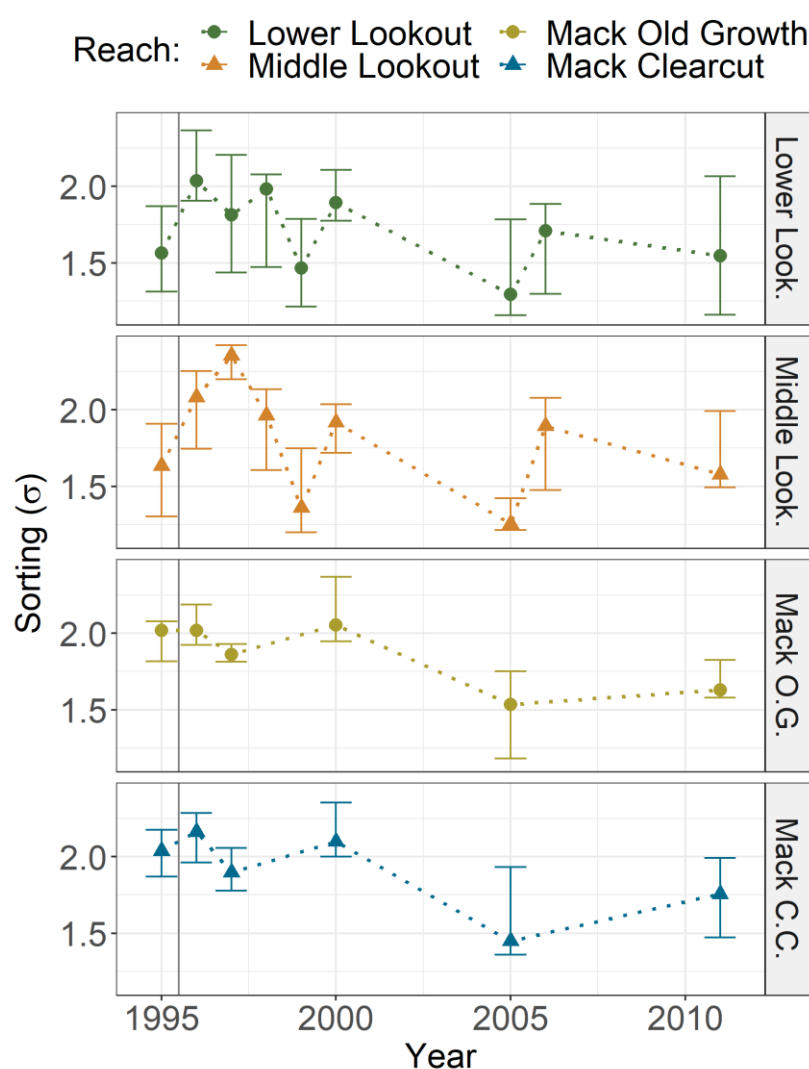


Figure 12: Sorting (σ , unitless) at each of the four reaches. Higher values indicate less sorted material and lower values indicate more sorted material. Lower Lookout Creek and Middle Lookout Creek show decreased sorting after the 1996 flood followed by increased sorting towards 1999. All reaches show increased sorting between 2000 and 2005.

3. Geomorphic patterns of response within the Lower Lookout

At Lower Lookout, post-flood changes in sediment storage and bankfull geometry varied by location within the reach (Figure 13). Spatial patterns in these changes suggest three distinct regions within this reach: an upper sub-reach consisting of two cross sections (LOL13 and LOL14) in a straight section of river, 20 meters of the top of the reach, a river bend sub-reach consisting of eight cross sections (LOL05 – LOL12) in and immediately downstream of a major bend in the river, between 70m and 280m from the top of the reach, and a lower sub-reach consisting of four cross sections (LOL01 – LOL04) in a straight section downstream of the bend, between 280m and the bottom of the reach (Figure 2).

Between 1978 and 1995, thirteen out of fourteen cross sections showed minimal changes of less than 8.8 m^2 (the 75th percentile of total change) in either direction of cumulative deposition (Figure 13c). The two cross sections within 20 m of the top of the reach continued to show minimal change throughout the monitoring period. In contrast, seven out of the eight cross sections near the river bend showed net scouring between 1995 and 1996. This scouring trend persisted over time, and by 2011 all eight of these cross sections had scoured by at least 3.3 m^2 relative to their initial conditions. In the lower sub-reach downstream of the river bend three of the four cross sections show net deposition by 1996 and all of them show net deposition by 2000. This depositional pattern mirrors the scouring seen in the cross sections directly upstream. By 2011, scouring had reversed the depositional trends on these four cross sections. Three of the four cross sections in this downstream sub-reach had returned to levels of deposition within the pre-flood range of variation and one of the four cross sections had scoured beyond the pre-flood range at a cumulative loss of 6.5 m^2 of sediment relative to 1978 (Figure 13c).

Thalweg aggradation followed similar zonal patterns after the 1996 flood. Between 1978 and 1995, thirteen out of fourteen cross sections showed minimal changes (i.e., less than 0.5 m in either direction) in thalweg elevation (Figure 13d). The two cross sections in the upstream sub-reach continued to show minimal changes throughout the remainder of the monitoring period. Every cross section near the river bend showed thalweg incision between 1995 and 1996, although only four of the eight cross sections showed thalweg incision that was deeper than any

previous thalweg observed at those cross sections. These four cross sections did not return to pre-flood thalweg elevations by 2011. Three of the four cross sections in the downstream sub-reach showed thalweg aggradation, and one of these (LOL03) returned to pre-flood thalweg elevations by 2011 (Figure 13d).

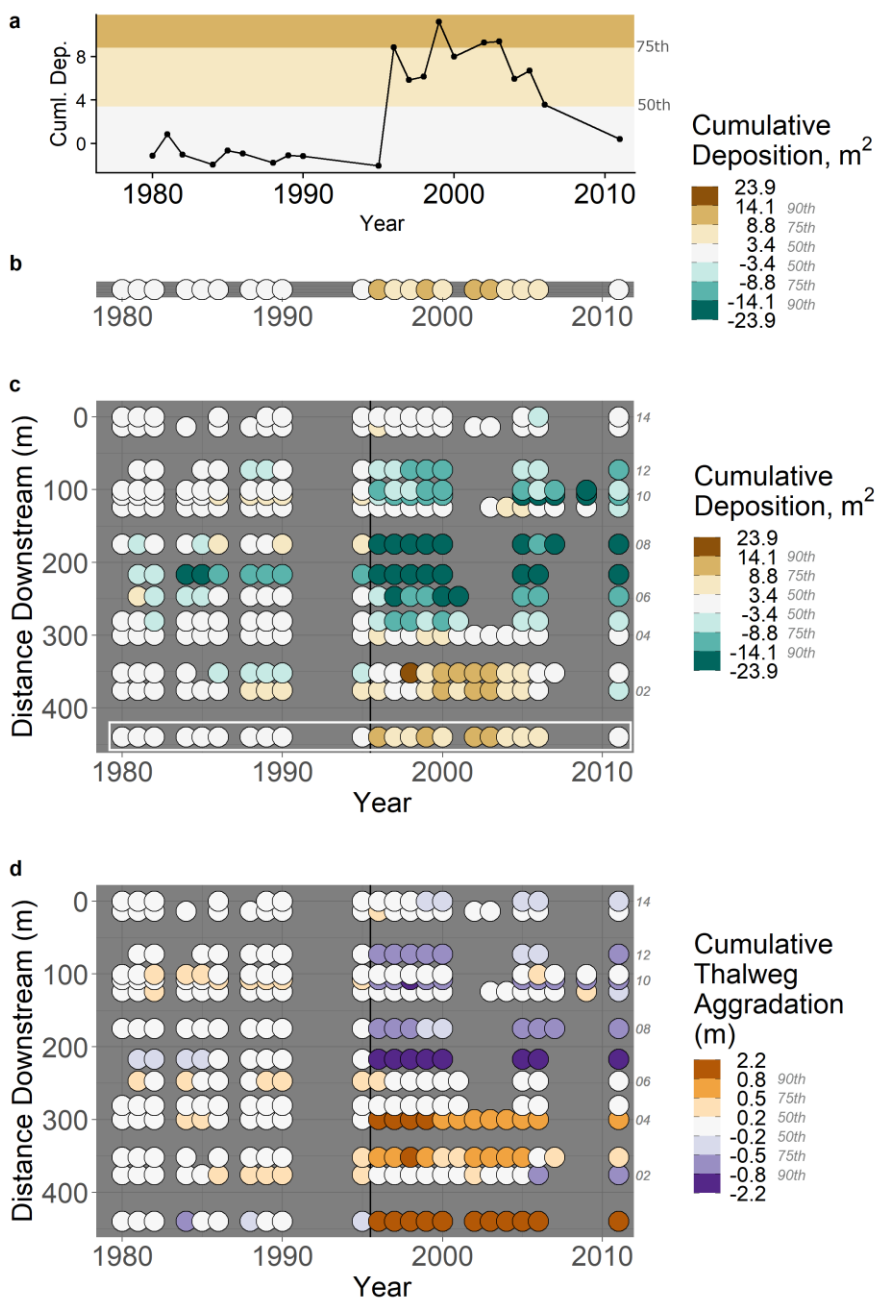


Figure 13: (a) Example of cumulative cross-sectional deposition (m^2) at a cross section (LOL01, Figure 2) over time. Black dots show values at each survey year and colored bands classify

values into ranges based on occurrence frequency (percentiles labeled on right axis). (b) Cumulative cross-sectional deposition values from panel a represented as colored dots. Percentiles are shown in italic text in the legend. (c) Cumulative cross-sectional deposition values from every cross section in Lower Lookout represented as colored dots. Cross section LOL01 is outlined by a white box for reference. The Y axis represents distance downstream from the top of the reach (flow direction if from top (distance 0) to bottom (distance 400-m). Brown colors (positive values) represent cumulative deposition while blue colors (negative values) represent cumulative scour. Cross section numbers are labeled on the right Y axis. Percentiles are shown in italic text in the legend. (d) Cumulative thalweg aggradation (m) over time represented by colored dots. The Y axis represents distance downstream from the top of the reach. Orange colors (positive values) represent cumulative thalweg aggradation while purple colors (negative values) represent cumulative thalweg incision.

Bankfull depths displayed relative stability between 1978 and 1995, with thirteen out of fourteen cross sections changing by no more than 50% during this time, and ten out of fourteen cross sections changing by no more than 20% (Figure 14a). Between 1995 and 1996, bankfull depths increased (i.e., became deeper) in one cross section of the upstream sub-reach but decreased (i.e., became shallower) in the other cross section. Near the bend in the river, bankfull depths increased at six out of eight cross sections. These adjustments did not always persist long-term. Three of these cross sections bankfull depths returned to the pre-flood range of conditions by 2011. In the downstream sub-reach, bankfull depths increased at two out of four cross sections (Figure 14a).

Between 1978 and 1995, twelve out of the fourteen cross sections varied in width by no more than 20%. While the bankfull depths generally increased near the bend and decreased downstream of the bend, the pattern was reversed for widths – bankfull widths generally decreased near the bend and increased downstream of the bed. Between 1995 and 1996, bankfull widths decreased at one out of two cross sections in the upstream subreach and decreased at six of the eight cross sections near the bend. Downstream of the bend, bankfull widths increased at all four cross sections. The increase in width downstream of the bend where substantial scour took place may represent the river widening to evacuate material (Figure 14).

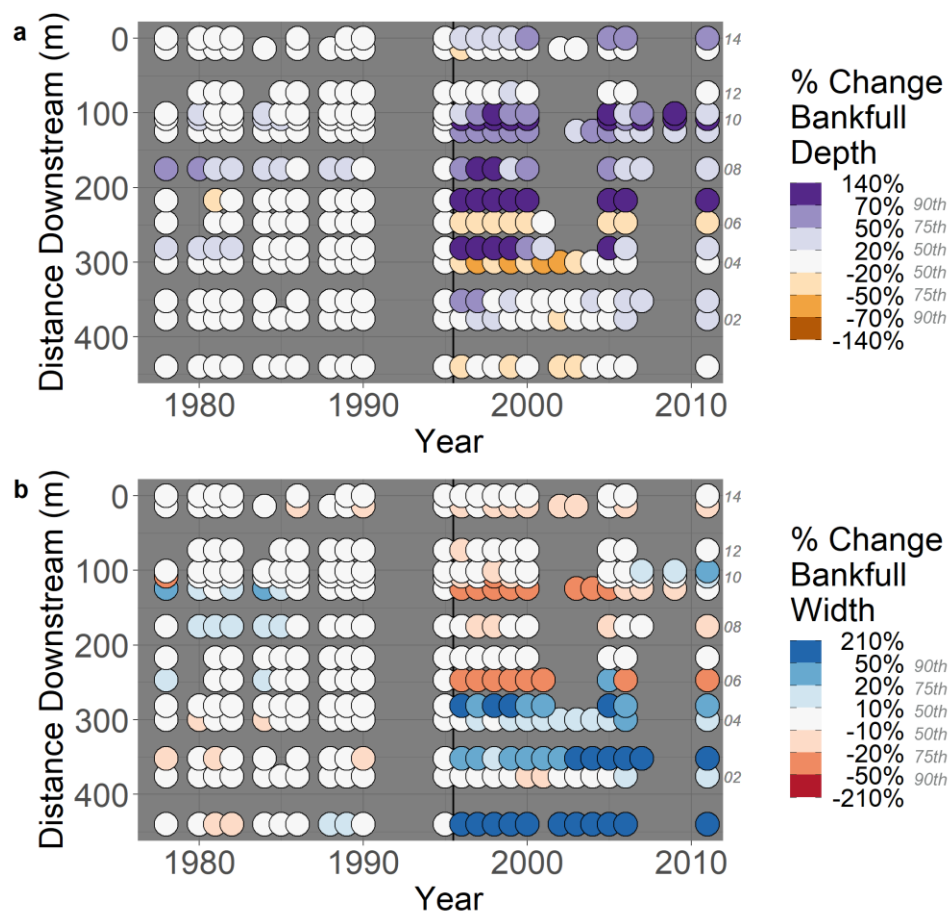


Figure 14: (a) Bankfull depths from every cross section in Lower Lookout represented as colored dots. Values are shown as percent change relative to 1995 values. The Y axis represents distance downstream from the top of the reach. Values are binned into divergent color groups based on the 50th, 75th, and 90th percentile of the absolute values of the data set. Brown colors (negative values) represent shallower bankfull depths relative to 1995 while purple colors (positive values) represent deeper bankfull depths relative to 1995. Select cross section numbers are labeled on the right axis. Percentiles are shown in italic text in the legend. (b) Bankfull widths from every cross section in Lower Lookout represented as colored dots. Values are shown as percent change relative to 1995 values. Red colors (negative values) represent narrower bankfull widths relative to 1995 while blue colors (positive values) represent wider bankfull widths relative to 1995.

Grain size data was not collected before 1995, but post-1995 spatial patterns in grain size adjustments also show a distinct pattern of change in the sub-reach near the bend of the reach. The median grain size at five of these eight cross sections increased 17–48% between 1995 and 1996 and four of these cross-sections (LOL06, LOL07, LOL08, LOL12) continued to coarsen through the late 1990s and early 2000s. As with other metrics, D_{50} showed little change in the

upstream sub-reach above the bend. There were also minimal changes in the lower sub-reach below the bend (Figure 15a).

Spatial patterns of grain sorting differed slightly from the patterns in sediment storage, bankfull geometry, and median grain size. While most changes in sediment storage and bankfull geometry occurred between sections LOL05 and LOL12, the largest changes in sorting occurred slightly downstream at cross sections LOL04–LOL08. This is the straighter section of the reach below the river bend. In this region, sediment became less sorted by at least 30% at all cross section between 1995 and 1996, while only two of the eight other cross sections showed changes in sorting greater than 30%. However, adjustments to sorting did not persist over time. By 2011 ten out of thirteen cross sections (LOL01 was not sampled in 1995) in the reach had returned to within 30% σ_ϕ of their 1995 distributions (Figure 15b).

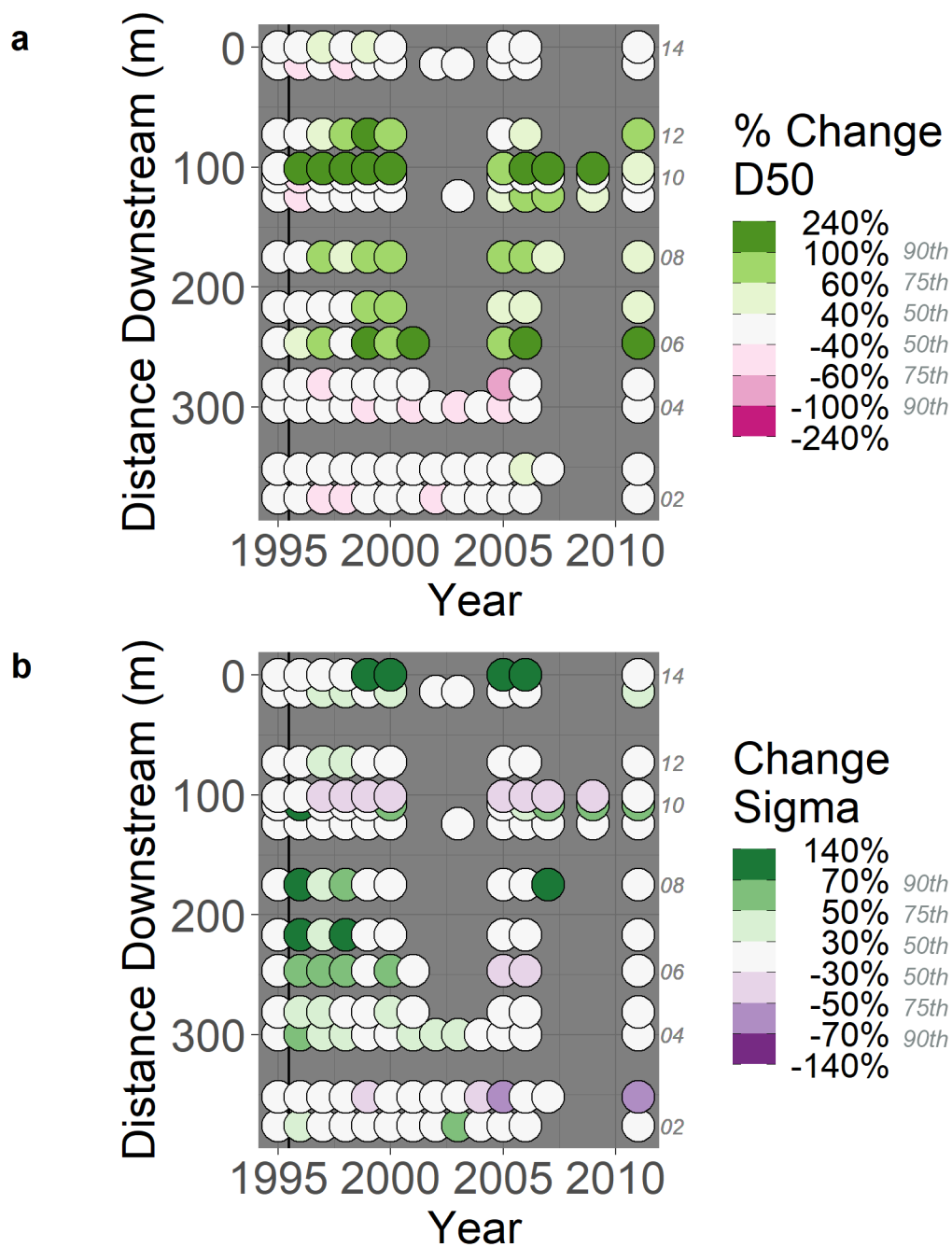


Figure 15: (a) D_{50} from every cross section in Lower Lookout represented as colored dots. Values are shown as percent change relative to 1995 values. The Y axis represents distance downstream from the top of the reach. Values are binned into divergent color groups based on the 50th, 75th, and 90th percentile of the absolute values of the data set. Magenta colors (negative values) represent finer median grain sizes relative to 1995 green colors (positive values) represent coarser median grain sizes relative to 1995. Select cross section numbers are labeled on the right axis. Percentiles are shown in italic text in the legend. (b) σ_ϕ from every cross

section in Lower Lookout represented as colored dots. Values are shown as percent change relative to 1995 values. Purple colors (negative values) represent a narrower distribution of grain sizes relative to 1995 while green colors (positive values) represent a wider distribution of grain sizes relative to 1995.

Changes in Shields stress and transport stage do not follow the same zonal patterns as sediment storage, bankfull geometry, or sediment size. From 1995 to 1996 Shields stress increased at eight cross sections scattered throughout the three zones and decreased in three others. The changes in Shield stress reflect concurrent changes in bankfull depth and median grain size as shear stress scales linearly with bankfull depth given a constant slope. The spatial discrepancy between changes in bankfull depth and changes in Shields stress may reflect a bed texture adjustment that accommodates some of the changes in shear stress. However, D_{50} and shear stress are linearly related only at cross sections LOL07 and LOL12 ($R^2 = 0.47\text{--}0.52$, $p = 0.03\text{--}0.04$, Table A.4, Figure A.6). By 2011, eight of the thirteen cross sections had Shields stresses within 30% of their 1995 values (Figure 15).

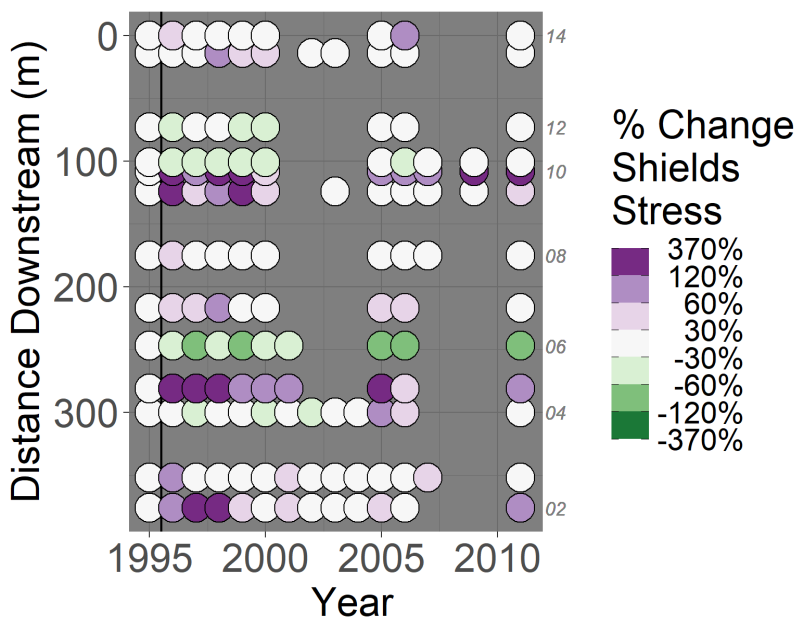


Figure 16: Percent change in shields stress from every cross section in Lower Lookout represented as colored dots. Values are shown as percent change relative to 1995 values. The Y axis represents distance downstream from the top of the reach. Values are binned into divergent color groups based on the 50th, 75th, and 90th percentile of the absolute values of the data set.

Red colors represent lower Shields stress values relative to 1995 while blue colors represent greater Shields stress values relative to 1995. Select cross section numbers are labeled on the right axis.

4.4. Geomorphic patterns of response at Middle Lookout

As in Lower Lookout, at Middle Lookout, changes in sediment storage and bankfull geometry varied by location in the reach after the 1996 flood. Many metrics show post-flood differences at or directly upstream of a large logjam crossing the stream at LOM08 and LOM09, around 230 m from the top of the reach (Figure 2).

In terms of sediment balance, Middle Lookout primarily experienced deposition and thalweg aggradation, but the effect was most prominent upstream of the logjam (between cross-sections LOM01 and LOM09). From 1978 to 1995, only two cross sections experienced more than 10.2 m^2 (i.e., the 75th percentile of scour or deposition) of net deposition in any year, and only one retained that amount of material in 1995. The flood of 1996 acted as a massive depositional event in Middle Lookout. By 1996, five cross sections had experienced more than 10.2 m^2 of net deposition, three of which experienced more than 21.7 m^2 (that is greater than the 90th percentile) Cross sections LOM03 to LOM08 showed both net deposition and aggradation following the 1996 flood. The effect was strongest closest to the logjam (cross sections LOM06–LOM08). By 2011, scouring had reversed only some of the depositional effects of the 1996 flood. In 2011, four cross sections showed net deposition greater than 10.2 m^2 and one of these, LOM10, was downstream of the site of initial deposition, suggesting downstream movement and deposition of bed load (Figure 17a).

Patterns in thalweg aggradation match those in sediment deposition, suggesting that the depositional event raised the entire stream bed. From 1978 to 1995, no cross section thalweg diverged more than 0.6 m from its original elevation, but in 1996, five cross sections (LOM03–LOM08) were 0.6 m greater than their initial conditions (Figure 17b). Aggradation continued for at least one more year at the three cross sections most directly upstream of the logjam (LOM06–LOM08). These three cross sections incised back to their 1996 elevations by 2011, but overall, the stream bed remained elevated relative to the 1995 conditions (Figure 17b).

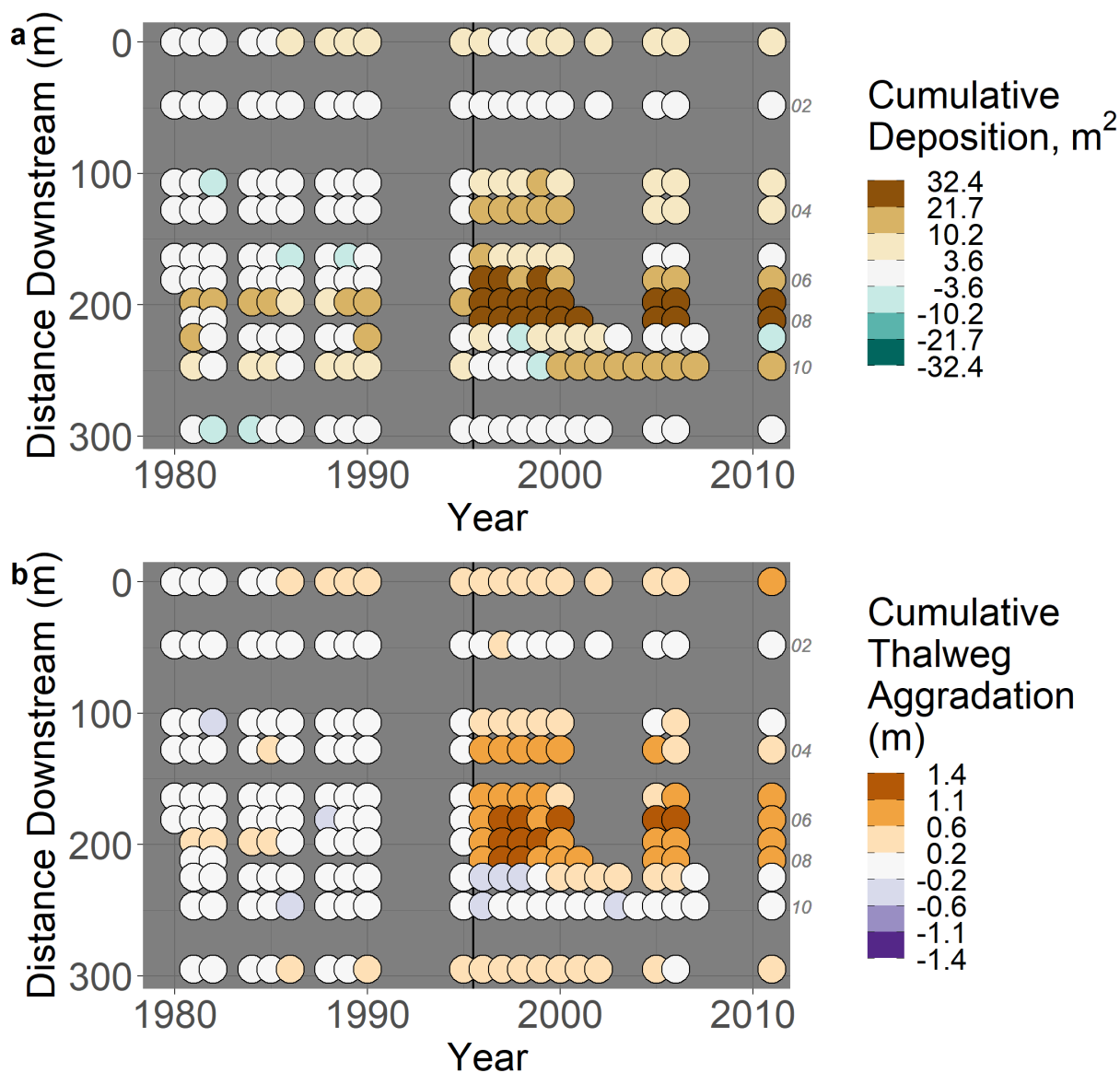


Figure 17: (a) Cumulative cross-sectional deposition values from every cross section in Middle Lookout represented as colored dots. The Y axis represents distance downstream from the top of the reach. Values are binned into divergent color groups based on the 50th, 75th, and 90th percentile of the absolute values of the data set. Brown colors (positive values) represent cumulative deposition while blue colors (negative values) represent cumulative scour. Cross section numbers are labeled on the right axis. (b) Cumulative thalweg aggradation (m) over time represented by colored dots. The Y axis represents distance downstream from the top of the reach. Orange colors (positive values) represent cumulative thalweg aggradation while purple colors (negative values) represent cumulative thalweg incision.

The aggradation of the streambed from 1995 to 1996 was associated with a reduction in bankfull depth along the entire reach. From 1995 to 1996, bankfull depths decreased by at least

20% in eight out of the ten cross sections. These changes also appeared to be most dramatic in the cross sections directly upstream of the large wood jam (Figure 2). The shallower bankfull geometry persisted through the end of monitoring in 2011 where seven out of ten cross sections were at least 20% shallower than their 1995 dimensions (Figure 18).

The reach accommodated the reduction in bankfull depth via widening. However, changes in bankfull width do not spatially coincide with the changes in depth and sediment storage. Cross sectional profiles suggest dynamic changes to bankfull width before 1995 in at least three cross-sections (LOM07, LOM08, and LOM10). From 1995 to 1996, five out of ten cross sections widened by at least 10% while two out ten narrowed by at least 10%. Cross-section LOM07 experienced the more dramatic relative increase in channel width of 12 m (87%) between 1995 and 1996. Between 1996 and 2011 the channel increased in width in nine out of eleven cross sections. Width adjustments in that time period ranged from -8% at LOM03 to +49% at LOM09. By 2011, five out of ten cross sections were still 14 – 90% wider than they were in 1995 (Figure 18).

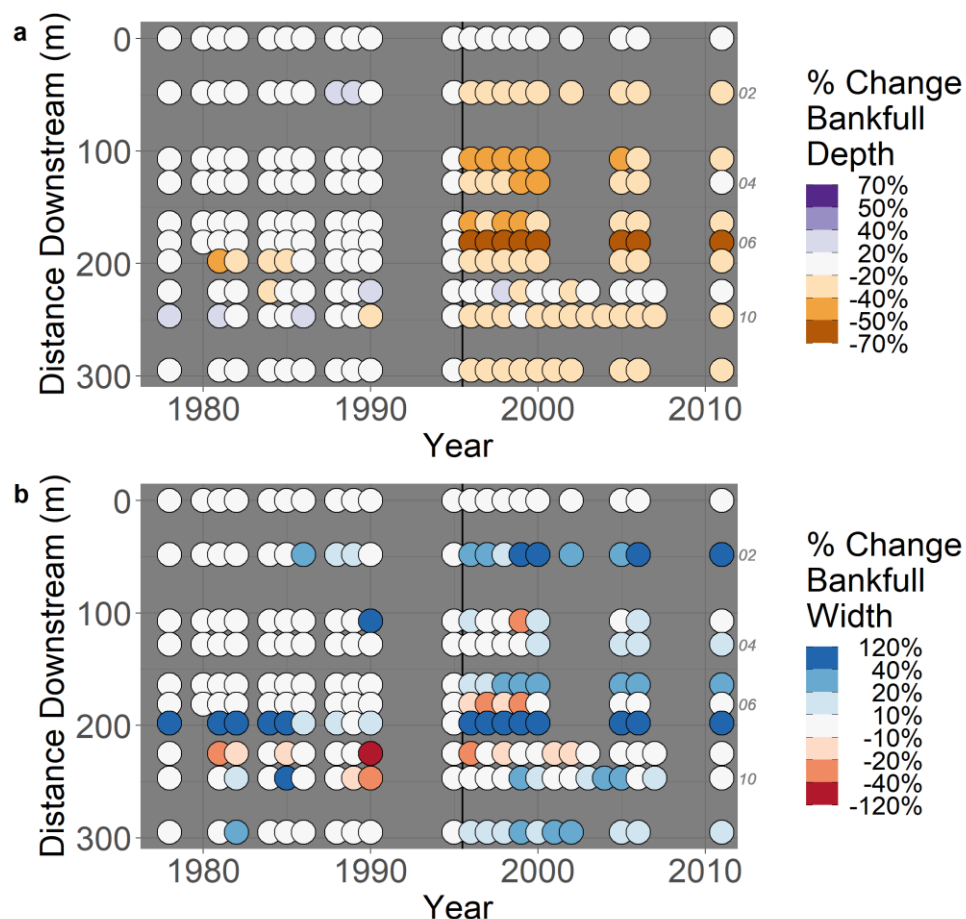


Figure 18: (a) Bankfull depths from every cross section in Middle Lookout represented as colored dots. Values are shown as percent change relative to 1995 values. The Y axis represents distance downstream from the top of the reach. Values are binned into divergent color groups based on the 50th, 75th, and 90th percentile of the absolute values of the data set. Brown colors (positive values) represent shallower bankfull depths relative to 1995 while purple colors (negative values) represent deeper bankfull depths relative to 1995. Select cross section numbers are labeled on the right axis. (b) Bankfull widths from every cross section in Lower Lookout represented as colored dots. Values are shown as percent change relative to 1995 values. Red colors (positive values) represent narrower bankfull widths relative to 1995 while blue colors (negative values) represent wider bankfull widths relative to 1995.

The events of 1996 resulted in a reduction in grain size at many of the cross sections in Middle Lookout, consistent with the widespread deposition and depth reduction. From 1995 to 1996, seven of the nine cross sections showed a reduction in D_{50} by at least 30%, the grain size in most of these cross sections continued to become finer in the subsequent two years. There is no clear evidence for a spatial pattern in these fining trends. The stream bed surface then coarsened at most cross sections throughout the 2000s, resulting in a 2005 bed surface D_{50} in 34 -

54 % finer than in 1995 in three of the ten cross sections, while one cross-section had coarsening (47 % coarser than 1995) and six cross sections had similar D_{50} (5%- 28% change relative to 1995 values, Figure 19).

In terms of sorting, cross sections upstream of the logjam, LOM01–LOM07, showed an increase in σ_ϕ from 1995–1996 (though the changes at LOM04 and LOM07 were small), indicating a reduction in sorting. The σ_ϕ value continued to increase through 1997 suggesting a temporally lagged effect likely as sediment delivered by debris flow move through the system. Individual cross sections did not appear to return to their pre-flood grain size distributions by 2011, but the distributions changed so that by 2011, four cross sections (LOM04 and LOM09–LOM11) were somewhat more sorted than their 1995 value, five (LOM01–LOM03, LOM05, and LOM07) were less sorted, and one (LOM01) ended up with nearly the same value as it started with in 1995 (Figure 19).

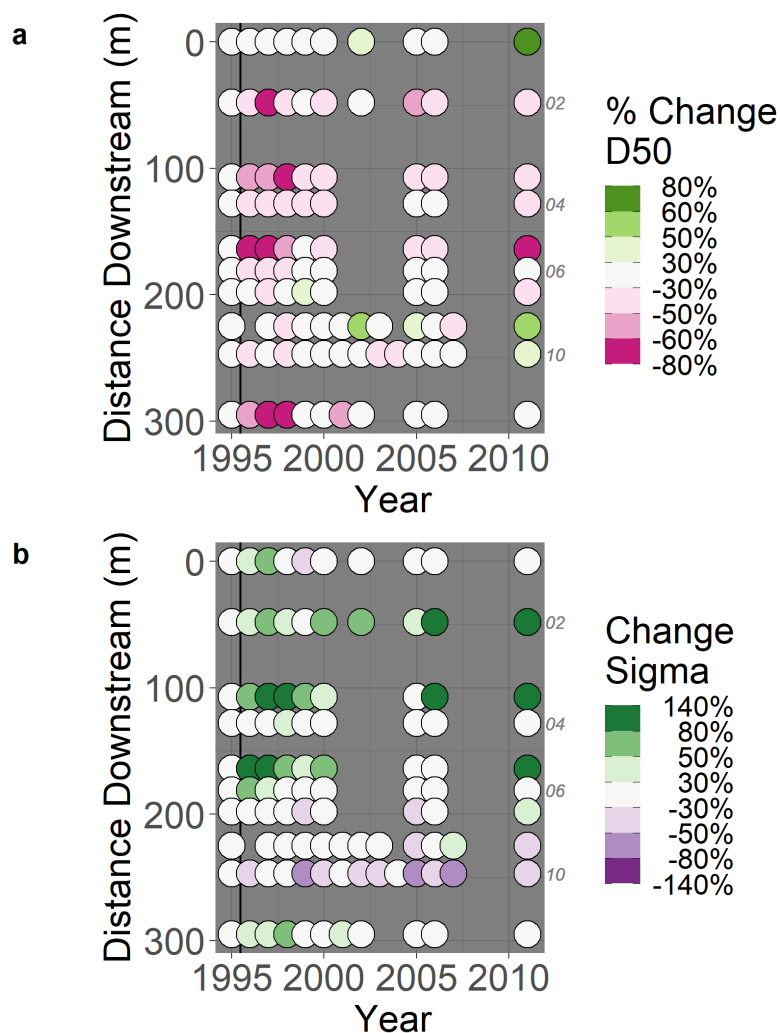


Figure 19: (a) D_{50} from every cross section in Middle Lookout represented as colored dots. Values are shown as percent change relative to 1995 values. The Y axis represents distance downstream from the top of the reach. Values are binned into divergent color groups based on the 50th, 75th, and 90th percentile of the absolute values of the data set. Magenta colors (positive values) represent finer median grain sizes relative to 1995 while purple colors (negative values) represent coarser median grain sizes relative to 1995. Select cross section numbers are labeled on the right axis. (b) σ_ϕ from every cross section in Lower Lookout represented as colored dots. Values are shown as percent change relative to 1995 values. Purple colors (positive values) represent a narrower distribution of grain sizes relative to 1995 while green colors (negative values) represent a wider distribution of grain sizes relative to 1995.

As in Lower Lookout, changes in Shields stress and at Middle Lookout do not follow the same zonal patterns as sediment storage, bankfull geometry, and grain sorting. From 1995 to 1996 Shields stress increased by at least 40% at four cross sections scattered across the reach and remained similar at the others. By 2006, Shields stress values were within 30% of the 1995

values at nine out of ten cross sections but they decreased below their 1995 values at five of nine cross sections by 2011 (

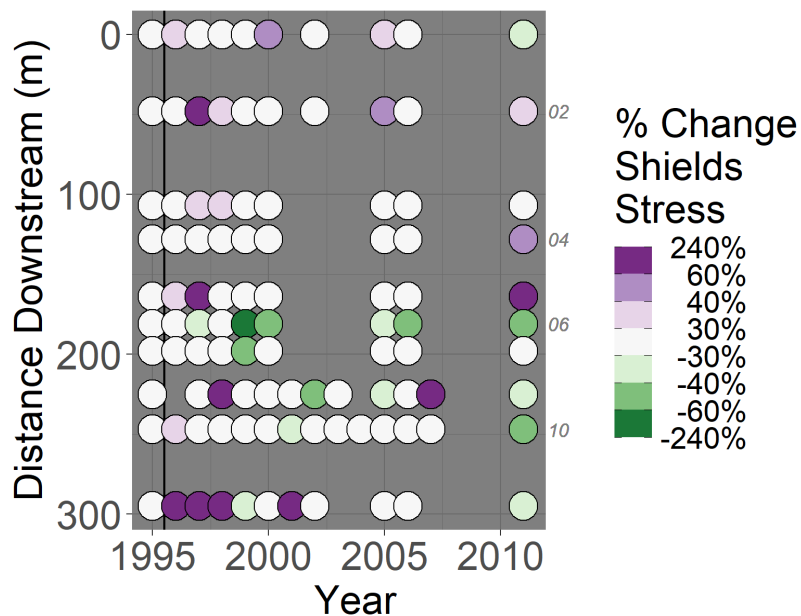


Figure 20). The spatial discrepancy between changes in bankfull depth and changes in Shields stress may reflect a bed texture adjustment (fining) that accommodates some of the reduction in shear stress. However, D_{50} and shear stress are linearly related only at cross sections LOM02 and LOM03 ($R^2 = 0.55-0.75$, $p = 0.003-0.01$, Table A.4, Figure A.7).

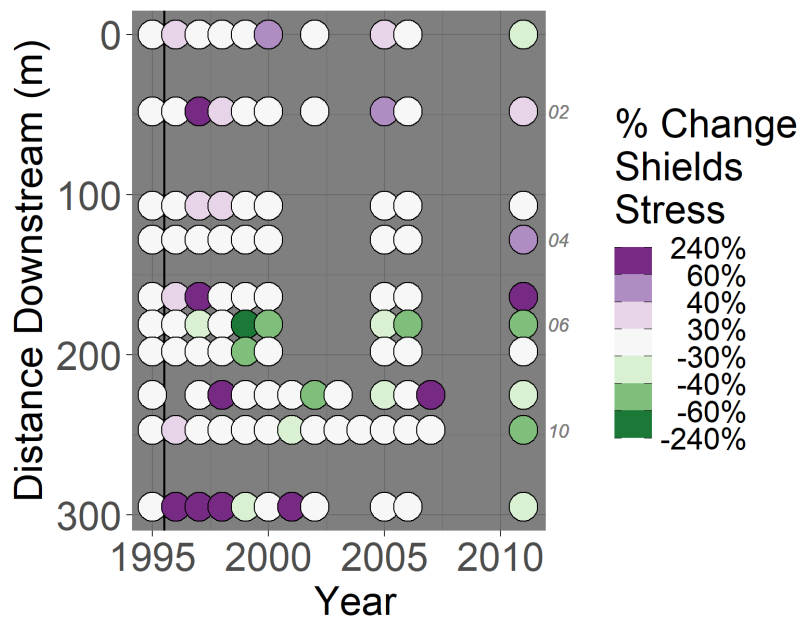


Figure 20: Percent change in shields stress from every cross section in Middle Lookout represented as colored dots. Values are shown as percent change relative to 1995 values. The Y axis represents distance downstream from the top of the reach. Values are binned into divergent color groups based on the 50th, 75th, and 90th percentile of the absolute values of the data set. Red colors represent lower Shields stress values relative to 1995 while blue colors represent greater Shields stress values relative to 1995. Select cross section numbers are labeled on the right axis.

5. Discussion

5.1. Relationships between channel adjustment and peak flows

The unusual geomorphic effectiveness of the 1996 flood (Figure 7) suggests an important role of thresholds in channel adjustments in forested mountain watersheds. This over-competence suggests that large, debris-laden flows may play a fundamentally different role in fluvial adjustment than smaller, lower density flows. Support for the exceptional nature of this type of event has been observed in a step pool stream in Switzerland (Turowski et al., 2009), in Redwood Creek in California (Janda et al., 1975; Madej, 1992), and in the Oregon Cascades (Grant & Swanson, 1995).

Additionally, the lagged responses in bankfull width and D_{50} (Figure 10, Figure 11) suggest that extreme events might place streams in a temporarily unstable configuration and make them more susceptible to additional changes. While there are fluvial and hydraulic mechanisms that might account for the presence of these thresholds (e.g. bank failure, altered fluid density, loss of armoring) non-fluvial interactions cannot be ignored. Patterns of adjustment in Lower Lookout and Middle Lookout suggest that colluvial sediment supply, the supply of instream wood, and patterns of valley confinement all have played major roles in shaping flood response. Previous work in Mack Creek in the Andrews Forest also suggests that in the absence of wood, boulders have also played a major role in shaping step-pool morphology of steep reaches (Faustini & Jones, 2003).

Even in less eventful years, peak flow magnitude was a significant driver of geomorphic change within the study reaches. Excluding the flood of record in 1996, peak flows were linearly related the amount of reworked cross-sectional area (scoured area plus deposited area) at three of the four study reaches (Table 2). Peak flow magnitude explained the greatest amount of variation

at Middle Lookout followed by Mack Clearcut and Lower Lookout. At Mack Old Growth, a V-shaped, wood loaded reach, peak flow magnitudes of small floods were not related to reworked cross-sectional area. This suggests that very large floods are needed to induce change in wood-forced step pool channels.

The combined influence of hydrologic events and landscape controls suggests that channel adjustment depends not only on the size of peak flows, but also the history of recent flood events and the land use history of the watershed. In essence, extreme flow events act as a mechanism by which characteristics from the upland landscape (e.g., lithology, forest cover, logging history, roads) propagate downward into the stream network and riparian areas. As extreme precipitation events become more common in the coming decades (Prein et al., 2017) and rain-on-snow events shift in distribution (Musselman et al., 2018), flow-related geomorphic thresholds might be more easily surpassed than in the recent historical record. In this context, the role of forest infrastructure and forest harvest practices may become more important as they can increase the likelihood of debris flows (Snyder, 2000; Wemple et al., 2001) thus modulating sediment and wood supply to streams.

It is difficult to compare the steep Mack Creek reaches to the lower-gradient Lookout Creek reaches because they differ not only in grade but also in forest history and flood magnitude. Because peak flows in 1996 at Mack Creek were substantially smaller than those at Lookout Creek, both relative to drainage area and mean annual peak discharge, it is challenging to discern whether the relatively mild response at Mack Creek represents intrinsic stability of steep step-pool channels (Montgomery & Buffington, 1997) or the relatively mellow flood history of that site compared to Lookout. A future, higher-magnitude, peak flow in that Mack Creek would provide an opportunity to further investigate the interaction between channel form, step features, peak flows, and geomorphic change.

5.2. Patterns of geomorphic adjustment in 1996 and subsequent years

Patterns of sediment storage in the study reaches differ somewhat from previous work. Previous studies described thalweg aggradation and deposition as a common response to large floods (Di Silvio, 1994; Lisle, 1981; Madej, 1999; Nelson & Dubé, 2016). However, we showed that while large events do trigger widespread aggradation and deposition in some places (as in

Middle Lookout), incision and erosion dominate in others (as in Lower Lookout), and other places show only very localized changes (as in Mack Clearcut and Mack Old Growth). The persistence of channel change also differed between this study and others. While aggradational and depositional signals lasted for only 5 to 10 years in other studies (Di Silvio, 1994; Madej, 1987), the flood-related thalweg aggradation at Middle Lookout has lasted at least 15 years, from the major flood of 1996 until the end of active monitoring in 2011. Overall, patterns at the Andrews Forest imply a complex and long-lasting sediment storage response not documented in prior research.

The changes in bankfull width we observed more closely match previous findings. Channel widening is known to be a common adjustment to large floods and increased sediment supply (Major et al., 2019; Nardi & Rinaldi, 2015; Sholtes et al., 2018; Sloan et al., 2001; Surian et al., 2016; Yochum et al., 2017), and three out of four study reaches experienced an increase in bankfull width after the 1996 flood. This study also clarified the timing of channel widening in response to extreme flows. In several cross sections at Middle Lookout, maximum bankfull width actually occurred several years after the 1996 flood. One explanation for this might be that the thalweg aggradation raised the water surface elevation during all flows which made the banks of the channel more susceptible to erosion during subsequent smaller flows. As with thalweg adjustments, width adjustments generally persisted through the end of active monitoring in 2011.

Adjustments in bankfull depth and grain size to peak flows are less frequently described in the literature. However, from well-documented patterns of thalweg aggradation, we might assume that depth reduction and surface fining would be the typical response, since those responses have been observed elsewhere in aggrading systems (Lisle, 1982; Miller & Benda, 2000a). In contrast, out of the four study reaches, only Middle Lookout, an unconfined reach, became shallower and finer-bedded following the 1996 flood. Mack Clear Cut and Lower Lookout both became deeper and the bed material at those sites coarsened. The wood-stabilized Mack Old Growth experienced little change in either bankfull depth or D_{50} .

Mountain streams might return to their pre-flood sediment transport conditions much more quickly than they return to their pre-flood cross-sectional geometries. While the 1996 flood produced a decadal-scale impact on channel geometry in many parts of the study reaches, grain size adjustment occurred on the 1 to 5-year time scale. Grain size adjustments both Lower

Lookout and Middle Lookout suggest that different parts of the reaches coarsened or fined their surface layer in response to cross sectional geometry adjustment (Figure 14a, Figure 15a, Figure 18a, Figure 19a). Sorting adjustments in cross sections LOL06 to LOL08 and LOM06 to LOM07 occurred on roughly a 5-year time scale as the stream reworked surface sediments (Figure 15b, Figure 19b). Bankfull Shields stress values suggest that from a sediment transport perspective, many parts of the study reaches returned to resemble their pre-flood state within 2–5 years after the major disturbance of 1996. This coevolution of grain size and channel depth supports the idea in recent literature that mountain streams can adjust to a large sediment pulse within a matter of years (Buffington & Montgomery, 1999; Eaton & Church, 2009; Fratkin et al., 2020; Madej et al., 2009; Mueller & Pitlick, 2013).

5.3. Variation within an unconfined and a confined reach

Prior research has widely demonstrated sediment storage and channel widening behind instream wood jams (Abbe & Montgomery, 2003; Adenlof & Wohl, 1994; Faustini & Jones, 2003; Nakamura & Swanson, 1993; Swanson et al., 1976; Swanson & Lienkaemper, 1978). This study provides a demonstration of how channel storage and cross-sectional geometry upstream of channel-spanning logjams evolve over both space and time. Two channel-spanning logjams strongly modulated channel adjustment in the unconfined Middle Lookout reach, impacting sediment storage, cross-sectional geometry, and grain size. A lower logjam developed before 1996 and an upper logjam was emplaced by the 1996 flood (Figure 2b). The broad, flat valley surrounding Middle Lookout mitigated flood energy during the 1996 flood, provided source wood for these instream wood accumulations, and allowed for wood persistence on the decadal timescale.

Middle Lookout experienced minor, localized deposition directly upstream of the lower logjam until 1996 (Figure 17a) when the flood racked additional wood onto the preexisting jam. The additional wood potentially combined with increased sediment input from the nearby valley wall landslide (Figure 1, point C) triggered sediment deposition, aggradation, and channel widening apparent for at least 100 meters upstream the lower jam. In 1996, summer field surveys showed that the upper logjam remained relatively small but played a role in anchoring a point bar near LOM04 (Faustini, 2000).

This wood-mediated depositional event modified the hydraulic energy gradient of the reach. As the total channel fall across the logjam increased, the channel gradient upstream of the logjam decreased. This gradient reduction is visible in thalweg aggradation measurements (Figure 17b): the magnitude of thalweg aggradation decreased with distance from the wood jam. The diminished slope and water depth (Figure 18a) facilitated deposition of relatively fine-grained sediment in the upstream zone (Figure 19a). Energy losses due to the fall over the wood jam (MacFarlane & Wohl, 2003; Swanson & Lienkaemper, 1978) might also account for the minor fining trend seen in the downstream cross sections (Figure 19a).

Middle Lookout's upper logjam appears to have influenced the evolution of the lower logjam and nearby channel in the years following 1996. Researchers (Julia Jones, personal communication) have hypothesized that as it grew, the upstream logjam deprived the lower logjam of additional wood by racking all of the large wood pieces entering the reach from the upstream end. Starting around 2000, this triggered the gradual disaggregation of the lower logjam which now exists as a large but diffuse structure (Figure B.4). This disaggregation increased the sediment supply to the lower part of the reach downstream of the lower logjam and triggered additional deposition and thalweg aggradation in those cross sections, which can be seen in the downstream cross sections beginning in 2000 (Figure 17).

While the upstream mass wasting event (Figure 1, point C) may have influenced Middle Lookout's adjustment by increasing fluid density and sediment supply, the role of the downstream debris flow (Figure 1, point B) remains unclear. If the downstream debris flow deposited a large amount of wood or other material close to the lower end of the reach, it could have had upward-propagating effects that could influence the lower end of the reach. However, there were no measurements of local channel changes where that debris flow entered Lookout Creek, so the exact nature of its effects are a matter of speculation.

The 1996 flood at Lower Lookout was marked by wood removal rather than wood emplacement. As the dense, debris-laden flow moved through the stream bend at this partially confined reach, it took with it several channel spanning logjams that had been situated between cross-sections LOL07 and LOL08 (Figure 3). In this section of the reach, the flow extensively scoured out the creek's left-bank (east) side-channel, creating a new primary channel away from where the rootwads of the instream wood had been located. The location of scour suggests that

the wood may have directed the flow towards the opposing (inner) bank (Abbe & Montgomery, 2003; Adenlof & Wohl, 1994; Daniels & Rhoads, 2003) before it was carried away. The relatively extreme channel changes observed near the wood removal zone match prior findings that show that wood removal is associated with scour and increased bedload transport in mountain streams (Adenlof & Wohl, 1994; Bugosh & Custer, 1989; Hogan, 1987). The depositional/aggradational zone immediately downstream of the wood removal zone suggests either that (a) the scoured sediment moved only a short distance and was deposited in the downstream subreach or (b) that bank failure and channel widening added sediment to the channel and promoted further deposition.

The relatively minor changes observed upstream of the river bend and wood removal zone suggest that in contrast to Middle Lookout, channel changes in this reach propagated in a primarily downstream rather than a primarily upstream direction. This may be due in part to the location of the river bends in this part of the stream. Cross sections LOL13 and LOL14 are located between two relatively sharp, confined bends (Figure 1, Figure 2) that may exert primary control on this straight channel section and protect these two cross sections from being affected by changes upstream or downstream.

The disparate and spatially variable channel responses within Lower Lookout reflect the dynamic history of the reach itself. Historic maps (Figure 3) show that large wood has moved frequently in and out of the system, especially following large peak flow events (Figure 3d, Figure 3f) and that the river has migrated within its valley several times since the late 1970s. Field work in 2019 showed additional large, channel-spanning wood structures that differed from those mapped in 2011 (Figure B.3). This suggests that wood in this moderate-gradient, partly confined reach is subject to frequent movement and rearrangement. The confined geometry may increase the hydraulic effectiveness of large floods and promote wood transport, as floated wood transport depends on water depth (Braudrick et al., 1997), and water depth during bank-exceeding flows is related to the cross sectional geometry of the valley (Leopold & Maddock, 1953). The greater flow depth in confined versus unconfined channels has been proposed as one explanation for lower frequency of logjams in confined valleys (Segura & Booth, 2010; Wohl & Cadol, 2011). This suggests that while large wood recruitment is possible in confined reaches,

large wood may not be able to play a stabilizing role during large flow events as it does in unconfined reaches.

Another potential cause of channel change in this reach is the influence of historical logging and roadbuilding that occurred before the start of the study. The flood of December 1964 triggered a record number of landslides and debris flows, which increased sediment supply to the stream (Johnson & Swanson, 2014; Jones & Grant, 1996; Snyder, 2000). Additionally, clearcutting in the early 1960s left a narrow riparian buffer near the bend of Lower Lookout (Figure A.2) as well as in many other areas upstream of the reach, further facilitating hillslope-channel interaction. If the increased sediment supply in 1964 led to deposition in Lower Lookout is possible that some of the scouring induced by the 1996 flood represent remobilization of large material emplaced by the 1964 flood.

5.4. Comparison to channel adjustment in other long-term study sites

The long term cross section study at the Andrews Forest is one of three long term mountain stream cross section monitoring projects in the Pacific Northwest established in the 1970s and 1980s. Other sites include Redwood Creek, in Northern California, the Toutle River at Mt. St. Helens, Washington, and Carnation Creek in coastal British Columbia. The sites vary in land use history, underlying lithology, and the timing of major disturbance events. Patterns of channel adjustment at the Andrews Forest differ from patterns seen at any of these other three sites. In comparison to the other long-term monitoring sites, the cross sections at the Andrews Forest appear relatively quiescent. The differences are likely due in a large part to lithology, which exerts strong controls on sediment transport and channel form (Mueller & Pitlick, 2013; O'Connor et al., 2014; Pfeiffer et al., 2017). An understanding of more subdued geomorphic responses as seen in the Andrews Forest might help inform those making watershed decisions in basins of similarly resistant lithology. The geologic composition of the Andrews Forest is in many ways similar to much of the rest of the Oregon Cascades which are dominated by Eocene and younger volcanic rocks (Peck et al., 1964). Geomorphic lessons learned in these streams might be applicable to other managed land within this part of Cascade Range.

The Redwood Creek study was started in 1975 and study reaches were resurveyed at various intervals until 2013 (Madej et al., 2018). Like the Andrews Forest, the Redwood Creek

watershed experienced logging and roadbuilding in the late 20th century, but the forest harvest at Redwood Creek was more extensive. A full 81% of the Redwood Creek watershed was logged by 1978, and second growth harvest has continued within the upper portion of the watershed (Madej, 2009). As in the Andrews forest, the Redwood Creek watershed experienced widespread landsliding in the winter of 1964, which was associated with forest harvest and roadbuilding (Madej, 1992). Redwood Creek is underlain by highly friable mudstones, sandstones, and schists (Madej, 1999). Long term monitoring at Redwood Creek showed that large (10–25-year) floods at that site triggered aggradation and pool in-filling followed by “recovery” periods of incision and pool formation in lower-flow years (Madej, 2009). Channel adjustment varied by location within the watershed – in the upper third of the channel, peak aggradation occurred quickly, and channel-stored sediment was evacuated within 5 to 10 years (Madej, 1987). In the lower portion of the watershed, peak aggradation occurred decades later in the 1990s, and the channel had not returned to its pre-aggradation condition by 2009 (Madej, 2009).

In contrast to the widespread aggradational response at Redwood Creek, the flood of record in the Andrews forest did not trigger aggradation in most cross sections, and most cross sections that experienced aggradation did not fully return to their pre-flood conditions within such a short time scale (Figure 13, Figure 17, and Figure A.5). The more rapid return to pre-flood conditions at Redwood Creek could be explained by that site’s highly friable lithology (Madej, 1992). The location of sediment storage also differs between the two sites. At Redwood Creek, channel-spanning wood pieces are rare, and much of the sediment was stored in pools (Madej, 2009). While we do not have a long term pool depth records at the Andrews Forest, the 1996 flood increased storage of sediment behind logjams in Mack Old Growth (Faustini & Jones, 2003) and in Middle Lookout (Figure 17). Likewise the removal of a logjam at Lower Lookout removed stored sediment upstream of the log. This suggest that wood may play a greater role in the placement of sediment storage reservoirs and the timing of their excavation in watersheds that have more resistant lithology.

The Toutle River at Mt. St. Helens, has been influenced by a number of processes related to very recent (May 1980) volcanism including pyroclastic flows, lahars, and avalanches. Thick, hummocky valley fill up to 150 m in depth completely reshaped the river valley. Redevelopment of a fluvial drainage network took several years (Janda et al., 1984). Shortly after the eruption,

researchers installed more than sixty permanent cross sections for long-term monitoring (D. F. Meyer et al., 1985). The Toutle River cross sections have shown dramatic changes in fluvial form in the decades since eruption (Major et al., 2019). Initial adjustment of the Toutle River was characterized by incision upstream and elevated downstream sediment delivery. Between the start of post-eruption monitoring in 1980 and 2010, vertical thalweg adjustment ranged from 40 m of incision in the upper North Fork Toutle to 39 m of aggradation at a site 33 km downstream (Zheng et al., 2014). From 1982 to 1985, water was pumped from Spirit Lake into part of the North Fork Toutle River at a rate similar to a 10-year flood flow, which triggered tens of meters of incision and tens of meters of channel widening. Since the start of monitoring, individual floods of natural origin caused incision and widening in the upper reaches of the North Fork Toutle River, and in some cases, deposited the displaced sediment several hundred meters downstream (Major et al., 2019).

Channel adjustments at the Toutle watershed are an order of magnitude greater than those observed in the Andrews Forest. The large adjustments in the Toutle watershed likely reflect the river vertically regrading (Zheng et al., 2014) as well as horizontally adjusting (widening) to accommodate a persistently high sediment supply (Major et al., 2019). The Toutle River experienced a major disruption to its long profile within the last 40 years, while the last major, grade-altering disturbance in the Andrews Forest, occurred more than 7,000 years ago (Swanson & James, 1975). In other studies (East et al., 2018; Yochum et al., 2017) as well as in Middle Lookout, channel widening is more often paired with aggradation than with incision. While both the Toutle watershed and the Andrews Forest responded to increased sediment supply, the sediment supply in the Andrews Forest increased via a single, relatively discrete pulse of debris flows, while the sediment increase in the Toutle was so much greater than the transport capacity of the stream that the sediment supply could be reasonably considered to be continuous. The results of this study may then provide insights into understanding pulsed rather than continuous sediment supply events in forested mountain watersheds.

While not strictly a cross section monitoring study, researchers at the Carnation Creek Experimental Watershed in British Columbia have been monitoring longitudinal profiles and detailed topographic surveys of study sections since 1970. The lithology at that site is dominated by Jurassic volcanics mantled by glacial till (Reid et al., 2019). This site experienced a large

debris flow between 10 and 40 times the estimated annual bed load volume in the early 1980s, and patterns of channel adjustment suggest that the excess sediment moves through the system on the multidecadal time scale (Reid et al., 2019). As in the Andrews Forest, large wood is locally associated with instream sediment storage, although large wood in Carnation Creek has decreased over time, while it has not decreased within the study reaches at the Andrews Forest.

5.5. Implications for aquatic habitat

The study reaches' varied response to the flood of 1996 event suggests potential implications for aquatic habitat. Although biotic communities in the Andrews forest recovered quickly after the 1996 flood (Swanson et al., 1998) the flood triggered persistent adjustments in characteristics relevant to aquatic habitat including cross-sectional geometry, particle size, and wood presence. Cross-sectional geometry influences both stream temperature water velocity, with impact for aquatic organisms (Aadland, 1993; Edington, 1968; Lister & Genoe, 1970; Meffe & Sheldon, 1988). Bed surface grain size distributions also affect the distribution, reproduction, and survival of aquatic organisms (Beard & Carline, 1991; Gayraud & Philippe, 2003). Wood creates both low-velocity areas and shelter in streams and is used by fish and other aquatic organisms (Bisson et al., 1987; Harmon et al., 1986; Lisle, 1986; Swanson et al., 1982). However, at high flows instream wood was much more resilient in the unconfined reach than the confined one, which suggests that wood-anchored habitats might be particularly vulnerable to flood effects in confined reaches.

5.6. Opportunities for Further Research

Additional metrics or methods could also be helpful for understanding channel form and function following a large flood. Width and depth analyses in this study were based on estimated bankfull water surface elevations, but the stream also experiences flows greater than or less than bankfull flows. Field-collected or remotely sensed information showing water surface elevation during various high flow events could provide better clues about the true hydraulic geometry at these study reaches under varied flow conditions. The particle count component of this study began nearly twenty years after the start of cross section monitoring, which makes it a much

shorter data set. Additional years of particle counts could provide useful information about the dynamics and natural variability of grain size changes in these streams.

While it would be convenient to have more study reaches to help disentangle the overlapping effects of instream wood, debris flows, and landscape structure, it seems economically infeasible to start additional cross section studies. Instead, it might be possible for new technology to facilitate related geomorphic studies that could be carried out over the long term at reduced field cost. Improvements in structure-from-motion technology and image processing mean that very low-elevation aerial photography, as used previously at this site (Swanson et al., 1998; Wondzell & Swanson, 1999) could potentially be used to image both the geometry and the grain sizes of parts of the streambed above the low-flow channel (Bird et al., 2010).

6. Conclusions

We investigated channel adjustment for 15 years following a large, debris-laden flood in a forested mountain watershed in the Oregon Cascades. The watershed has resistant volcanic lithology and a history of disturbance via logging and roadbuilding that is typical of other watersheds in this region. Our results indicate that large floods in these systems can trigger persistent changes in channel width, depth, and in-stream sediment storage that last for at least 15 years after disturbance. Valley width appeared to play a major role in the stability of in-stream wood features during high flow events. In turn, channel-spanning logjams appeared to strongly influence the location of areas of scour and fill. Valley width and wood supply should be considered when assessing similar watersheds for vulnerability to flood-induced channel change, especially around critical habitat or infrastructure.

Patterns of flood response documented in this study differ from those seen in previous long-term studies on account of differences in lithology, disturbance history, sediment supply, and wood recruitment. This study expands our understanding of possible disturbance responses in watersheds that appear relatively “quiet” in terms of channel change. Rapid (1 to 5-year) adjustment of bed surface textures and concurrent adjustments of Shields stress values suggest that from a sediment transport perspective, these streams may return quickly to pre-flood

conditions. Longer-term monitoring of bed surface texture could help clarify the behavior of bed surface sediment during and after large floods and its role in channel adjustment.

7. References

- Aadland, L. P. (1993). Stream Habitat Types: Their Fish Assemblages and Relationship to Flow. *North American Journal of Fisheries Management*, 13(4), 790–806.
[https://doi.org/10.1577/1548-8675\(1993\)013<0790:SHTTFA>2.3.CO;2](https://doi.org/10.1577/1548-8675(1993)013<0790:SHTTFA>2.3.CO;2)
- Abbe, T. B., & Montgomery, D. R. (2003). Patterns and processes of wood debris accumulation in the Queets river basin, Washington. *Geomorphology*, 51(1), 81–107.
[https://doi.org/10.1016/S0169-555X\(02\)00326-4](https://doi.org/10.1016/S0169-555X(02)00326-4)
- Adenlof, K. A., & Wohl, E. E. (1994). Controls on Bedload Movement in a Subalpine Stream of the Colorado Rocky Mountains, U.S.A. *Arctic and Alpine Research*, 26(1), 77–85.
<https://doi.org/10.1080/00040851.1994.12003043>
- Anderson, S. W., & Konrad, C. P. (2019). Downstream-Propagating Channel Responses to Decadal-Scale Climate Variability in a Glaciated River Basin. *Journal of Geophysical Research: Earth Surface*, 124(4), 902–919. <https://doi.org/10.1029/2018JF004734>
- Baker, V. R. (1977). Stream-channel response to floods, with examples from central Texas. *GSA Bulletin*, 88(8), 1057–1071. [https://doi.org/10.1130/0016-7606\(1977\)88<1057:SRTFWE>2.0.CO;2](https://doi.org/10.1130/0016-7606(1977)88<1057:SRTFWE>2.0.CO;2)
- Batalla, R. J., Jong, C. D., Ergenzinger, P., & Sala, M. (1999). Field observations on hyperconcentrated flows in mountain torrents. *Earth Surface Processes and Landforms*, 24(3), 247–253. [https://doi.org/10.1002/\(SICI\)1096-9837\(199903\)24:3<247::AID-ESP961>3.0.CO;2-1](https://doi.org/10.1002/(SICI)1096-9837(199903)24:3<247::AID-ESP961>3.0.CO;2-1)
- Beard, T. D., & Carline, R. F. (1991). Influence of Spawning and Other Stream Habitat Features on Spatial Variability of Wild Brown Trout. *Transactions of the American Fisheries Society*, 120(6), 711–722. [https://doi.org/10.1577/1548-8659\(1991\)120<0711:IOSAOS>2.3.CO;2](https://doi.org/10.1577/1548-8659(1991)120<0711:IOSAOS>2.3.CO;2)
- Benda, L., & Dunne, T. (1997). Stochastic forcing of sediment supply to channel networks from landsliding and debris flow. *Water Resources Research*, 33(12), 2849–2863.
<https://doi.org/10.1029/97WR02388>
- Bierlmaier, F. A. (1989). *Climatic Summaries and Documentation for the Primary Meteorological Station, H.J. Andrews Experimental Forest, 1972 to 1984*. U.S. Department of Agriculture, Forest Service, Pacific Northwest Research Station.
- Bird, S., Hogan, D., & Schwab, J. (2010). Photogrammetric monitoring of small streams under a riparian forest canopy. *Earth Surface Processes and Landforms*, 35(8), 952–970.
<https://doi.org/10.1002/esp.2001>

- Bisson, P. A., Bilby, R. E., Bryant, M. D., Dolloff, C. A., Grette, G. B., House, R. A., Murphy, M. L., Koski, K. V., & Sedell, J. R. (1987). Large Woody Debris in Forested Streams in the Pacific Northwest: Past, Present, and Future. In *Streamside management, forestry and fishery interactions* (p. 51). Institute of Forest Research, University of Washington.
- Braudrick, C. A., Grant, G. E., Ishikawa, Y., & Ikeda, H. (1997). Dynamics of Wood Transport in Streams: A Flume Experiment. *Earth Surface Processes and Landforms*, 22(7), 669–683. [https://doi.org/10.1002/\(SICI\)1096-9837\(199707\)22:7<669::AID-ESP740>3.0.CO;2-L](https://doi.org/10.1002/(SICI)1096-9837(199707)22:7<669::AID-ESP740>3.0.CO;2-L)
- Brummer, C. J., & Montgomery, D. R. (2006). Influence of coarse lag formation on the mechanics of sediment pulse dispersion in a mountain stream, Squire Creek, North Cascades, Washington, United States. *Water Resources Research*, 42(7). <https://doi.org/10.1029/2005WR004776>
- Buffington, J. M., & Montgomery, D. R. (1997). A systematic analysis of eight decades of incipient motion studies, with special reference to gravel-bedded rivers. *Water Resources Research*, 33(8), 1993–2029. <https://doi.org/10.1029/96WR03190>
- Buffington, J. M., & Montgomery, D. R. (1999). Effects of hydraulic roughness on surface textures of gravel-bed rivers. *Water Resources Research*, 35(11), 3507–3521. <https://doi.org/10.1029/1999WR900138>
- Bugosh, N., & Custer, S. G. (1989). Effect of a log-jam burst on bedload transport and channel characteristics in a headwaters stream. *Proceedings of the Symposium on Headwaters Hydrology. American Water Resources Association, Bethesda Maryland. 1989. p 203-211, 5 Fig, 1 Tab, 15 Ref, 1989.*
- Bunte, K., & Abt, S. R. (2001). *Sampling surface and subsurface particle-size distributions in wadable gravel-and cobble-bed streams for analyses in sediment transport, hydraulics, and streambed monitoring* (RMRS-GTR-74). U.S. Department of Agriculture, Forest Service, Rocky Mountain Research Station. <https://doi.org/10.2737/RMRS-GTR-74>
- Cenderelli, D. A., & Wohl, E. E. (2003). Flow hydraulics and geomorphic effects of glacial-lake outburst floods in the Mount Everest region, Nepal. *Earth Surface Processes and Landforms*, 28(4), 385–407. <https://doi.org/10.1002/esp.448>
- Church, M. (2002). Geomorphic thresholds in riverine landscapes. *Freshwater Biology*, 47(4), 541–557. <https://doi.org/10.1046/j.1365-2427.2002.00919.x>
- Costa, J. E. (1984). Physical Geomorphology of Debris Flows. In J. E. Costa & P. J. Fleisher (Eds.), *Developments and Applications of Geomorphology* (pp. 268–317). Springer. https://doi.org/10.1007/978-3-642-69759-3_9
- Daniels, M. D., & Rhoads, B. L. (2003). Influence of a large woody debris obstruction on three-dimensional flow structure in a meander bend. *Geomorphology*, 51(1), 159–173. [https://doi.org/10.1016/S0169-555X\(02\)00334-3](https://doi.org/10.1016/S0169-555X(02)00334-3)

- de Jong, C. (1992). A catastrophic flood/multiple debris flow in a confined mountain stream: An example from the Schmedlaine, southern Germany. *Proceedings of Chengdu Symposium on Erosion, Debris Flows and Environment in Mountain Regions*, 209.
- Di Silvio, G. (1994). Floods and sediment dynamics in mountain rivers. In G. Rossi, N. Harmancioğlu, & V. Yevjevich (Eds.), *Coping with Floods* (pp. 375–392). Springer Netherlands. https://doi.org/10.1007/978-94-011-1098-3_21
- Dunne, T., & Leopold, L. B. (1979). Water in environmental planning, Thomas Dunne and Luna Leopold, W. H. Freeman & Co. San Francisco. Price: £17.40. *Earth Surface Processes*, 4(3), 305–306. <https://doi.org/10.1002/esp.3290040322>
- Dyrness, T., Swanson, F. J., Grant, G., Gregory, S., Jones, J., Kurosawa, K., Levno, A., Henshaw, D., & Hammond, H. (1996). *Flood of February, 1996 in the H.J. Andrews Experimental Forest* (p. 34).
- East, A. E., Logan, J. B., Mastin, M. C., Ritchie, A. C., Bountry, J. A., Magirl, C. S., & Sankey, J. B. (2018). Geomorphic Evolution of a Gravel-Bed River Under Sediment-Starved Versus Sediment-Rich Conditions: River Response to the World’s Largest Dam Removal. *Journal of Geophysical Research: Earth Surface*, 123(12), 3338–3369. <https://doi.org/10.1029/2018JF004703>
- Eaton, B. C., & Church, M. (2009). Channel stability in bed load–dominated streams with nonerodible banks: Inferences from experiments in a sinuous flume. *Journal of Geophysical Research: Earth Surface*, 114(F1). <https://doi.org/10.1029/2007JF000902>
- Edington, J. M. (1968). Habitat Preferences in Net-Spinning Caddis Larvae with Special Reference to the Influence of Water Velocity. *Journal of Animal Ecology*, 37(3), 675–692. JSTOR. <https://doi.org/10.2307/3081>
- Faustini, J. M. (2000). *Stream channel response to peak flows in a fifth-order mountain watershed* [Dissertation, Oregon State University]. https://ir.library.oregonstate.edu/concern/graduate_thesis_or_dissertations/t722hc913
- Faustini, J. M., & Jones, J. A. (2003). Influence of large woody debris on channel morphology and dynamics in steep, boulder-rich mountain streams, western Cascades, Oregon. *Geomorphology*, 51(1–3), 187–205. [https://doi.org/10.1016/S0169-555X\(02\)00336-7](https://doi.org/10.1016/S0169-555X(02)00336-7)
- Folk, R. L., & Ward, W. C. (1957). Brazos River bar [Texas]; a study in the significance of grain size parameters. *Journal of Sedimentary Research*, 27(1), 3–26. <https://doi.org/10.1306/74D70646-2B21-11D7-8648000102C1865D>
- Fratkin, M. M., Segura, C., & Bywater-Reyes, S. (2020). The influence of lithology on channel geometry and bed sediment organization in mountainous hillslope-coupled streams. *Earth Surface Processes and Landforms*, 45(10), 2365–2379. <https://doi.org/10.1002/esp.4885>

- Gayraud, S., & Philippe, M. (2003). Influence of Bed-Sediment Features on the Interstitial Habitat Available for Macroinvertebrates in 15 French Streams. *International Review of Hydrobiology*, 88(1), 77–93. <https://doi.org/10.1002/iroh.200390007>
- Gintz, D., Hassan, M. A., & Schmidt, K.-H. (1996). Frequency and Magnitude of Bedload Transport in a Mountain River. *Earth Surface Processes and Landforms*, 21(5), 433–445. [https://doi.org/10.1002/\(SICI\)1096-9837\(199605\)21:5<433::AID-ESP580>3.0.CO;2-P](https://doi.org/10.1002/(SICI)1096-9837(199605)21:5<433::AID-ESP580>3.0.CO;2-P)
- Gomi, T., & Sidle, R. C. (2003). Bed load transport in managed steep-gradient headwater streams of southeastern Alaska. *Water Resources Research*, 39(12). <https://doi.org/10.1029/2003WR002440>
- Grant, G. E., & Swanson, F. J. (1995). Morphology and Processes of Valley Floors in Mountain Streams, Western Cascades, Oregon. In *Natural and Anthropogenic Influences in Fluvial Geomorphology* (pp. 83–101). American Geophysical Union (AGU). <https://doi.org/10.1029/GM089p0083>
- Harmon, M. E., Franklin, J. F., Swanson, F. J., Sollins, P., Gregory, S. V., Lattin, J. D., Anderson, N. H., Cline, S. P., Aumen, N. G., Sedell, J. R., Lienkaemper, G. W., Cromack, K., & Cummins, K. W. (1986). Ecology of Coarse Woody Debris in Temperate Ecosystems. In A. MacFadyen & E. D. Ford (Eds.), *Advances in Ecological Research* (Vol. 15, pp. 133–302). Academic Press. [https://doi.org/10.1016/S0065-2504\(08\)60121-X](https://doi.org/10.1016/S0065-2504(08)60121-X)
- Harrelson, C. C., Rawlins, C. L., & Potyondy, J. P. (1994). *Stream channel reference sites: An illustrated guide to field technique* (RM-GTR-245). U.S. Department of Agriculture, Forest Service, Rocky Mountain Forest and Range Experiment Station. <https://doi.org/10.2737/RM-GTR-245>
- Hartman, G. F., & Scrivener, J. C. (1993). Impacts of forestry practices on a coastal stream ecosystem, Carnation Creek, British Columbia (Canadian bulletin of fisheries and aquatic sciences No. 223). *Reviews in Fish Biology and Fisheries*. <https://doi.org/10.1007/BF00043304>
- Hassan, M. A., Hogan, D. L., Bird, S. A., May, C. L., Gomi, T., & Campbell, D. (2005). Spatial and Temporal Dynamics of Wood in Headwater Streams of the Pacific Northwest. *JAWRA Journal of the American Water Resources Association*, 41(4), 899–919. <https://doi.org/10.1111/j.1752-1688.2005.tb03776.x>
- Hogan, D. L. (1987). The Influence of Large Organic Debris on Channel Recovery in the Queen Charlotte Islands, British Columbia, Canada. In *Erosion and Sedimentation in the Pacific Rim* (Vol. 165). http://hydrologie.org/redbooks/a165/iahs_165_0343.pdf
- Hogan, D. L., Bird, S. A., & Hassan, M. A. (1998). Spatial and Temporal Evolution of Small Coastal Gravel-Bed Streams. In *Gravel-bed rivers in the environment* (pp. 365–392). Water Resources Publications. <https://coast.noaa.gov/data/czm/pollutioncontrol/media/Technical/D48%20->

%20Hogan,%20D.L.,%20S.A.%20Bird,%20and%20M.A.%20Hassan.%201998.%20Spatial
%20and%20Temporal%20Evolution%20of%20Small%20Coastal%20Gravel-
Bed%20Streams.pdf

- Janda, R., Meyer, D., & Childers, D. (1984). Sedimentation and Geomorphic Changes During and Following the 1980-1983 Eruption of Mt. St. Helens, Washington. *Sabo Gakkaishi*, 37(3), 5–19. https://doi.org/10.11475/sabo1973.37.3_5
- Janda, R., Nolan, K. M., Harden, D. R., & Colman, S. M. (1975). Watershed conditions in the drainage basin of Redwood Creek, Humboldt County, California, as of 1973. In *Open-File Report* (No. 75–568). United States Geological Survey,. <https://doi.org/10.3133/ofr75568>
- Johnson, S. L., Grant, G. E., Swanson, F. J., & Wemple, B. C. (1997). Lessons from a flood: An integrated view of the February 1996 flood in the McKenzie River basin. *The Pacific Northwest Floods of February 6-11, 1996: Proceedings of the Pacific Northwest Water Issues Conference*, 159–167.
- Johnson, S. L., & Swanson, F. J. (2014). *Stream cross-section profiles in the Andrews Experimental Forest and Hagan Block RNA 1978 to present (Version 10) [database]*. <http://andlter.forestry.oregonstate.edu/data/abstract.aspx?dbcode=GS002>
- Johnson, S. L., Swanson, F. J., Grant, G. E., & Wondzell, S. M. (2000). Riparian forest disturbances by a mountain flood—The influence of floated wood. *Hydrological Processes*, 14(16–17), 3031–3050. [https://doi.org/10.1002/1099-1085\(200011/12\)14:16/17<3031::AID-HYP133>3.0.CO;2-6](https://doi.org/10.1002/1099-1085(200011/12)14:16/17<3031::AID-HYP133>3.0.CO;2-6)
- Johnson, S. L., Wondzell, S. M., Rothacher, J. S., & Jones, J. A. (2019). *Stream discharge in gaged watersheds at the HJ Andrews Experimental Forest, 1949 to present (Version 31) [database]*. <http://andlter.forestry.oregonstate.edu/data/abstract.aspx?dbcode=HF004>
- Jones, J. A., & Grant, G. E. (1996). Peak Flow Responses to Clear-Cutting and Roads in Small and Large Basins, Western Cascades, Oregon. *Water Resources Research*, 32(4), 959–974. <https://doi.org/10.1029/95WR03493>
- Jones, J. A., & Perkins, R. M. (2010). Extreme flood sensitivity to snow and forest harvest, western Cascades, Oregon, United States. *Water Resources Research*, 46(12). <https://doi.org/10.1029/2009WR008632>
- Klingeman, P. C. (1973). *Indications of Streambed Degradation in the Willamette Valley* (p. 96) [Project Completion Report]. Office of Water Resources Research U .S . Department of the Interior.
- Krapesch, G., Hauer, C., & Habersack, H. (2011). Scale orientated analysis of river width changes due to extreme flood hazards. *Natural Hazards and Earth System Sciences*, 11(8), 2137–2147. <https://doi.org/10.5194/nhess-11-2137-2011>

- Lenzi, M. A., Mao, L., & Comiti, F. (2006). Effective discharge for sediment transport in a mountain river: Computational approaches and geomorphic effectiveness. *Journal of Hydrology*, 326(1), 257–276. <https://doi.org/10.1016/j.jhydrol.2005.10.031>
- Leopold, L. B., & Maddock, T. (1953). *The hydraulic geometry of stream channels and some physiographic implications* (Report No. 252; Professional Paper, p. 64). USGS Publications Warehouse. <https://doi.org/10.3133/pp252>
- Lisle, T. E. (1981). The recovery of aggraded stream channels at gauging stations in northern California and southern Oregon. *Erosion and Sediment Transport in Pacific Rim Steeplands*, 132, 12.
- Lisle, T. E. (1982). Effects of aggradation and degradation on riffle-pool morphology in natural gravel channels, northwestern California. *Water Resources Research*, 18(6), 1643–1651. <https://doi.org/10.1029/WR018i006p01643>
- Lisle, T. E. (1986). Stabilization of a gravel channel by large streamside obstructions and bedrock bends, Jacoby Creek, northwestern California. *Geological Society of America Bulletin* 97: 999-1011. <https://www.fs.usda.gov/treearch/pubs/7838>
- Lister, D. B., & Genoe, H. S. (1970). Stream Habitat Utilization by Cohabiting Underyearlings of Chinook (*Oncorhynchus tshawytscha*) and Coho (*O. kisutch*) Salmon in the Big Qualicum River, British Columbia. *Journal of the Fisheries Research Board of Canada*, 27(7), 1215–1224. <https://doi.org/10.1139/f70-144>
- MacFarlane, W. A., & Wohl, E. (2003). Influence of step composition on step geometry and flow resistance in step-pool streams of the Washington Cascades. *Water Resources Research*, 39(2). <https://doi.org/10.1029/2001WR001238>
- Madej, M. A. (1987). Residence times of channel-stored sediment in Redwood Creek, northwestern California. In *Publication* (No. 165; pp. 429–438). International Association of Hydrological Sciences. <https://pubs.er.usgs.gov/publication/2002171>
- Madej, M. A. (1992). *Changes in Channel-Stored Sediment, Redwood Creek, Northwestern California, 1947 to 1980* (USGS Numbered Series No. 92–34; Open-File Report, p. 43). Geological Survey (U.S.).
- Madej, M. A. (1999). Temporal and spatial variability in thalweg profiles of a gravel-bed river. *Earth Surface Processes and Landforms*, 24(12), 1153–1169. [https://doi.org/10.1002/\(SICI\)1096-9837\(199911\)24:12<1153::AID-ESP41>3.0.CO;2-8](https://doi.org/10.1002/(SICI)1096-9837(199911)24:12<1153::AID-ESP41>3.0.CO;2-8)
- Madej, M. A. (2009). Persistence of effects of high sediment loading in a salmon-bearing river, northern California, in James, L.A., Rathburn, S.L., and Whittecar, G.R., eds., *Management and Restoration of Fluvial Systems with Broad Historical Changes and Human Impacts. Special Paper of the Geological Society of America.*

- Madej, M. A., & Ozaki, V. (1996). Channel response to sediment wave propagation and movement, Redwood Creek, California, USA. *Earth Surface Processes and Landforms*, 21, 911–927.
- Madej, M. A., Ozaki, V., Truesdell, R., Falvo, C. I., Enns, K. D., Bell, T. M., Everette, A. L., & Faundeen, J. L. (2018). *River Channel Survey Data, Redwood Creek, California, 1953-2013* [Data set]. U.S. Geological Survey. <https://doi.org/10.5066/P9G0N0TN>
- Madej, M. A., Sutherland, D. G., Lisle, T. E., & Pryor, B. (2009). Channel responses to varying sediment input: A flume experiment modeled after Redwood Creek, California. *Geomorphology*, 103(4), 507–519. <https://doi.org/10.1016/j.geomorph.2008.07.017>
- Maita, H. (1991). Sediment Dynamics of a High Gradient Stream in Oi River Basin of Japan. In *Proceedings of the IUFRO Technical Session on Geomorphic Hazards in Managed Forests: August 5-11, 1990, Montreal, Canada*. Pacific Southwest Research Station.
- Major, J. J., Zheng, S., Mosbrucker, A. R., Spicer, K. R., Christianson, T., & Thorne, C. R. (2019). Multidecadal Geomorphic Evolution of a Profoundly Disturbed Gravel Bed River System—A Complex, Nonlinear Response and Its Impact on Sediment Delivery. *Journal of Geophysical Research: Earth Surface*, 124(5), 1281–1309. <https://doi.org/10.1029/2018JF004843>
- Mao, L., & Lenzi, M. A. (2007). Sediment mobility and bedload transport conditions in an alpine stream. *Hydrological Processes*, 21(14), 1882–1891. <https://doi.org/10.1002/hyp.6372>
- Marks, D., Kimball, J., Tingey, D., & Link, T. (1998). The sensitivity of snowmelt processes to climate conditions and forest cover during rain-on-snow: A case study of the 1996 Pacific Northwest flood. *Hydrological Processes*, 12(10–11), 1569–1587. [https://doi.org/10.1002/\(SICI\)1099-1085\(199808/09\)12:10/11<1569::AID-HYP682>3.0.CO;2-L](https://doi.org/10.1002/(SICI)1099-1085(199808/09)12:10/11<1569::AID-HYP682>3.0.CO;2-L)
- Meffe, G. K., & Sheldon, A. L. (1988). The Influence of Habitat Structure on Fish Assemblage Composition in Southeastern Blackwater Streams. *American Midland Naturalist*, 120(2), 225. <https://doi.org/10.2307/2425994>
- Meyer, D. F., Nolan, K. M., & Dodge, J. E. (1985). Post-Eruption Changes in Channel Geometry of Streams in the Toutle River Drainage Basin, 1980-82, Mount St. Helens, Washington. In *Post-Eruption Changes in Channel Geometry of Streams in the Toutle River Drainage Basin, 1980-82, Mount St. Helens, Washington* (USGS Numbered Series No. 85–412; Open-File Report, Vols. 85–412). Geological Survey (U.S.). <https://doi.org/10.3133/ofr85412>
- Meyer, G. A., Pierce, J. L., Wood, S. H., & Jull, A. J. T. (2001). Fire, storms, and erosional events in the Idaho batholith. *Hydrological Processes*, 15(15), 3025–3038. <https://doi.org/10.1002/hyp.389>

- Miller, D. J., & Benda, L. E. (2000a). Effects of punctuated sediment supply on valley-floor landforms and sediment transport. *Geological Society of America Bulletin*, 11.
- Miller, D. J., & Benda, L. E. (2000b). Effects of punctuated sediment supply on valley-floor landforms and sediment transport. *GSA Bulletin*, 112(12), 1814–1824. [https://doi.org/10.1130/0016-7606\(2000\)112<1814:EOPSSO>2.0.CO;2](https://doi.org/10.1130/0016-7606(2000)112<1814:EOPSSO>2.0.CO;2)
- Montgomery, D. R., & Buffington, J. M. (1997). Channel-reach morphology in mountain drainage basins. *GSA Bulletin*, 109(5), 596–611. [https://doi.org/10.1130/0016-7606\(1997\)109<0596:CRMIMD>2.3.CO;2](https://doi.org/10.1130/0016-7606(1997)109<0596:CRMIMD>2.3.CO;2)
- Montgomery, D. R., Buffington, J. M., Smith, R. D., Schmidt, K. M., & Pess, G. (1995). Pool Spacing in Forest Channels. *Water Resources Research*, 31(4), 1097–1105. <https://doi.org/10.1029/94WR03285>
- Mueller, E. R., & Pitlick, J. (2005). Morphologically based model of bed load transport capacity in a headwater stream. *Journal of Geophysical Research: Earth Surface*, 110(F2). <https://doi.org/10.1029/2003JF000117>
- Mueller, E. R., & Pitlick, J. (2013). Sediment supply and channel morphology in mountain river systems: 1. Relative importance of lithology, topography, and climate. *Journal of Geophysical Research: Earth Surface*, 118(4), 2325–2342. <https://doi.org/10.1002/2013JF002843>
- Musselman, K. N., Lehner, F., Ikeda, K., Clark, M. P., Prein, A. F., Liu, C., Barlage, M., & Rasmussen, R. (2018). Projected increases and shifts in rain-on-snow flood risk over western North America. *Nature Climate Change*, 8(9), 808–812. <https://doi.org/10.1038/s41558-018-0236-4>
- Nakamura, F., & Swanson, F. J. (1993). Effects of coarse woody debris on morphology and sediment storage of a mountain stream system in western Oregon. *Earth Surface Processes and Landforms*, 18(1), 43–61. <https://doi.org/10.1002/esp.3290180104>
- Nakamura, F., & Swanson, F. J. (2003). Dynamics of wood in rivers in the context of ecological disturbance. *American Fisheries Society Symposium*, 2003, 279–297.
- Nakamura, F., Swanson, F. J., & Wondzell, S. M. (2000). Disturbance regimes of stream and riparian systems—A disturbance-cascade perspective. *Hydrological Processes*, 14(16–17), 2849–2860. [https://doi.org/10.1002/1099-1085\(200011/12\)14:16/17<2849::AID-HYP123>3.0.CO;2-X](https://doi.org/10.1002/1099-1085(200011/12)14:16/17<2849::AID-HYP123>3.0.CO;2-X)
- Nardi, L., & Rinaldi, M. (2015). Spatio-temporal patterns of channel changes in response to a major flood event: The case of the Magra River (central–northern Italy). *Earth Surface Processes and Landforms*, 40(3), 326–339. <https://doi.org/10.1002/esp.3636>

- Nelson, A., & Dubé, K. (2016). Channel response to an extreme flood and sediment pulse in a mixed bedrock and gravel-bed river. *Earth Surface Processes and Landforms*, *41*(2), 178–195. <https://doi.org/10.1002/esp.3843>
- O'Connor, J. E., Mangano, J. F., Anderson, S. W., Wallick, J. R., Jones, K. L., & Keith, M. K. (2014). Geologic and physiographic controls on bed-material yield, transport, and channel morphology for alluvial and bedrock rivers, western Oregon. *GSA Bulletin*, *126*(3–4), 377–397. <https://doi.org/10.1130/B30831.1>
- Parker, G., & Klingeman, P. C. (1982). On why gravel bed streams are paved. *Water Resources Research*, *18*(5), 1409–1423. <https://doi.org/10.1029/WR018i005p01409>
- Peck, D. L., Griggs, A. B., Schlicker, H. G., Wells, F. G., & Dole, H. M. (1964). Geology of the central and northern parts of the Western Cascade Range in Oregon. In *Geology of the central and northern parts of the Western Cascade Range in Oregon* (USGS Numbered Series No. 449; Professional Paper, Vol. 449, p. 62). U.S. Government Printing Office. <https://doi.org/10.3133/pp449>
- Pfeiffer, A. M., Collins, B. D., Anderson, S. W., Montgomery, D. R., & Istanbuluoglu, E. (2019). River Bed Elevation Variability Reflects Sediment Supply, Rather Than Peak Flows, in the Uplands of Washington State. *Water Resources Research*, *55*(8), 6795–6810. <https://doi.org/10.1029/2019WR025394>
- Pfeiffer, A. M., Finnegan, N. J., & Willenbring, J. K. (2017). Sediment supply controls equilibrium channel geometry in gravel rivers. *Proceedings of the National Academy of Sciences*, *114*(13), 3346–3351. <https://doi.org/10.1073/pnas.1612907114>
- Pitlick, J. (1993). Response and recovery of a subalpine stream following a catastrophic flood. *GSA Bulletin*, *105*(5), 657–670. [https://doi.org/10.1130/0016-7606\(1993\)105<0657:RAROAS>2.3.CO;2](https://doi.org/10.1130/0016-7606(1993)105<0657:RAROAS>2.3.CO;2)
- Prein, A. F., Rasmussen, R. M., Ikeda, K., Liu, C., Clark, M. P., & Holland, G. J. (2017). The future intensification of hourly precipitation extremes. *Nature Climate Change*, *7*(1), 48–52. <https://doi.org/10.1038/nclimate3168>
- Priest, G. R., Black, G. L., Woller, N. M., & Taylor, E. M. (1988). *Geologic map of the McKenzie Bridge quadrangle* [Map]. Oregon Department of Geology and Mineral Industries.
- Reid, D. A., Hassan, M. A., Bird, S., & Hogan, D. (2019). Spatial and temporal patterns of sediment storage over 45 years in Carnation Creek, BC, a previously glaciated mountain catchment. *Earth Surface Processes and Landforms*, *44*(8), 1584–1601. <https://doi.org/10.1002/esp.4595>

- Rickenmann, D. (1991). Hyperconcentrated Flow and Sediment Transport at Steep Slopes. *Journal of Hydraulic Engineering*, 117(11), 1419–1439. [https://doi.org/10.1061/\(ASCE\)0733-9429\(1991\)117:11\(1419\)](https://doi.org/10.1061/(ASCE)0733-9429(1991)117:11(1419))
- Robison, D. E. G., Mills, K. A., Paul, J., & Dent, L. (1999). *Oregon Department of Forestry Storm Impacts and Landslides of 1996: Final Report*. 157.
- Schumm, S. A. (1979). Geomorphic Thresholds: The Concept and Its Applications. *Transactions of the Institute of British Geographers*, 4(4), 485–515. JSTOR. <https://doi.org/10.2307/622211>
- Segura, C., & Booth, D. B. (2010). Effects of Geomorphic Setting and Urbanization on Wood, Pools, Sediment Storage, and Bank Erosion in Puget Sound Streams I. *JAWRA Journal of the American Water Resources Association*, 46(5), 972–986. <https://doi.org/10.1111/j.1752-1688.2010.00470.x>
- Sholtes, J. S., Yochum, S. E., Scott, J. A., & Bledsoe, B. P. (2018). Longitudinal variability of geomorphic response to floods. *Earth Surface Processes and Landforms*, 43(15), 3099–3113. <https://doi.org/10.1002/esp.4472>
- Sloan, J., Miller, J. R., & Lancaster, N. (2001). Response and recovery of the Eel River, California, and its tributaries to floods in 1955, 1964, and 1997. *Geomorphology*, 36(3), 129–154. [https://doi.org/10.1016/S0169-555X\(00\)00037-4](https://doi.org/10.1016/S0169-555X(00)00037-4)
- Snyder, K. U. (2000). *Debris flows and flood disturbance in small, mountain watersheds* [Oregon State University]. https://ir.library.oregonstate.edu/concern/graduate_thesis_or_dissertations/gf06g706q
- Spies, T. A. (2016). *LiDAR data (August 2008) for the Andrews Experimental Forest and Willamette National Forest study areas (Version 7) [geospatial data set]*. <http://andlter.forestry.oregonstate.edu/data/abstract.aspx?dbcode=GI010>
- Stoffel, M., Wyżga, B., & Marston, R. A. (2016). Floods in mountain environments: A synthesis. *Geomorphology*, 272, 1–9. <https://doi.org/10.1016/j.geomorph.2016.07.008>
- Surian, N., Righini, M., Lucía, A., Nardi, L., Amponsah, W., Benvenuti, M., Borga, M., Cavalli, M., Comiti, F., Marchi, L., Rinaldi, M., & Viero, A. (2016). Channel response to extreme floods: Insights on controlling factors from six mountain rivers in northern Apennines, Italy. *Geomorphology*, 272, 78–91. <https://doi.org/10.1016/j.geomorph.2016.02.002>
- Swanson, F. J. (2014). *Landslide inventory (1953-1996), Andrews Experimental Forest and Blue River Basin (Version 5) [database]*. <http://andlter.forestry.oregonstate.edu/data/abstract.aspx?dbcode=GE012>
- Swanson, F. J., Benda, L. E., Duncan, S. H., Grant, G. E., Megahan, W. F., Reid, L. M., & Ziemer, R. R. (1987). Mass failures and other processes of sediment production in Pacific

- northwest forest landscapes. *Chapter Two, In: Ernest O. Salo and Terrance W. Cundy (Eds.), Streamside Management: Forestry and Fishery Interactions, Proceedings of a Symposium Held at University of Washington, 12-14 February 1986. Contribution No. 57, Institute of Forest Resources, Seattle, Washington.*
<https://www.fs.usda.gov/treesearch/pubs/8628>
- Swanson, F. J., Gregory, S., Sedell, J., & Campbell, A. (1982). *Land-water interactions: The riparian zone.*
- Swanson, F. J., & James, M. E. (1975). *Geology and geomorphology of the H.J. Andrews Experimental Forest, Western Cascades, Oregon.* <https://agris.fao.org/agris-search/search.do?recordID=US201300715326>
- Swanson, F. J., Johnson, S. L., Gregory, S. V., & Acker, S. A. (1998). Flood Disturbance in a Forested Mountain Landscape Interactions of land use and floods. *BioScience*, 48(9), 681–689. <https://doi.org/10.2307/1313331>
- Swanson, F. J., & Jones, J. A. (2002). Geomorphology and Hydrology of the H.J. Andrews Experimental Forest, Blue River, Oregon. *Field Guide to Geologic Processes in Cascadia: Oregon Department of Geology and Mineral Industries, Special Paper 36.*
https://people.wou.edu/~taylors/g473/refs/swanson_jones_2002_field_guide.pdf
- Swanson, F. J., & Lienkaemper, G. W. (1978). *Physical Consequences of Large Organic Debris in Pacific Northwest Streams* (USDA Forest Service General Technical Report PNW-69). Department of Agriculture, Forest Service, Pacific Northwest Forest and Range Experiment Station.
- Swanson, F. J., Lienkaemper, G. W., & Sedell, J. R. (1976). History, physical effects, and management implications of large organic debris in western Oregon streams. *Gen. Tech. Rep. PNW-GTR-056. Portland, OR: U.S. Department of Agriculture, Forest Service, Pacific Northwest Research Station. 15 p, 056.* <https://www.fs.usda.gov/treesearch/pubs/22618>
- Thompson, C. J., Fryirs, K., & Croke, J. (2016). The Disconnected Sediment Conveyor Belt: Patterns of Longitudinal and Lateral Erosion and Deposition During a Catastrophic Flood in the Lockyer Valley, South East Queensland, Australia. *River Research and Applications*, 32(4), 540–551. <https://doi.org/10.1002/rra.2897>
- Turowski, J. M., Yager, E. M., Badoux, A., Rickenmann, D., & Molnar, P. (2009). The impact of exceptional events on erosion, bedload transport and channel stability in a step-pool channel. *Earth Surface Processes and Landforms*, 34(12), 1661–1673.
<https://doi.org/10.1002/esp.1855>
- Wallick, J. R., Anderson, S. W., Cannon, C., & O'Connor, J. E. (2012). *Channel change and bed-material transport in the Lower Chetco River, Oregon* (USGS Numbered Series No. 2010–5065; Open-File Report). U.S. Geological Survey.
<http://pubs.er.usgs.gov/publication/ofr20091163>

- Wells, S. G., & Harvey, A. M. (1987). Sedimentologic and geomorphic variations in storm-generated alluvial fans, Howgill Fells, northwest England. *GSA Bulletin*, 98(2), 182–198. [https://doi.org/10.1130/0016-7606\(1987\)98<182:SAGVIS>2.0.CO;2](https://doi.org/10.1130/0016-7606(1987)98<182:SAGVIS>2.0.CO;2)
- Wemple, B. C., Swanson, F. J., & Jones, J. A. (2001). Forest roads and geomorphic process interactions, Cascade Range, Oregon. *Earth Surface Processes and Landforms*, 26(2), 191–204. [https://doi.org/10.1002/1096-9837\(200102\)26:2<191::AID-ESP175>3.0.CO;2-U](https://doi.org/10.1002/1096-9837(200102)26:2<191::AID-ESP175>3.0.CO;2-U)
- Wohl, E., & Cadol, D. (2011). Neighborhood matters: Patterns and controls on wood distribution in old-growth forest streams of the Colorado Front Range, USA. *Geomorphology*, 125(1), 132–146. <https://doi.org/10.1016/j.geomorph.2010.09.008>
- Wolman, M. G. (1954). A method of sampling coarse river-bed material. *Eos, Transactions American Geophysical Union*, 35(6), 951–956. <https://doi.org/10.1029/TR035i006p00951>
- Wolman, M. G., & Miller, J. P. (1960). Magnitude and Frequency of Forces in Geomorphic Processes. *The Journal of Geology*, 68(1), 54–74. <https://doi.org/10.1086/626637>
- Wondzell, S. M., & King, J. G. (2003). Postfire erosional processes in the Pacific Northwest and Rocky Mountain regions. *Forest Ecology and Management*, 178(1), 75–87. [https://doi.org/10.1016/S0378-1127\(03\)00054-9](https://doi.org/10.1016/S0378-1127(03)00054-9)
- Wondzell, S. M., & Swanson, F. J. (1999). Floods, channel change, and the hyporheic zone. *Water Resources Research*, 35(2), 555–567. <https://doi.org/10.1029/1998WR900047>
- Yochum, S. E., Sholtes, J. S., Scott, J. A., & Bledsoe, B. P. (2017). Stream power framework for predicting geomorphic change: The 2013 Colorado Front Range flood. *Geomorphology*, 292, 178–192. <https://doi.org/10.1016/j.geomorph.2017.03.004>
- Zheng, S., Wu, B., Thorne, C. R., & Simon, A. (2014). Morphological evolution of the North Fork Toutle River following the eruption of Mount St. Helens, Washington. *Geomorphology*, 208, 102–116. <https://doi.org/10.1016/j.geomorph.2013.11.018>

8. Appendices

A. Appendix A: Study and Site Information

Table A.1: Table of survey years with number of cross sections surveyed at each reach. “Full” surveys are designated as surveys that included at last 75% of permanent cross sections. “Partial” surveys included fewer than 75% of the permanent cross sections. An additional cross section, “LOL19”, was added to Lower Lookout in 2004 and is not included in analysis. Cross section “MCC116” was not sampled at the Mack Clear Cut reach after 1990. Cross section “LOM 109” was not sampled at Middle Lookout after 1995. From 1995 onwards, pebble counts were conducted in conjunction with cross section surveys, except at cross sections “LOL01” in 1995 and “LOM09” in 1996. These pebble counts were not conducted at these cross sections during these years because surveyors could not access the substrate.

Survey Year	Lower Lookout	Middle Lookout	Mack Old Growth	Mack Clear Cut
1978	Full (14)	Full (11)	Full (12)	None
1980	Full (13)	Partial (6)	Full (12)	None
1981	Full (14)	Full (11)	Full (12)	Full (20)
1982	Full (14)	Full (11)	Full (12)	Full (20)
1983	None	None	Full (12)	Partial (9)
1984	Full (14)	Full (10)	Full (12)	Full (20)
1985	Full (11)	Full (10)	Full (12)	Full (20)
1986	Full (14)	Full (11)	Full (12)	Full (20)
1988	Full (14)	Full (11)	Full (12)	Full (20)
1989	Full (14)	Full (11)	None	None
1990	Full (14)	Full (11)	Full (12)	Full (20)
1995	Full (14)	Full (11)	Full (12)	Full (18)
1996	Full (14)	Full (11)	Full (12)	Full (19)
1997	Full (14)	Full (11)	Full (12)	Full (19)
1998	Full (14)	Full (11)	None	None
1999	Full (14)	Full (11)	None	None
2000	Full (14)	Full (11)	Full (12)	Full (19)
2001	Partial (5)	Partial (4)	None	None
2002	Partial (5)	Partial (5)	None	None
2003	Partial (6)	Partial (2)	None	None
2004	Partial (6)	Partial (1)	None	None
2005	Full (15)	Full (11)	Full (12)	Full (19)
2006	Full (15)	Full (11)	None	None
2007	Partial (6)	Partial (2)	None	None
2009	Partial (4)	None	None	None

2011	Full (15)	Full (11)	Full (12)	Full (19)
------	-----------	-----------	-----------	-----------

Table A.2: Substrate descriptions from survey metadata and whether or not each substrate class was included in cross-sectional change calculations.

Substrate Code	Description	Included in Profile
NR	Not recorded	no
BL	Boulder	yes
BR	Bedrock	yes
CB	Cobble	yes
FO	Fine organics	yes
FS	Fine sediment	yes
GR	Gravel	yes
IB	Eye-bolt/bedrock	no
LG	Log (> 10 cm diameter)	no
LI	Litter	yes
LS	Suspended log	no
MS	Bare mineral soil / colluvium	yes
OD	Organic debris (< 10 cm diameter)	yes
OS	Suspended organic debris	no
RW	Rootwad / stump	no
TF	Turf / grass	yes
TR	Trail	yes

Table A.3: Table of cross section-year pairs that were excluded from analysis.

Reach	Cross Section Code	Years excluded	Reason for Exclusion
Lower Lookout	LOL06	1980	Bank placement misaligned with prior and subsequent surveys
Lower Lookout	LOL12	1978, 1984	Incomplete survey (1978), Poor survey quality (1984)
Lower Lookout	LOL14	1984	Poor Survey quality
Lower Lookout	LOL19	2004 – 2011	Temporary cross section
Middle Lookout	LOM109	1986–1995	Temporary cross section

Mack Clearcut	MCC111	1981 – 2011	Inconsistent survey
Mack Clearcut	MCC112	1981, 1985 & 1990	Tilted and/or incomplete survey coordinates
Mack Clearcut	MCC116	1981 – 1990	Temporary cross section
Mack Clearcut	MCC117	1983 – 1984	Poor alignment to prior and subsequent surveys
Mack Old Growth	MAC09	1978	Incomplete survey

Table A.4: R^2 values and p values for linear regressions between cross section D50 and cross section shear stress.

Reach	Cross Section	R^2	p
Lower Lookout	LOL01	0.05	0.51
Lower Lookout	LOL02	0.06	0.41
Lower Lookout	LOL03	0.16	0.15
Lower Lookout	LOL04	0.21	0.11
Lower Lookout	LOL05	0.32	0.09
Lower Lookout	LOL06	0.19	0.21
Lower Lookout	LOL07	0.47	0.04
Lower Lookout	LOL08	0.27	0.12
Lower Lookout	LOL09	0.09	0.33
Lower Lookout	LOL10	0.01	0.79
Lower Lookout	LOL11	0.32	0.07
Lower Lookout	LOL12	0.52	0.03
Lower Lookout	LOL13	0.29	0.08
Lower Lookout	LOL14	0.06	0.53
Middle Lookout	LOM01	0.04	0.59
Middle Lookout	LOM02	0.55	0.01
Middle Lookout	LOM03	0.75	0.003
Middle Lookout	LOM04	0.35	0.09
Middle Lookout	LOM05	0.38	0.08
Middle Lookout	LOM06	0.10	0.40
Middle Lookout	LOM07	0.01	0.81
Middle Lookout	LOM08	0.09	0.42
Middle Lookout	LOM09	0.13	0.25
Middle Lookout	LOM10	0.06	0.42
Middle Lookout	LOM11	0.15	0.23

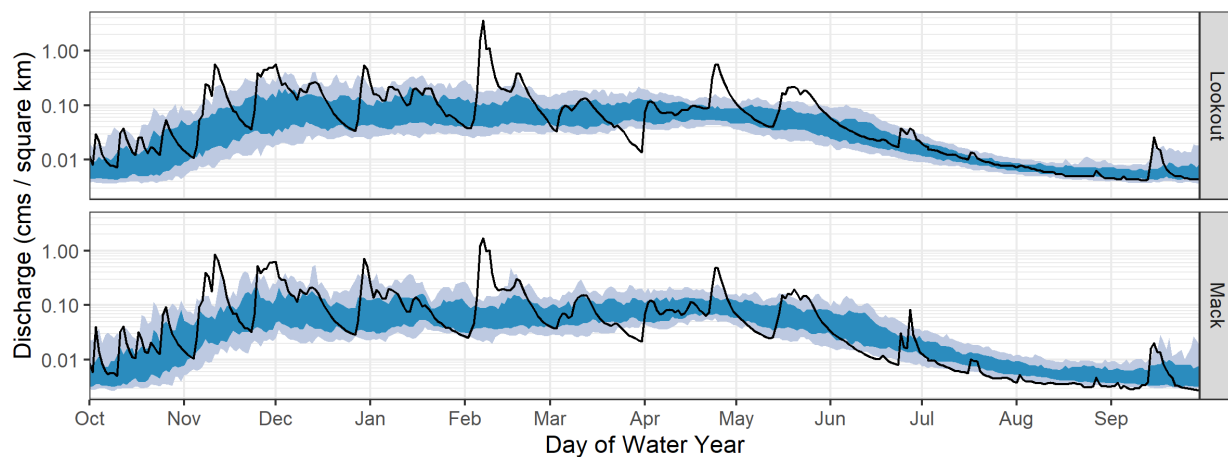


Figure A.1: Summary of daily maximum discharge values for the Lookout Creek gage (top) and Mack Creek gage (bottom). The 10th–90th percentile flows are shown as a light blue band. 25th–75th percentile flows are shown in dark blue. Daily maximum flows for the 1996 water year are shown in black.

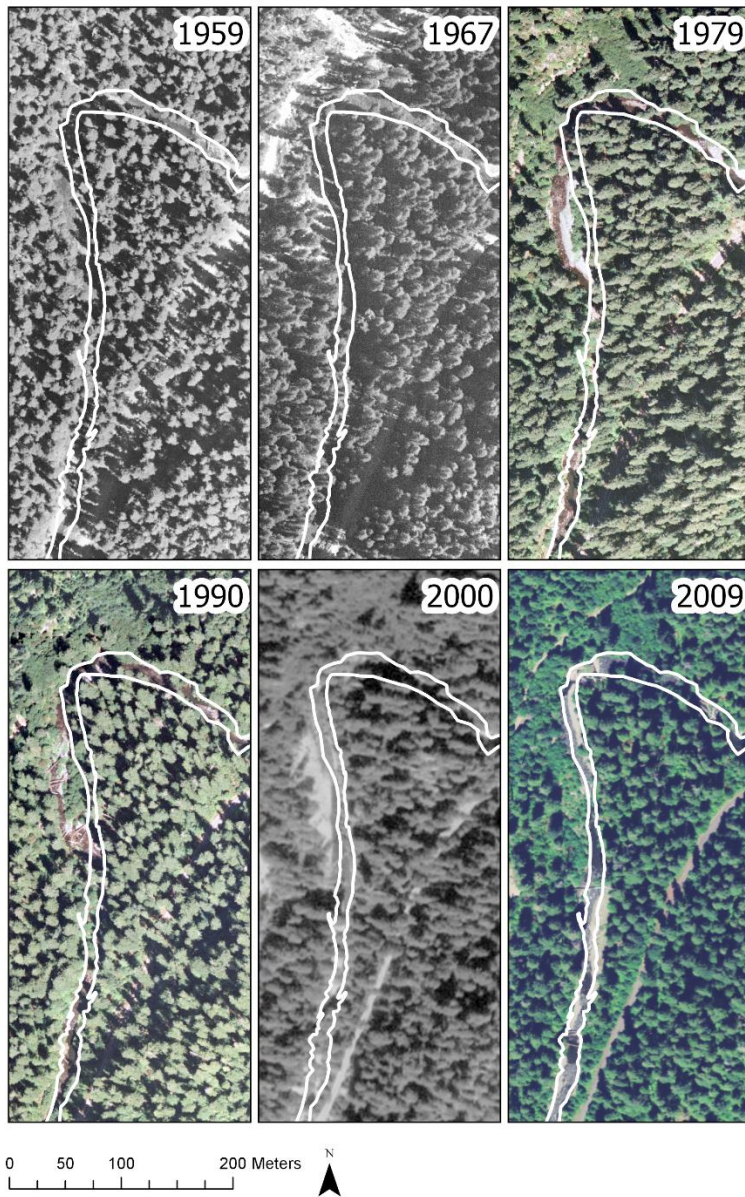


Figure A.2: Historical aerial photos of Lower Lookout from 1959 to 2009. Map extent and scale is identical to that in Figure 2a. The 1996 low-flow channel boundary is shown in white for comparison. Data 1959-1990 are courtesy of the HJ Andrews Experimental Forest. The 2000 and 2009 imagery comes from the USDA National Agricultural Imagery Program (NAIP).

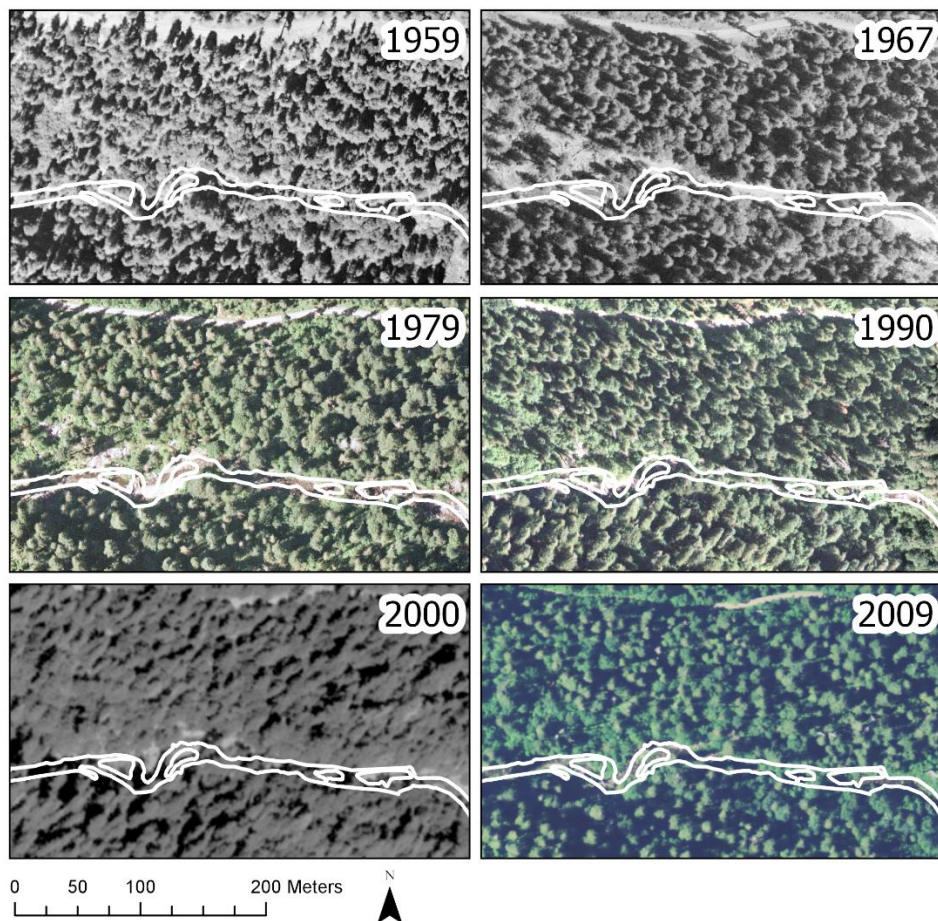


Figure A.3: Historical aerial photos of Middle Lookout from 1959 to 2009. Map extent and scale is identical to that in Figure 2a. The 1996 low-flow channel boundary is shown in white for comparison. Data 1959-1990 are courtesy of the HJ Andrews Experimental Forest. The 2000 and 2009 imagery comes from the USDA National Agricultural Imagery Program (NAIP).

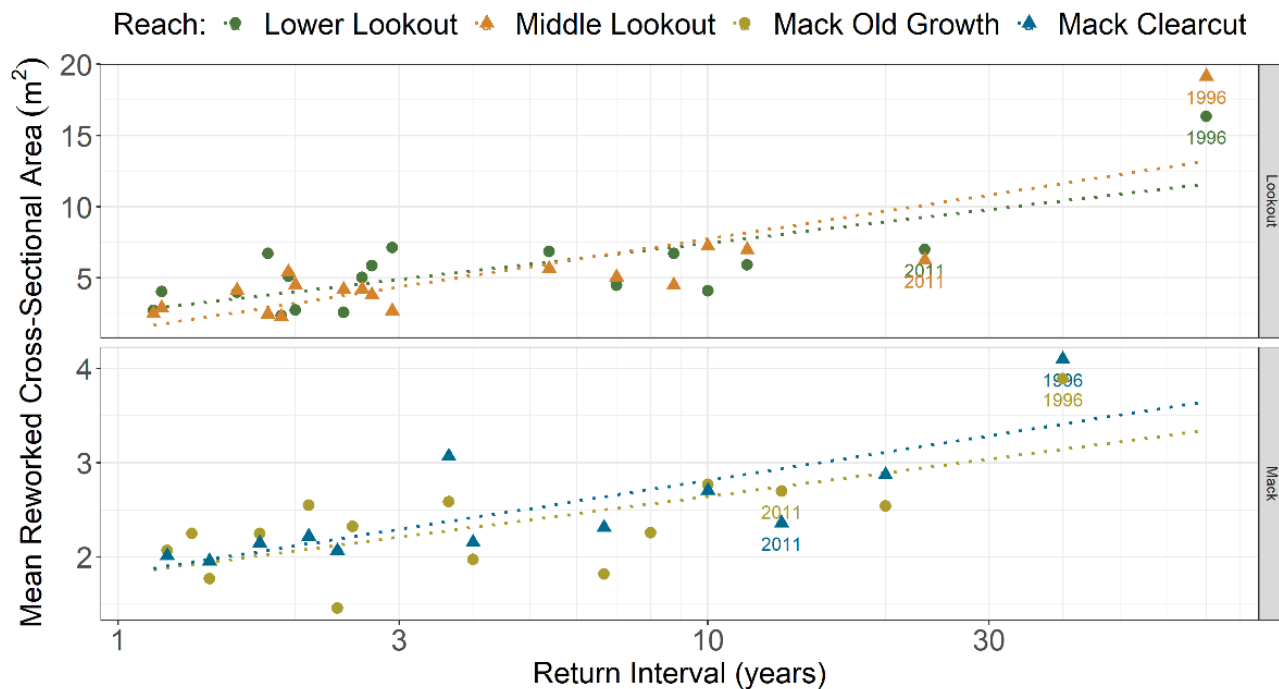


Figure A.4: Total reworked channel area (i.e., area eroded plus area deposited) plotted against flood return interval for all reaches, with linear trendlines. The x-axis is on a log scale to better show the distribution of data. Points from 1996 and 2011 are labeled.

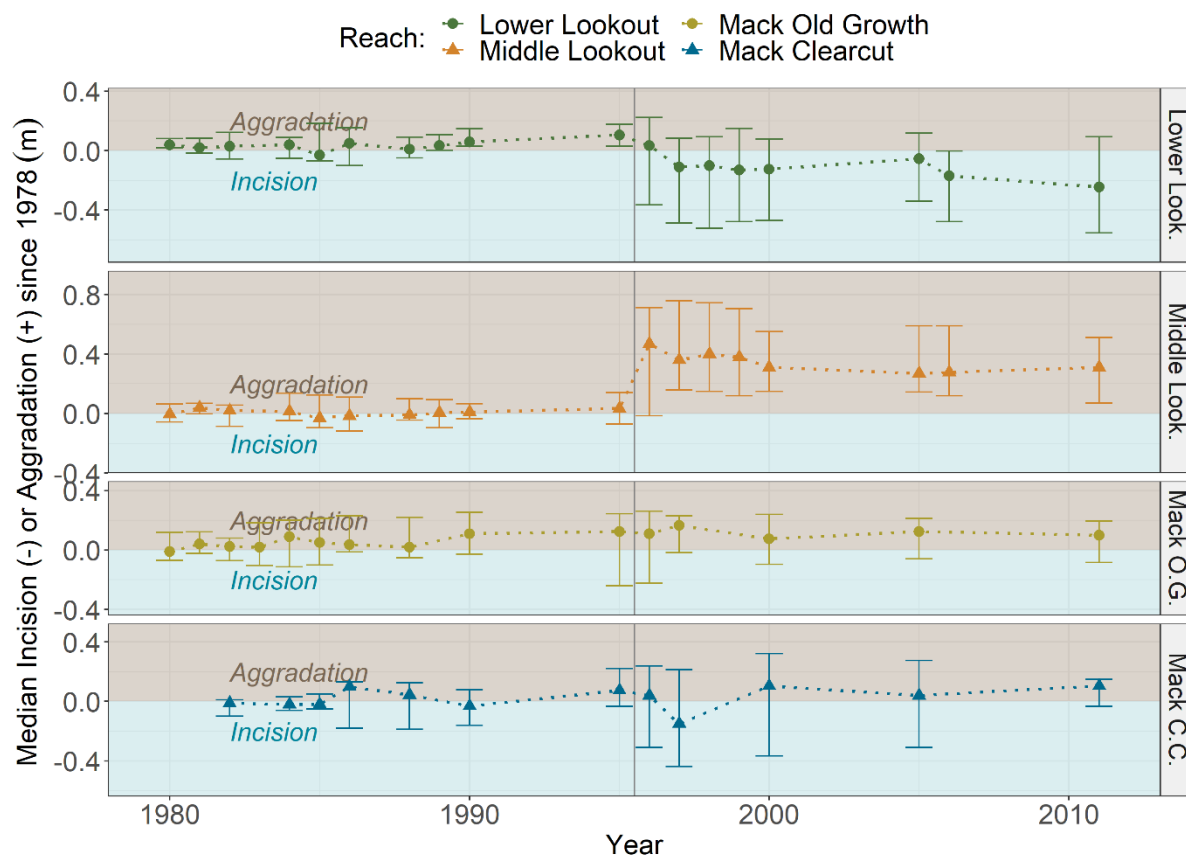


Figure A.5: Median (dots) and interquartile range (bars) of cumulative thalweg incision and aggradation relative to the start of monitoring in 1978 (or 1981 for Mack Clearcut). Points in the brown field represent cumulative aggradation while points in the blue field represent cumulative incision. Lower Lookout overall incised while Middle Lookout experienced aggradation. Median values changed very little at the Mack Creek reaches between 1995 and 1996, but the interquartile range increased after the flood of 1996. The black vertical line shows the 1996 flood.

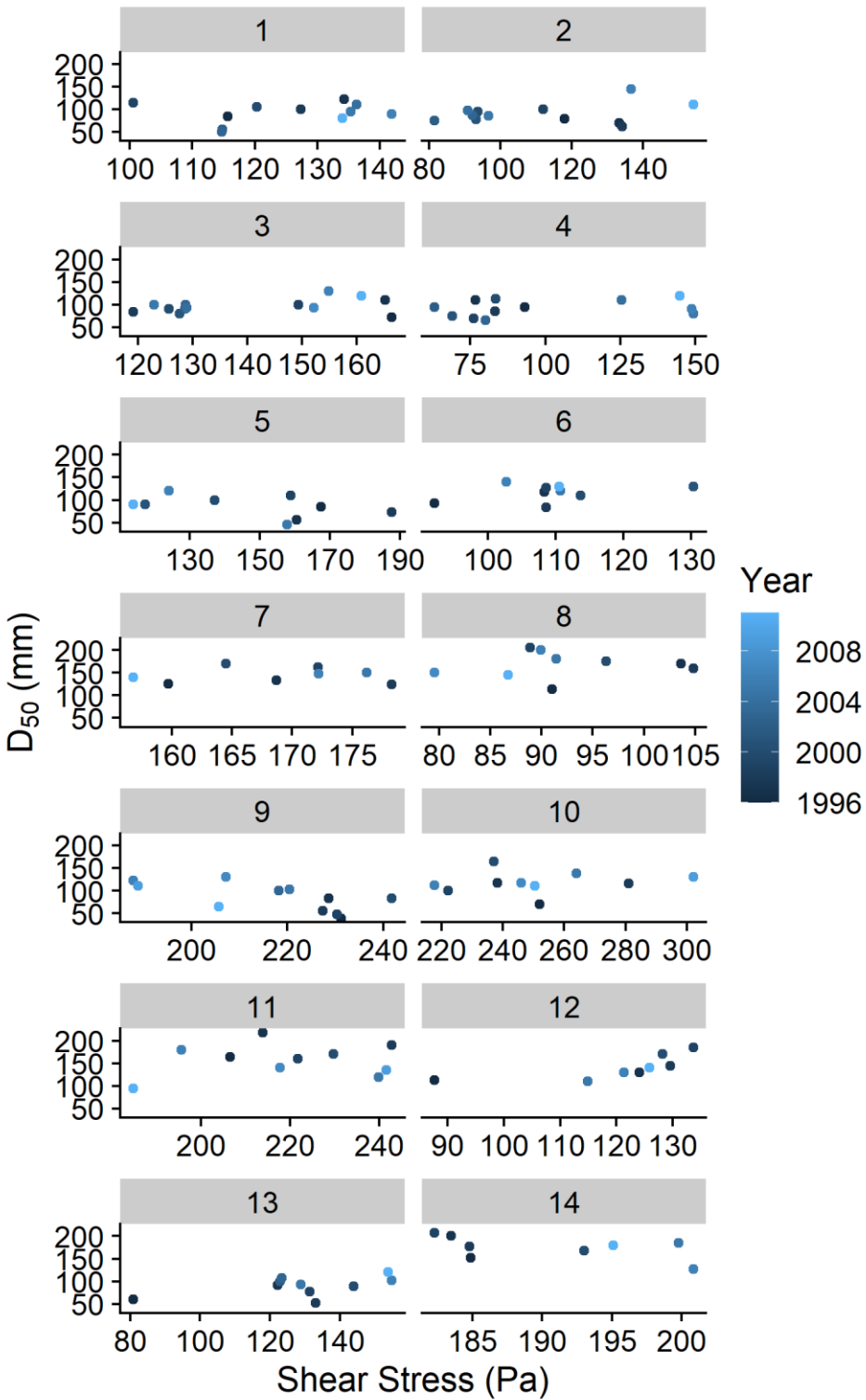


Figure A.6: Scatter plots of shear stress (Pa) versus D_{50} (mm) for each cross section in Lower Lookout. Significant relationships are seen at cross sections LOL07 and LOL12

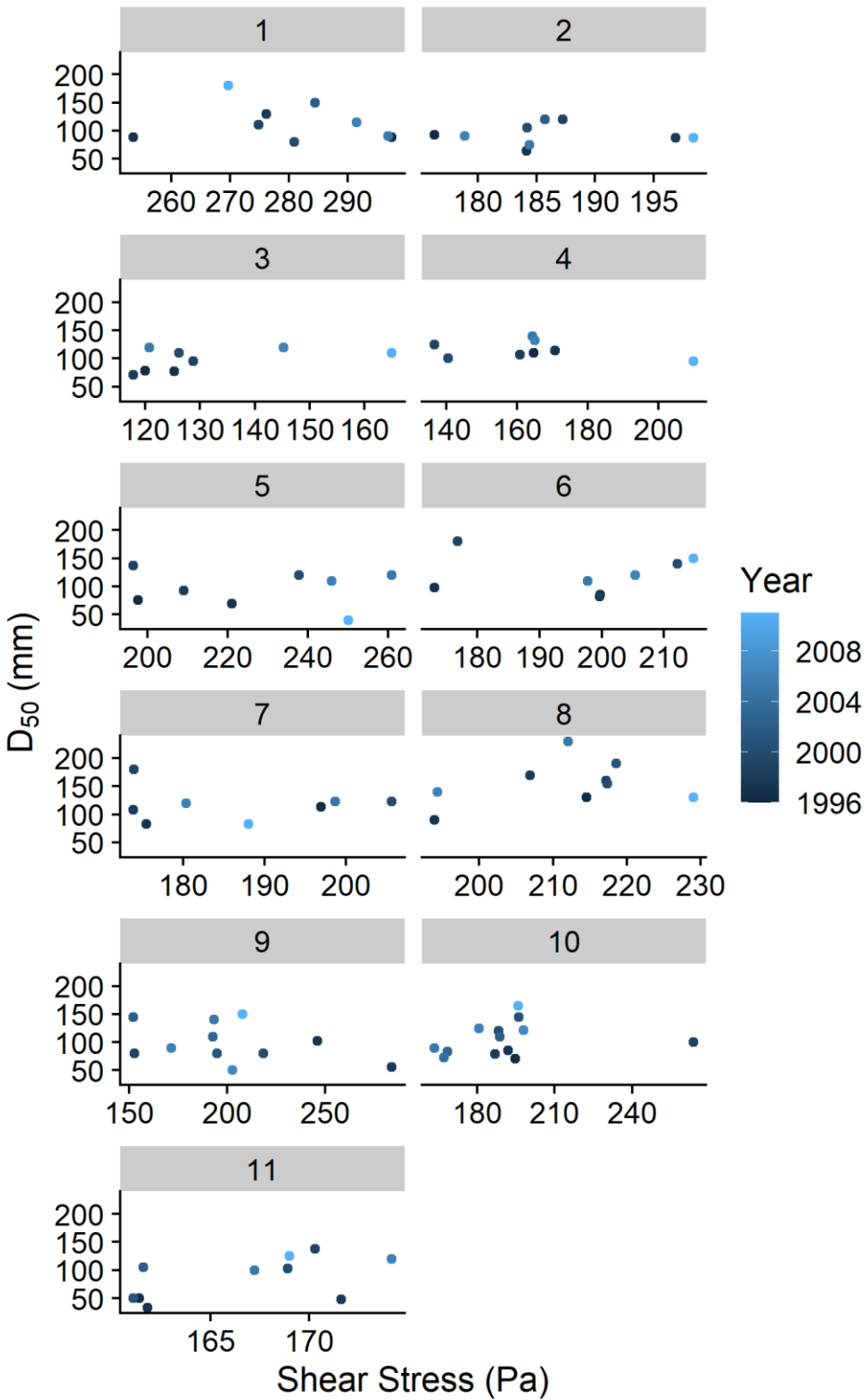


Figure A.7: Scatter plots of shear stress (Pa) versus D_{50} (mm) for each cross section in Middle Lookout. Significant relationships are seen at cross sections LOM02 and LOM03

B. Appendix B: Site Photos



Figure B.1: Total station surveying in Lower Lookout during summer 2019



Figure B.2: Midchannel bar visible at low flow in Lower Lookout during summer 2019



Figure B.3: Large channel-spanning wood jam in Lower Lookout near channel bend during summer 2019



Figure B.4: Channel-spanning wood jam in Middle Lookout near LOM08 during summer 2019



Figure B.5: Boulders in stream near Mack Clearcut during summer 2019



Figure B.6: Field assistant holding RTK GPS unit above channel spanning logjam at Mack Old Growth near cross section MAC07